Electronic Sensing Systems for Next Generation SDS PAGE Technologies

Mohamed Adam bin Mohamed Ibrahim

MSc by Research

University of York

Electronic Engineering

January 2018

1 Abstract

This document presents an assessment on the viability of an electronically measured, miniaturised alternative to “sodium dodecyl sulphate polyacrylamide gel electrophoresis”, abbreviated as SDS-PAGE or simply Gel Electrophoresis. An understanding of alternating electrical fields and its effects on dielectrics with and without the presence of ionic substances suggests that a capacitive electrode could be used as a sensor in detecting the motion of ions under a large external electrostatic field.

Photolithography was used to manufacture small scale interdigitated capacitor loops to be used in conjunction with a sensor holder to measure effects of varying electric field strength on the motion of salt ions through agarose gel. The polarity of the electric field was also reversed to determine whether the process of ionic motion was reversible. The sensor was capable of measuring the gradual introduction of salt ions through the gel but unsuccessful in reversing the process of ionic measurement.

A second double mesh experiment was also conducted to enable salt ions to pass through the sensor in order to detect the possibility of a peak and then reduction of voltage readings. This experiment also studied the effects of varying salt concentration and showed a higher voltage reading for higher salt concentrations as well as a slightly faster transition time when an electric field was present compared to the absence of a field however was unable to record a drop of voltage after 24 hours.

2 Table of Contents

3 Introduction

This thesis will describe a new approach to gel electrophoresis that could result in low cost, miniaturised instruments which measure the dielectric properties of the samples rather than using the traditional fluorescent technique widely used today. Two instruments are presented. The first is a substrate based electrode, the second is a pass-through, double mesh design. In both cases the transit time of the sample to the sensor will be dependent on the mass charge ratio of the sample as is the case with current technique. Electrophoresis is a method of separating macromolecules according to their size and this study aims to determine whether these molecules can be measured electrically rather than visually.

Both instruments act as a capacitor with the gel as a dielectric medium. The technique explored in this experiment involves measuring the output voltage across the capacitor structures as salt ions are introduced, therefore affecting the electrical permittivity of the capacitive structure by altering the dielectric constant within the electrodes. The reason NaCl solution is used is because table salt is cheap and readily available. NaCl also contains ions which can be measured as using DNA samples can be costly. Copper plates are used to provide an Electrostatic field that will be responsible for providing salt ions with the ability to travel through agarose gel solution.

The experiments conducted will attempt to differentiate between initial salt ion arrival time, saturation time and final saturation voltage. For the nanofabricated electrodes, it is investigated whether reversing the polarity of the electrostatic field plates midway through the experiment will reverse the process of ionic motion and cause an inverted trend on the voltage output readings. The double mesh experiment will investigate whether salt ions that pass through the mesh will cause a parabolic trend in the measurement of output voltage across the mesh, signifying the loss of voltage output as the salt ions pass through the mesh and collects to the bottom of the setup.

The ionic transfer experiment uses the nanofabricated electrodes to determine the presence of an ionic trap on the electrode by slowly reducing the concentration of salt ions within the sensor through slow funnelling of de-ionized water. The supplemental Iodine visual experiment is a simple visual experiment to analyse the motion of iodine crystal solution within an agarose gel in a 1ml sealed vial.

4 List of Figures

5 List of Tables

6 List of Abbreviations

CAD – Computer Aided Design

DI – De-Ionized

SDS-PAGE - Sodium Dodecyl Sulfate Polyacrylamide Gel Electrophoresis

Na - Natrium or Sodium

Cl – Chloride

IPA – Isopropyl Alcohol

CHD – Coronary Heart Disease

DNA – Deoxyribonucleic Acid

RNA – Ribonucleic Acid

TAE – Tris-Acetate-EDTA

EDTA - Ethylenediaminetetraacetic acid

7 Acknowledgements

I would like to thank my supervisors, Dr Iain Will and Professor Yongbing Xu for their tremendous support, guidance and feedback throughout this project. Thanks also to the support staff, Charan Panesar and Jonathan Cremer for their time and assistance. A special note of thanks also to Stephen Thorpe, Dr Martin Robinson and Dr Katherine Dunn for their sound advice and suggestions.

8 Declaration

I declare that this thesis is a presentation of original work and I am the sole author. This work has not previously been presented for an award at this, or any other, University. All sources are acknowledged as References.

9 Literature Review

This section discusses literature surrounding the field of medicine that benefit from advances in Nanotechnology processes. Areas such as medical diagnostics, drug delivery and cell repair have all benefitted from Nanotechnology from the use of principles such as photolithography of substrates, quantum dots, carbon nanotubes and magnetic nanoparticles.

9.1 Nanotechnology in Medicine

As newer technologies emerge, it has become increasingly easier for medical patients to seek more effective treatments for medical conditions. The lowering production costs, and higher processing power of medical and diagnostic machinery has been beneficial to the modern medical industry in helping to combat illness and provide the best care possible at a faster rate and hopefully cheaper cost. One such developing field that is involved in helping in the research, manufacture and development of newer technologies in medicine is Nanotechnology. The process of using nanotechnology in medicine can be simply described as Nanomedicine, where medical processes using nano-scaled devices to assist in medical applications such as drug delivery systems, medical diagnoses, medical imaging, disease prevention and therapy. Nanomedicine can also involve using nanofabrication methods to manufacture
medical devices that improve current available technologies involved in these processes. There are many benefits nanotechnology can provide in the medical field such as the reduction in the size of large medical devices and analytical tools, allowing hospitals and other medical facilities to make use of more spaces to conduct their practices. Smaller scale medical devices also allow for easy to use interfaces for stay-at-home patients to still be monitored remotely as they would not need bulkier hospital monitoring tools[1]. Patients that require the use of invasive implants also tend to benefit from miniaturization as larger analytical and therapeutic devices usage can be cumbersome.
Nanotechnology also has the possibility of improving target area diagnosis and treatment, being able to accurately target problem areas without damaging surrounding healthy or undamaged tissue for purposes of treatment and improving accuracy of treatment methods.
If automation within nanomedical devices can be further developed, this will create a more cost-efficient and improve resource management for medical treatment as less manual labour is needed to support larger medical infrastructure.
Some other key benefits that Nanotechnology will bring to medicine include[2]

- Cheaper and more elegant surgical and diagnostic tools

- Cost efficient research and diagnosis
- Small permanent medical implantable medical devices
- General health improvement and higher lifespans
- Potential of fully replaceable organs

Finally it is worth noting that nanotechnology, while being an emerging and ever improving field will allow for wider area of study and also improvements of other fields of study such as agriculture, environment and aeronautics.

The use of nanoparticles can some day revolutionise the medical field with the use of nanorobots and other nano or micro scaled systems for the diagnosis and eventual treatment of illnesses.

9.1.1 Nanotechnology in Drug Delivery Systems

One of the most profound uses of nanotechnology in the field of medicine involves engineered “Nanoparticles” and other systems to transfer life-saving curative drugs to problem areas within the patient's’ anatomy.

Demand for newer drug delivery methods are now a high priority considering that there will be a need to replace older, more established pharmaceutical drugs as their patents are being challenged[3].

The benefits nanotechnology can have for the pharmaceutical industry is undeniable as studies have shown that it is possible to achieve;

i) better drug solubility

ii) improved drug targetting and specificity

iii) drug protection from degradation in the gastrointestinal tract

For example [4] Researchers at the University of California in San Diego have collected red blood cells and wrapping them around biodegradable polymer nanoparticles that have been stuffed with drugs. These wraps act as a camouflage to evade the human body’s immune system as it travels through the human body while delivering powerful drugs to combat cancerous tumours.

This is particularly useful as the human body can be an effective tool when fighting foreign substances that enter it. Having this camouflage means the drugs can be safely transported to the tumour as the body only recognises it as a red blood cell.

As the polymer is biodegradable, this ensures that the drugs are dissolved naturally over time and provides an excellent means of delivering pharmaceutical treatment.

Another such example of using nanoparticles in the treatment of cancer is a study done by the researchers at the UCLA Henry Samueli School of Engineering and Applied Science where “Tiny shells composed of a water-soluble polymer that safely deliver a protein complex to the nucleus of cancer cells to induce their death”[5] where cancer cells are

destroyed by a protein complex that has been derived from an anemia virus in birds.
Coronary heart and coronary artery disease (CHD and CAD respectively) are terms that are used interchangeably regarding the disease that involves the buildup of plaque in the human artery. According to the NHS [6] this disease is responsible for many deaths not only within the United Kingdom, but also worldwide.
According to a study in 2016[7] nanotechnology may play a huge rule in the treatment of CAD and plays a variety of roles such as

- increasing systematic agent circulation time
- lowering off-target cytotoxicity of drugs
- improving the solubility of drugs
- decreasing the required dosage of drugs

Similarly to the treatment of cancerous cells, the treatment of CAD involves the formation of nanomembranes or the transportation of drugs encased within nanoparticles for targeted drug delivery. Such membranes or particles may be in the form of polymer coatings, magnetic nanoparticles and “nanotextured” ceramic coatings.
In conclusion nanolayered membranes and nanoparticles show great promise in the pharmaceutical industry, as laboratory and other trials on small animals such as mice have shown great success.

9.1.2 Nanotechnology in Cell Repair

Cell repair is another developing section within medical nanotechnology that is involved in the regeneration and reassembly of deteriorated or decomposing cells that maintain function within the human body.
The integrity of organs and physical homeostasis is maintained by the body’s ability to control the rate at which the death of cells and the division of existing cells occur. Not all cell death is harmful however, as unwanted or damaged cells are removed from the human body and such these cells do not consume resources that could be used to feed and nourish healthier cells[8].
Alternatively, systems or organs within the human body may not always be within peak condition to maintain the balance ratio of cell death to cell division, meaning that there must be systems in place to assist the recreation and healing of lost cells to maintain organ efficiency. Such causes in these imbalances include [9]

- Aging
- Diseases
- Poor health and dietary habits

Researchers at the Northwestern University have managed to heal the spinal cord of

paralyzed lab mice in 6 weeks, returning their ability to use their hind legs. This process was done by “injecting molecules that were designed to self assemble into nanostructures in the spinal tissue”. Nanofibres were used to rescue and regrow rapidly damaged neurons, prevent the formation of harmful scar tissue to assist in spinal cord healing by stimulating the body into regenerating lost or damaged cells [10].

One study suggests that nanorobots could also be injected into the human body to repair human cells and even organs. The working principal behind these “nanites” are that programmable medical robots could be introduced within infected or damaged tissue and use laser to remove them. The structure of these nanites, which consist of several moving parts such as; a propeller and fins to assist in forward motion and to create stability and lift, a nanocamera for detection and visual aid and lasers for harmful cell removal[11]

9.1.3 Nanotechnology in Diagnostics

The process of using Nanotechnology in the assistance of medical diagnostics, also known as nanomolecular diagnostics, is the clinical application of molecular technologies to interpret, diagnose and monitor human diseases.

There are several examples of which nanotechnology-influenced diagnostic tools could be used in the field of medicine.

i) Biochips and Microarrays – these include a type of chip that allows for multiple analytic procedures to take place called “multiplex assays”. A microarray is then simply a multiplex assay “lab-on-a-chip” that is fabricated on a substrate such as glass or silicone. Such examples of Microarrays in diagnostics include “Nanofluidic Arrays” which can be used for size selective protein fractionation [12] and saliva based nano-biochip tests for acute myocardial infarction, which utilize saliva as an alternative diagnostic fluid for identifying those with Acute Myocardial Infarction (AMI) [13]

ii) Nanobiosensors – A biosensor can be defined as a “sensing device or a measurement system designed specifically for estimation of a material by using the biological interactions and then assessing these interactions into a readable form with the help of transduction and electromechanical interpretation”[14] . There are several working components that make up a biosensor[15,16,17],

   a. The bioreceptor – a component that act as the recognition element of a biosensor that identifies biological analytes. These include enzymes, proteins, nucleic acids, antigens and antibodies
   b. The transducer – a conversion device capable of converting biological stimuli or behaviour into electrical signals. Examples of transducers are

electrochemical, optical, piezoelectrical, mass-based and calorimetrical transducers.

c. Amplifier – these simply amplify signals received from the transducer
d. Data processor – a component that receives the amplified data and converts them into a readable format
e. Display – A screen or device that displays the data to the user

The core principals of a dependable biosensor include[15,16,17],

a. Specificity
b. Accuracy and repeatability
c. Sensitivity and resolution
d. High speed of response
e. Insensitivity to external responses

iii) Nanoparticles – particles that possess unique characteristics that allow for non-invasive methods of diagnostics through optical and physio-chemical means. The three most frequently used in nanoparticle diagnostics area

a. Gold Nanoparticles
b. Quantum Dots
c. Magnetic nanoparticles

Nanoparticles are particularly interesting as they seem to have use in not only diagnostics but also drug delivery as previously discussed earlier in the chapter.

As stated in the abstract [18], the influenza virus can be detected rapidly by functionalizing gold particles to glycan forming a glycan-functionalized gold nanoparticles (gGNPs). The flu virus diagnosis was also researched by the University of Georgia [19] where the flu virus could be photonically detected by coating gold nanoparticles with antibodies that attach themselves to specific strains of the flu virus and measured how these particles scattered laser light. Sigma Aldrich describe quantum dots as “tiny particles or nanocrystals of a semiconducting material with diameters in the range of 2-10 nanometers”[20] . Quantum dots exhibit a property called fluorescence, which emit light depending on its size upon being illuminated. Fluorescence enables the process of immunolabelling to occur through immunofluorescence, which is a technique for “fluorescently labelling a specific biological target within a specific biological target using an antibody”[21]. Fluorescent Immunolabelling allows quantum dots to be coupled with cancer specific target ligands for fluorescent cancer visualization [22] . Other studies that uses quantum dots as immunolabels include using commercial streptavidin-coated quantum dots for the detection of

- prostate tumour cells [23]
- human fetal fibroblasts [24]
- Ovarian cells [25]
- Liver cells [26]

And using commercial quantum dots in the detection of human monocytic cells and atherosclerotic tissue sections [27] and peripheral blood [28].

Magnetic nanoparticles are simply particles that can be manipulated with magnetic fields. In medical diagnosis, magnetic particles can be bound to bacteria under controlled biorecognition events. This binding process helps bacterial detection and separation using magnets[29]. Magnetic nanoparticles can also improve the detection rate and help distinguish between benign and malignant tumours for breast cancer patients through the use of ultra-sensitive magnetic field sensors [30]

10 Theory

This section discusses the relevant theoretical principles that build the foundations of the experimental processes. The knowledge of electrical fields is essential in understanding motion of charged particles. A basic understanding of Gel electrophoresis processes is outlined and current gel electrophoresis processes are discussed. A brief section on capacitors and dielectric changes is explained to provide an alternative measurement and analysis method for gel electrophoresis. The section will also provide relationships on the change of voltage across an alternating field when a dielectric medium is present and also how this will change as charged particles or ions enter the field as well as the effects of higher frequency on the polarization of dielectric materials.

10.1 Electrical Fields

An electric field is defined as electric force, F, per unit charge, q.

$$E = \frac{F}{q} \tag{1}$$

The direction of the field is determined by the direction of the force it would exert on a positive test charge. Electric fields emit radially outward for positive point charges and radially inward for negative point charge.

10.1.1 Static Electric Field

When an electric field does not vary over time, it is said that the electric field is “static” and are characterized by steady direction, flow rate and strength[31]. This can also be referred to as “Electrostatic Field”

10.1.2 Charge density

Charge density refers to the amount of charge is accumulated in an area. This is commonly known as the charge density formula, denoted by σ.

$$\sigma = \frac{q}{A} \tag{2}$$

Or that the charge density is equal to the charge,q, over unit area, A.

10.1.3 Gauss's Law

Gauss's Law states that the total electric flux, Φ, which is "the measure of flow of the electric field through a given area", out of a closed surface area is equal to the charge enclosed divided by the permittivity, ε. The permittivity is a constant proportionality that exists between electric displacement and electric field intensity. This value is usually given by a constant ε = 8.85 x10 $^{-12}$ farad per meter (F/m) in free space[32].

10.1.4 Electric fields for a sheet charge

For an infinite sheet of charge, the electric field will be perpendicular to the surface of the sheet. This can be visualized by Figure 1 below

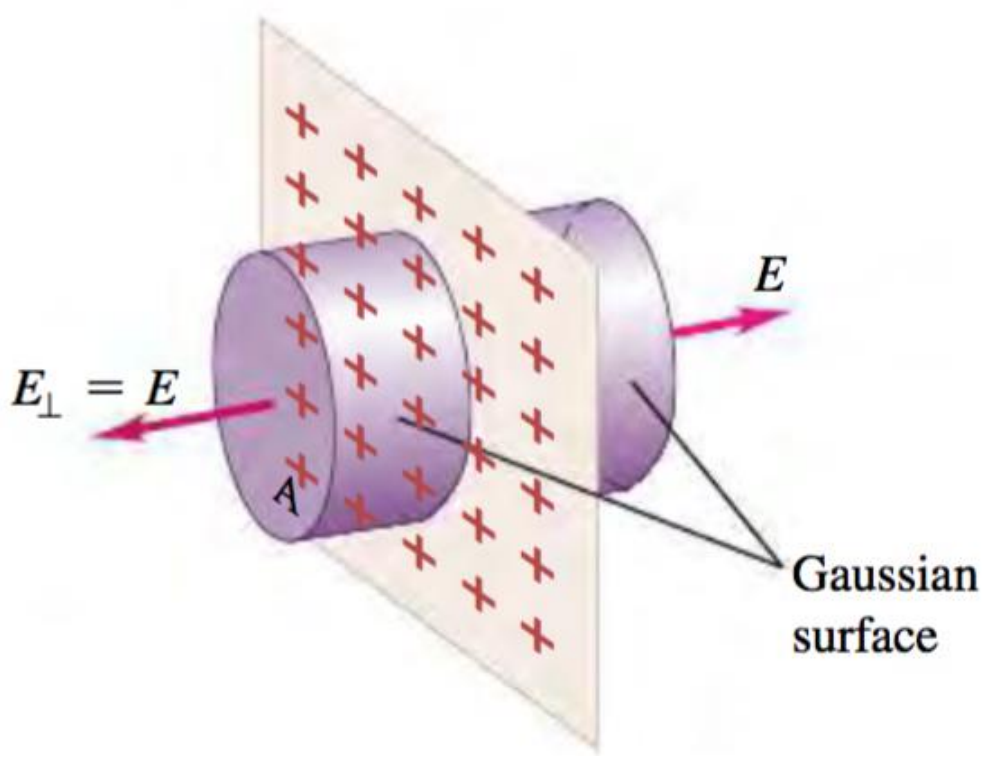

Figure 1- Image of the electric field on an infinite charge [33]

A simplified formula to explain the electric field due to the sheet charge, while conforming to Gauss's law for a cylinder is

$$E = \frac{\sigma}{2\varepsilon} \quad (3)$$

10.1.5 Electric field for parallel planes

The second of the two instruments described in this work measures ionic flow past two parallel plates. For parallel plates of opposite charge, assuming that there are no electric fields within the two conductors, the electric field strength will carry equal but opposite uniform charge densities. This means that the electric fields formed, superposed by each plane is simply a uniform field directed from the positive plate to the negative plate. The electric field form is then

$$E = \frac{\sigma}{\varepsilon} \tag{4}$$

10.1.6 Voltage generated by parallel electrostatic field plates

As stated earlier, the Electric field is defined as Force per unit Charge and it is known from conventional physics knowledge that Work is done by overcoming the force over a certain displacement;

$$W = Fd \tag{5}$$

Where d is displacement.
Introducing this to the Electric field equation then gives;

$$Ed = \frac{Fd}{q} \tag{6}$$

Or

$$Ed = \frac{W}{q} \tag{7}$$

Energy is required to move a charged object between two points in an electric field. The total potential difference, ΔV is then a byproduct caused when work is done per unit charge, to move the charge across an electric field;

$$\Delta V = Ed \tag{8}$$

10.1.7 The effect of Electric force on the motion of atoms

Electrical mobility is a phenomenon where charged particles move through a medium,

either gas or liquid (electrophoresis) under the influence of an Electrical field.
For a particle with net zero charge, this is also called “ion mobility” and can be described as the velocity attained by an ion under an electric field.
When a test charge exists anywhere between two parallel plates exhibiting an electrostatic field, the net force acting on it will always be equal. This is due to the repulsion forces from the one plate will diminish as the test charge moves from one plate to another, however simultaneously the attraction force will increase and the net force is always conserved.
Manipulating the electric formula will give

$$F = qE \tag{9}$$

The acceleration due to force can then be appropriated by

$$F = ma \tag{10}$$

$$a = \frac{F}{m} \tag{11}$$

$$a = \frac{qE}{m} \tag{12}$$

Where q is the charge, E is the electric field, m is mass of the charge and a is acceleration.
As the force is constant throughout the electrostatic field, it can also be assumed that velocity of the charge throughout the parallel plates will be constant. This means by using suvat equations will give;

$$v = u + at \tag{13}$$

Where v is the final velocity, u is the initial velocity, a is acceleration, and t is time.
However as time is an irrelevant factor in this analysis, an alternative form of is taken using kinematic equations

$$v^2 = u^2 + 2\,ad \tag{14}$$

If it is assumed that the charge moves from rest, the initial velocity, u, can then be set to 0 or just ignored. Velocity of a charged particle travelling through a uniform electrostatic field

can then be described by the equation

$$v = \sqrt{2\frac{qE}{m}d} \tag{15}$$

Equation (11) could be used to estimate the transit times of ions through gels used in the instruments described in this work. The transit times allow different ionic species to be differentiated on the basis of their mass charge ratio (q/m). However, there is expected to be a constant retarding force on the ions, produced by the gel through which they pass. Consequently, we rely on experimental results for the exact transit times.

10.2 Gel Electrophoresis

Gel electrophoresis is the technique used to separate DNA, RNA and protein fragments according to their molecular size. DNA samples are placed in wells at one end of a gel and an electrical field is applied using a power supply that will draw them from one end of the well to the other. This is because these particles are negatively charged and the electric field from the positive end of the gel will attract the particles through the gel. Larger DNA fragments or strands move slower compared to smaller strands, allowing for a separation of these strands according to size.

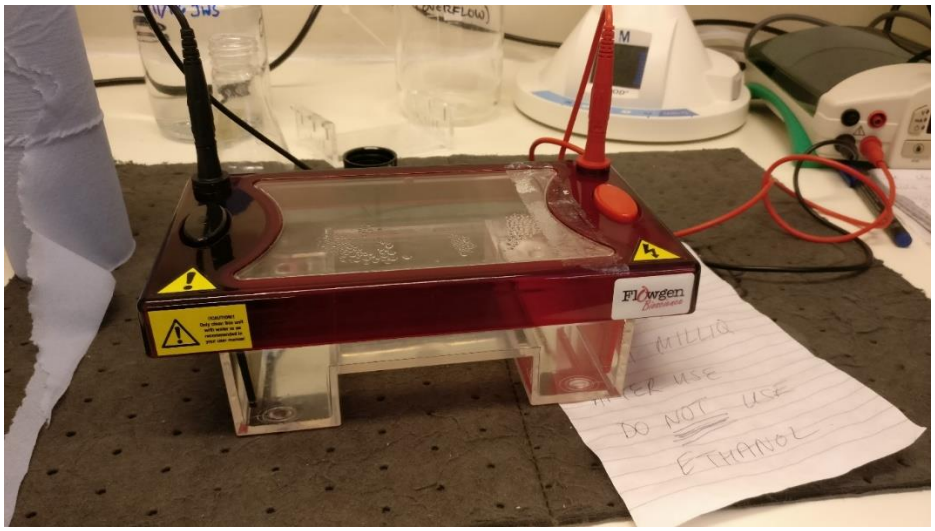

Figure 2 - Gel electrophoresis machine

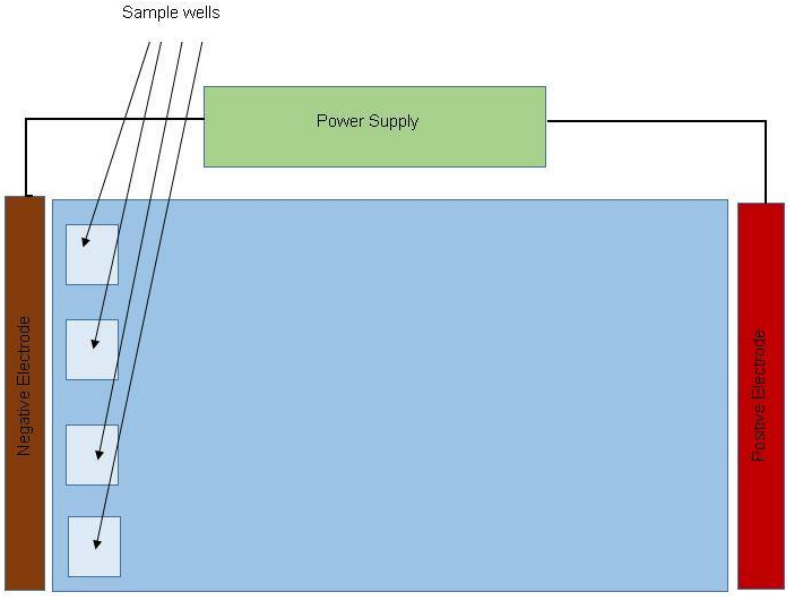

Figure 3 - Schematic of a gel electrophoresis machine

10.2.1 Mediums in Gel Electrophoresis.

The primary medium used in gel electrophoresis is the gel itself. The purpose of the gel is to prevent thermal convection of molecules when applied with electrical fields and as to reduce the motion of molecules through the gel. The primary gel used in electrophoresis, as well the only gel used in this study is agarose. Agarose exists in powder form and must be mixed with water and heated before the gel can be formed.
A buffer is also used in the preparation of gels. The purpose of a buffer solution is to act as an ion carrier to assist in the mobility of ions through the gel. However, due to the scale and size of the experiments run in this study, the effect of electrophoresis without the use of buffer solutions is conducted.

10.2.2 Visualisation in Electrophoresis

In order for individual DNA strands to be visualised, the gel must be stained with a dye or stains. The most common stain used in laboratory experimentation are fluorescent DNA stains that use an ultraviolet light source to detect and visualise DNA fragments [34]. Under UV light, the DNA strands will begin to glow and DNA bands will be separated by size as larger fragments will move slower than smaller strands. The brighter the strands under light also correlates to the amount of strands with the same size.

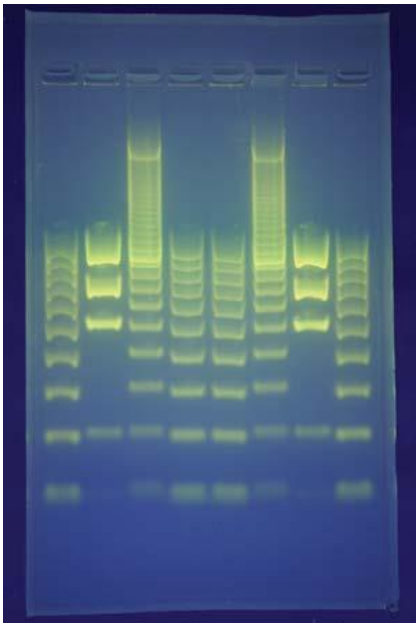

Figure 4 - DNA strands separated by size [35]

10.3 Capacitors and Dielectrics

A capacitor is a plate that has the ability to store charge. Capacitors usually consist of two terminals that are separated by a dielectric material or medium such as glass, air or distilled water. Dielectrics are simply substances that are poor conductors of electricity. Dielectrics usually consist of dipoles that are only polarized when an electrostatic field is present. The model that best represents dielectric is that it is a “dipole” containing both positive and negative charges. These charges will stretch out according to its polarity, with the positive charges attracted to the negative plate and vice versa.
When a dielectric is placed inbetween two conducting plates, this will reduce the amount of voltage across the plates as the voltages are negated by the presence of non-conducting atoms of the dielectric material and also because electric charges do not flow through dielectric materials. This is because the dielectric becomes polarized in the presence of an electric field. The dielectric material however does re-orient their positions through a process called dielectric polarization. This increases the capacitance of the capacitor as the relationship between voltage and capacitor is such that a decrease of voltage correlates to an increase of capacitance.

$$C = \frac{Q}{V} \tag{16}$$

This means that increasing the presence of conducting ions within the capacitor will not only reduce the capacitance, but increase the voltage reading across the capacitor as the ions causes more electrical charge to flow through the capacitor. This forms the basis of the measurement system used in this work.

10.3.1 Conclusion

To conclude, it is sufficed to say that the presence of dielectric material within a capacitor will cause voltage across the capacitor to drop. The presence of ions, for example Na^+, will cause more charge to be introduced into the capacitor and if a voltage reading was to be taken across the capacitor, the voltage will increase as a higher current is allowed to pass thorough the field.

10.4 Dielectrics in an alternating field

When a dielectric becomes polarized in an electrostatic field, altering the direction of the polarity will cause a certain delay, called “dielectric relaxation”. After overcoming this dielectric relaxation period, the dielectric will be repolarized according to the direction of the field.

The dielectric will require some time to readjust to the new polarity, called the “relaxation time”. This means that if the frequency of the alternation of Electrostatic fields is too high, the dipoles cannot keep up with the speed of repolarization, causing the overall dielectric constant to drop. This can be explained in the image;

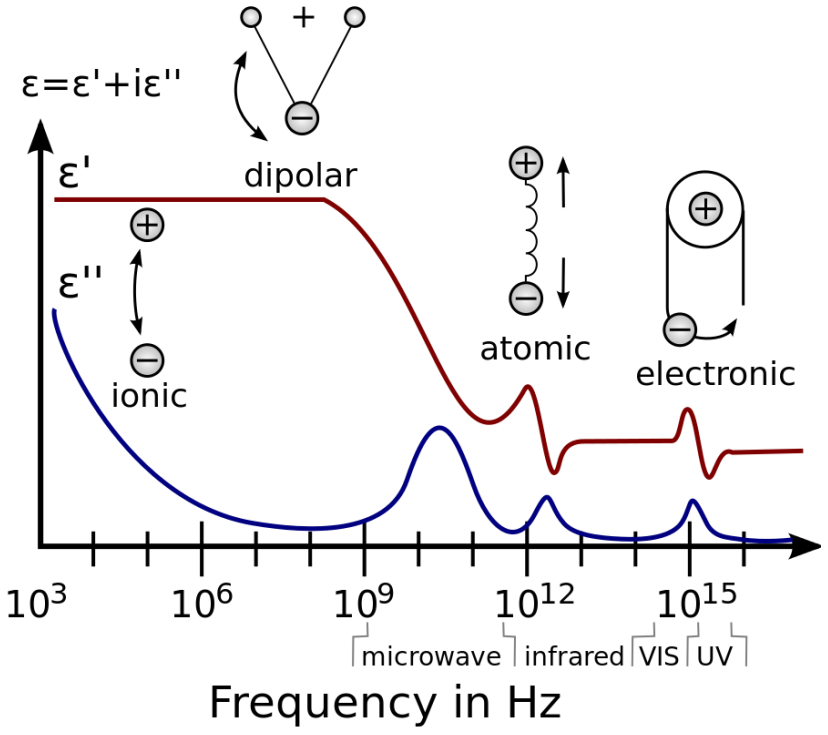

Figure 5 - Image showing the effect of dielectric constant over time[36]

Figure 5 above shows the drop of dielectric constant as the frequency of oscillating fields increase. Dielectric constant is simply another term to describe relative permittivity, which was the ratio of permittivity of a substance in relative to the permittivity of vacuum. The graph conveniently shows that at 1000 Hz, the dielectric constant is at the highest point,

meaning that the material has enough time to polarize due to the change of electrostatic field direction.

10.4.1 Conclusion

As the rate of alternating Electrostatic Fields increases, the ability of polarization of dielectric materials becomes increasingly more difficult. This means that when the sensor is activated a 1000 Hz frequency must be applied to the electrode to ensure peak dielectric permittivity. As the sensors used are basically capacitors, this can be applied to the sensors that will be manufactured in this experiment as both are capable of generating alternating Electrostatic Fields.

10.5 Theory conclusion

To finalize the discussion on theory, the basic concepts proposed for this experiment includes.

1) Using electrostatic fields to “push” the ionic substances through a medium
2) The medium used in this experiment is agarose gel, which is a common gel used in commercial gel electrophoresis
3) Detection of Ions using dielectric principles such as the manipulation of change of voltage generated across an alternating Electric field as highly conductive particles enter a region of high dielectric constant.
4) Measuring the change in voltage relative to the mass per charge ratio of ionic substances.
5) Ensuring 1000 Hz across the alternating field to ensure high dielectric constant.

11 Procedures

This section explains the variety of procedures involved in the creation of capacitive electrodes, the measurement techniques during experimental analysis and several other clean room and laboratory procedures carried throughout the course of the study.

11.1 Measurement Techniques

To ensure that the experimental setup will function as intended and provide accurate, consistent and repeatable data, several calibration methods and accuracy tests must be conducted. These tests are also conducted to determine whether the laboratory equipments used for providing the signal and also measuring data can be used in conjunction with the manufactured capacitors.

11.1.1 Equipment calibration

To generate the signal that would power the equipment, an AFG1062 Tektronix Arbitrary function generator was used. Before any calculations and experimental procedures are made, some exercises were carried out to familiarize and explore the functions of the signal generator.

A PDF could be downloaded online at the Tektronix website that acted as a datasheet containing a list of specifications, list of performance and features and a list of suitable applications. This device was used as it had the ability to run electrical and electronic experiments, simulate sensors and had an easy-to-use colour display system as well as a wide frequency and amplitude range.

The function generator has a built in “sweep” function that could sweep between a range of frequencies. Firstly, there were some modulation issues with this function as it was only able to start at a low frequency and increase itself over time, and then promptly reset. Increasing the sweep time would allow the prolonging of this process to allow the user to fine tune the rate of which results are captured on the oscilloscope. This is particularly useful as using an older oscilloscope means that at lower sweep times, the oscilloscope would have a harder time keeping up with the rate at which the sweep would output data onto the oscilloscope display.

There is also a logarithmic sweep function however there is no method of fine-tuning this control to allow for manual control over the rates at which certain frequency ranges are displayed.

11.1.2 Equipment accuracy

A simple setup was constructed in order to verify the accuracy of the oscilloscope, or rather how theoretical values would differ from measured values in simple electrical systems.

11.1.2.1 Using traditional voltage divider equations

A potential divider circuit consisting of two capacitors in series was installed on a breadboard and was driven with 1V peak to peak from the function generator. A lead was placed in between the capacitors and the voltage was measured.
At 1V peak to peak, the measured output was 300mV and at 2V peak to peak the measured voltage was 592mV. For both measurements the frequency was at 1000Hz. When reduced to 500Hz the new readings were measured at 196mV output for a 1V peak to peak input and when frequency was increased to 5000Hz, the output was measured at 396mV.
The Capacitive Voltage Divider equations can be used to verify the accuracy of these measurements.

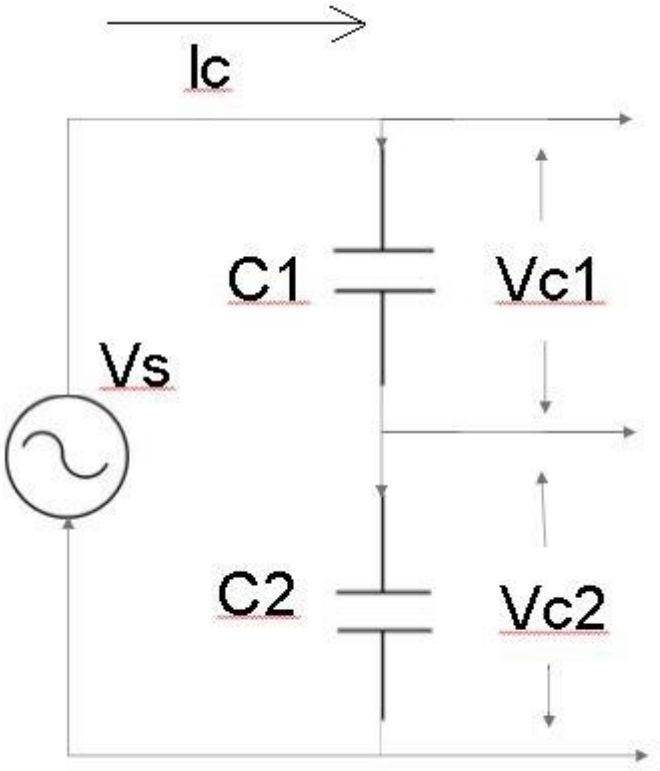

Figure 6 - Image shows a basic capacitve voltage divider circuit

Using Figure 6 as a guide, using the parameters below;

Vs – 1V

C1 & C2 – 33pF or $33x10^{-12}$

f - 1000 Hz

the formula that can be used is then;

$$X_{c1} = \frac{1}{2\pi f C} = \frac{1}{2\pi \times 1000 \times 33 \times 10^{-12}} = 4.823M\Omega \quad (17)$$

Similarly to find X_{C2}

$$X_{c2} = \frac{1}{2\pi f C} = \frac{1}{2\pi \times 1000 \times 33 \times 10^{-12}} = 4.823M\Omega \quad (18)$$

Then using the voltage divider equation to find the appropriate voltage V_{c2} the voltage across the second capacitor can be found as

$$V_{c2} = \frac{V_s \times X_{c2}}{X_{c2} + X_{c1}} \quad (19)$$

$$V_{c2} = \frac{1 \times (4.823 \times 10^6)}{\left((4.823 \times 10^6) + (4.823 \times 10^6)\right)} = 500mv \quad (20)$$

As the measured voltage is 300mV, there is definitely some voltage loss or inaccuracy in the setup. Following the change of voltage in the second set of measurements. The new parameters are below;

Vs – 2V

C1 & C2 – 33pF or $33x10^{-12}$

f - 1000 Hz

using the established reactance X values into the voltage divider equation;

$$V_{c2} = \frac{V_s \times X_{c2}}{X_{c2} + X_{c1}} \quad (21)$$

$$V_{c2} = \frac{2 \times (4.823 \times 10^6)}{\left((4.823 \times 10^6) + (4.823 \times 10^6)\right)} = 1V \quad (22)$$

Now with the increased supply voltage the recorded measurement is further away from the theoretical calculated value. To further see how varying the frequency would affect the accuracy of the measured voltages, the theoretical voltage values are then recalculated

with the established parameters listed below;

Vs – 1V

C1 & C2 – 33pF or $33x10^{-12}$

f1 - 500 Hz

f2 – 5000 Hz

At f1, the impedance values are calculated to be;

$$X_{c1} = X_{c2} = \frac{1}{2\pi f_1 C} = \frac{1}{2\pi \times 500 \times 33 \times 10^{-12}} = 9.646M\Omega \quad (23)$$

And to find the voltage across the second capacitor

$$V_{c2} = \frac{V_s \times X_{c2}}{X_{c2} + X_{c1}} \quad (24)$$

$$V_{c2} = \frac{1 \times (9.646 \times 10^6)}{\left((9.646 \times 10^6) + (9.646 \times 10^6)\right)} = 500mV \quad (25)$$

And at f2, the impedance values are calculated to be

$$X_{c1} = X_{c2} = \frac{1}{2\pi f_2 C} = \frac{1}{2\pi \times 5000 \times 33 \times 10^{-12}} = 0.965M\Omega \quad (26)$$

Finding the voltage at the second capacitor will give;

$$V_{c2} = \frac{V_s \times X_{c2}}{X_{c2} + X_{c1}} \quad (27)$$

$$V_{c2} = \frac{1 \times (9.646 \times 10^5)}{\left((9.646 \times 10^5) + (9.646 \times 10^5)\right)} = 500mF \quad (28)$$

To summarize the results

At 500Hz, 1 volt peak to peak the measured output is 196mV and calculated theoretical output is 500mV

And

At 5000Hz, 1 volt peak to peak the measured output is 396mV and calculated theoretical output is 500mV.

It can be concluded then this method of calculation and comparing the measured to

theoretical values are inconclusive and has a pattern of deviation away from the measured values according to the peak to peak and frequency changes.
To ratify this, an alternate method of calculating the theoretical output is conceived to determine whether these inaccuracies are part of the intrinsic properties of the circuit or whether some mathematical error is present.

11.1.2.2 Alternative current measurement

With the calculated values for each of the parameters in the section above, the values for current can then be found.
Using the values for the first set of parameters
Vs – 1V
C1 & C2 – 33pF or $33x10^{-12}$
f - 1000 Hz
X_{c1} & X_{c2} – 4.832MΩ
The total capacitive reactance is then

$$X_{total} = X_{c1} + X_{c2} \tag{29}$$

$$X_{total} = (4.832 \times 10^6) + (4.832 \times 10^6)$$
$$X_{total} = 9.664 \times 10^6$$

Then finding the overall circuit current would be

$$I = \frac{V_s}{X_{total}} \tag{30}$$

$$I = \frac{1}{9.664 \times 10^6}$$
$$I = 1.035 \times 10^{-7}$$

Now using the established current value, the value for voltage for the potential divider is then

$$V_{c2} = I \times X_{c2} \tag{31}$$

$$V_{c2} = 1.035 \times 10^{-7} \times 4.832 \times 10^6$$

$$V_{c2} = 0.5V$$

This value shows no difference between the first calculated theoretical values, meaning that the other values will probably not differ from earlier calculations thus implying that

there is a parameter within the calculations that have not been taken into account, the internal impedance of the oscilloscope.

11.1.2.3 Internal impedance.

For most oscilloscopes, there is a fixed input impedance value at around 1MΩ. The current equations can be modified to allow for the new values of the output voltage across the second capacitor C_2.

The new circuit diagram, now taking into account the internal impedance of the oscilloscope is

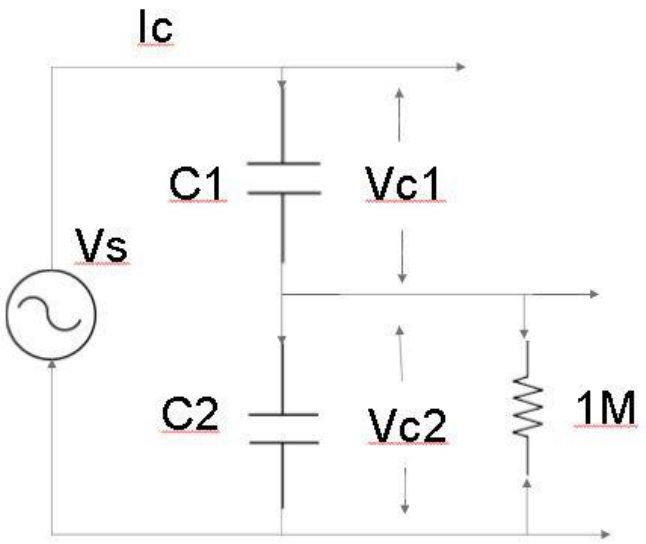

Figure 7 - Schematic diagram of the source voltage

Assuming the above calculations for C1 and C2 and their impedance values are correct, the voltage divider formula can then be used to find the value for voltage across the 1MΩ resistor.

The new equation to find the new Vout, which is the voltage across the 1MΩ resistor is

$$V_{out} = \frac{X_{c2} \,//1 \times 10^6}{(X_{c1} + (X_{c2}//1 \times 10^6))} \times V_s$$

Where

$$X_{c2} \,//1 \times 10^6 = \frac{X_{c2} \times (1 \times 10^6)}{X_{c2} + (1 \times 10^6)}$$

Now using the parameters,

Vs – 1v

C1 & C2 – 33pF or $33x10^{-12}$

f - 1000 Hz

X_{c1} & X_{c2} – 4.832MΩ

$$V_{out} = \frac{4.832 \times 10^6 \,//\, 1 \times 10^6}{(4.832 \times 10^6 + (4.832 \times 10^6 // 1 \times 10^6))} \times 1$$

$$V_{out} = 0.146V$$

A peculiar thing to note is that the calculated theoretical value is half of the measured value. This can be explained from the fact that the signal generator too has its own characteristic internal impedance. This means that the voltage from the signal generator may differ from the programmed input voltage.
This can be explained in a simple diagram;

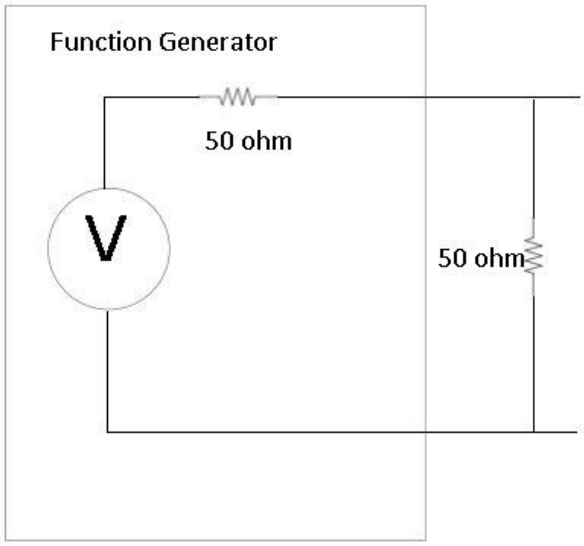

Figure 8 - Schematic diagram of the function generator termination

This shows that the function generator has a built in 50ohm internal impedance with a terminated 50ohm load. Most function generators are designed to function in such a way and therefore when a typically high input impedance oscilloscope is used to display measurements, this value will then double the input voltage from the function generator. To ratify this, some oscilloscopes are able to change their input impedances to 50ohms. Alternatively, a 50ohm resistor can be added to the end of the coaxial cable that is fed into the oscilloscope.

11.1.3 Conclusion

Considering the circuits designed above were not terminated with a 50ohm load, the results that were measured were twice the calculated values. However, since the measurements in future experiments will be relative to their input values, this may not negatively impact the results as the results do not necessarily have to be accurate as long

as the methods are consistently applied to all experiments.

11.2 Agarose solution preparation for electrophoresis experiments

The agarose powder used throughout the course of the study is “Agarose, Molecular Biology Grade” by Melford.

The concentration of agarose gel used for the majority of the experiments conducted are at 1%. To achieve this, an amount of de-ionized water is placed into a beaker and the mass of the water is measured using a digital weighing scale. Small amounts of agarose powder is added into the beaker until a mix of 99:1 is achieved.

In Gel electrophoresis, a buffer known as TAE or Tris Acetate-EDTA Buffer is used as a working solution, however the simplicity of the experiments conducted allow for de-ionized water to replace the buffer solution. TAE buffer solution helps improve the mobility of DNA samples within the agarose gel and improves the separation of DNA strands. However this separation assistance is unnecessary if the sample used only has a simple chemical composition. For example, the analyte used in majority of the preliminary studies is salt, containing Na (sodium) and Cl (chloride) ions, each with one positive and negative charge respectively, which means only one element is analysed at a particular instance. As the solutions measured increase in complexity, TAE buffer may be used, however as the method used of detecting ionic transfer is a mathematical model and not visual, it may still be unnecessary to us the buffer solution. Further studies may be carried out to determine the viability of TAE buffer solution later on, and how using de-ionized water negatively impacts the results of the experiments.

As the powder is added into the beaker of water, it will settle to the bottom of the beaker. For the gel to fully form, the beaker must first be introduced to some heat. A hot plate is heated up to 150 degrees Celsius and the beaker is placed on the top of the heating element. The mixture is first stirred to prevent the powder from clumping and ensure equal distribution throughout the liquid. This is then done periodically as the solution gets hotter to ensure heat is linear throughout the liquid and to further spread the agarose powder. At higher temperatures the powder will begin to fully dissolve in the de-ionized water and will turn the powder white solution clear. A sheet of aluminium is used to cover the opening of the beaker to prevent the de-ionized water from evaporating and affecting the concentration of the agarose solution.

After the powder has fully dissolved, the hotplate is turned down to around 60 degrees celcius to allow the mixture to cool slightly. A thermometer is placed in the beaker to ensure the solution remains at around 60 degrees as the solution may harden to form a

gel at lower temperatures. If this does happen, the mixture may be stirred and the hotplate temperature should be increased slightly.

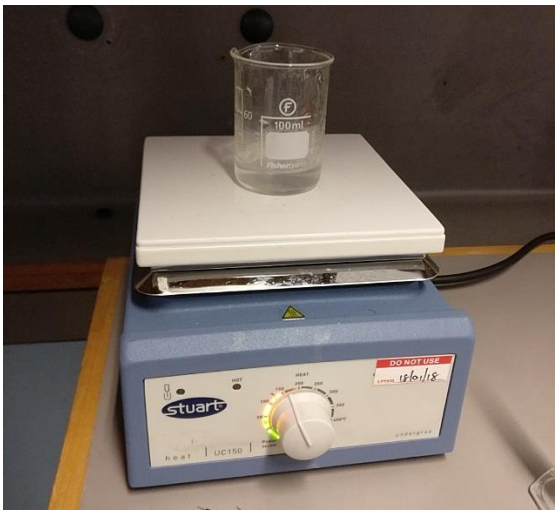

Figure 9 - Image shows a beaker of molten agarose solution

Figure 9 shows the clear solution formed by heating the agarose powder and de-ionized water mix after being heated at 150 degrees Celsius for around 20 minutes. There are no longer any powdered remains from the agarose powder and the water is clear.

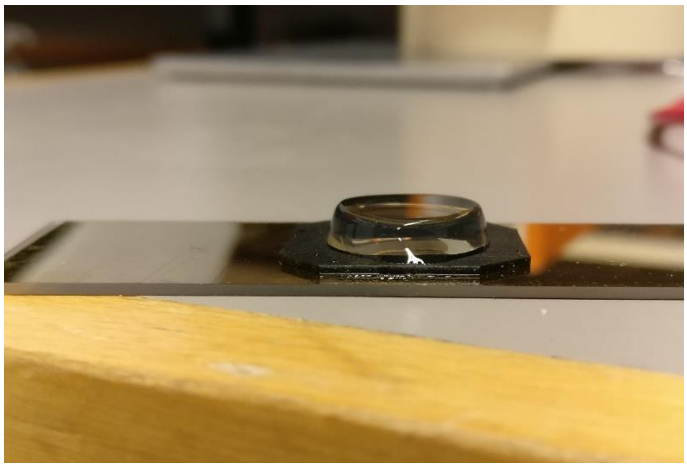

Figure 10 - an imperfect gel mixture

Figure 10 above shows the result of inadequate mixture of DI-water to agarose. The gel does not hold its shape well at all as a result of too little agarose powder used.

11.3 Feasibility Study

Feasibility studies are done as simple introductory experiments to verify the viability of certain resource intensive procedures. These are usually simplified variants of these

studies and help provide the basis of understanding of core principles revolved around them. The procedures for feasibility studies differ from experiment to experiment and therefore each section in the document will have its own procedure on how they are carried out and the underlying theory that will support the results. Therefore feasibility studies act as a bridge between the underlying theory and the primary experimental procedure, explaining the thought process that goes into why the experiment is carried out in the first place, in its most basic form.

11.4 Hardware creation – Sensor Enclosure

The metal enclosure that supports the majority of the transducer is 18.8cm in length, 12cm in width and 7.6cm in height.

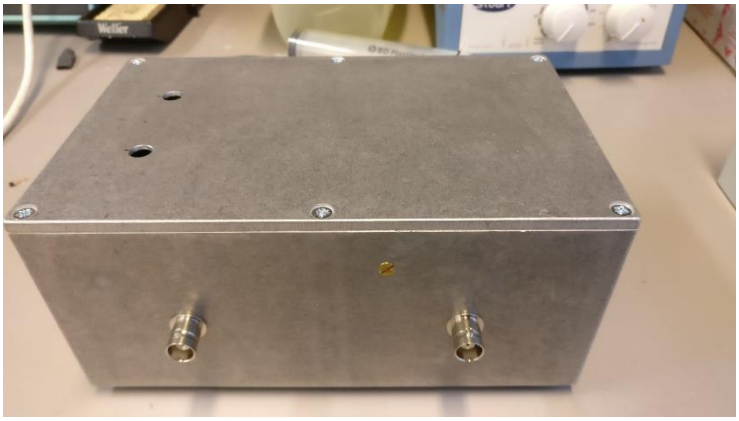

Figure 11 - The metal enclosure used as a sensor holder

Two holes were drilled in the front as shown in Figure 11 so that BNC connector points could be inserted and used to make a connection to and from the oscilloscope and signal generator. There are six screws on top of the box so that the lid may be placed on top to seal the enclosure. On the bottom there are 4 rubber stops to ensure that the sensor enclosure does not move about when experiments are conducted.
The enclosure also prevents electrical inteferences such as noise from affecting the results of the experiments.

11.5 Water Bath

The diffusion rate of ions through the gel is temperature dependent. Control of gel temperature is therefore vital for accurate results. In the laboratory where most experiments are conducted, there is a water bath present which provides a way of keeping laboratory solvents at a constant temperature. The bath contains a thermostat that constantly measures liquid temperature within its container.

Placing the agarose solution within a beaker and into the water bath ensures the agarose solution is always in its molten form by providing accurate amount of heat. The main benefit of using a water bath is the equal distribution of heat throughout the surface area of the beaker that holds the agarose as placing a beaker directly on a hot plate will mean that the majority of the heat is focussed on the bottom of the beaker and the solution must be continuously stirred. However the water bath takes a while to reach the desired temperature therefore it is advised to heat initially with a hot plate, and then the agarose solution can be placed in the water bath for later use. This is especially useful if multiple experiments using agarose solution is conducted on the same day.

11.6 Mask Preparation

This section outlines the steps in order to create the functioning electrode capacitors used in the first part of the experimental phase, outlining how the electrodes are first drawn on a computer aided design software, printing and assembly of the mask, preparation of the substrate and growth of the electrode array onto the substrate. The aim is to produce electrodes with a large active area between the electrodes so as to produce a compact, but sensitive, electrode design.

11.6.1 Computer Aided Design of Electrode Capacitors

Masks are required for the photolithographic process. The concept of the mask is first hand-drawn and once the dimensions and basic shape have been established, the outlines for the design can be transferred to the CAD software. There are three different primary arrangements for each of the electrode arrays, two array electrode, three array electrode and four array electrode, and for each array there are two thickness and separation parameters. For each arrangement, several loops are drawn of equal thickness and gap width, these are made wider for the electrodes that have thicker arrays and wider gaps. As the thicker electrodes have a higher volume, this means that the number of individual loops are reduced so that they may fit the parameters of the sensor holder. Once the loops are drawn, connective lines are drawn in so that “cutting” excess portions of the loop can form the gaps.

The basic loops can then be colour coded individually to correspond to which electrode array they belong to. For example, the positive lead of a two array electrode system will be in red, the negative lead will be in black, and the gap is left in white. This will make it easier to determine if any mistake has been made during the process and to ensure that loops are uniform in arrangement. If done correctly, using the fill colour function of autocad will fill in individual loops with each of the corresponding colour for each loop

separately.
Finally for each electrode, depending on the number of arrays, are then connected by a series of squares and rectangles on each corner following the dimensions of a glass slide. The colours of each loop are filled in black as a final measure to allow for them to be printed on acetate paper.

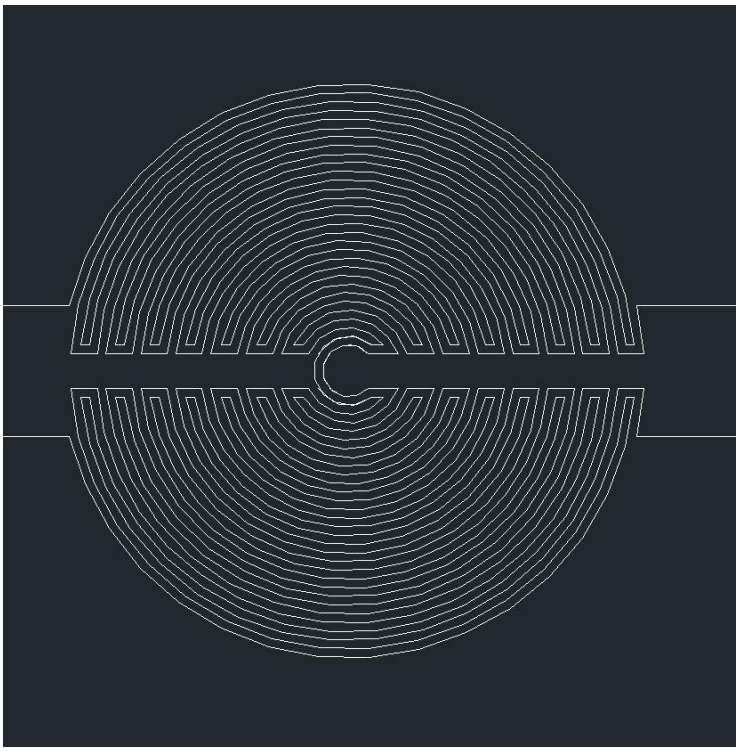

Figure 12 - image of two array electrode

Figure 12 shows the interdigitating nature of two-contact electrode in the spiral formation. Both contacts then form a narrower primary lead and meet in the centre, with the right contact ending a circular fashion and the left contact surrounding the right central contact in a pincer-like shape. The two narrow central-reaching contacts then form additional circular fingers that loop semi-circularly one after another in an “interdigitated” fashion, with a small 100 micro-meter gap in between them.

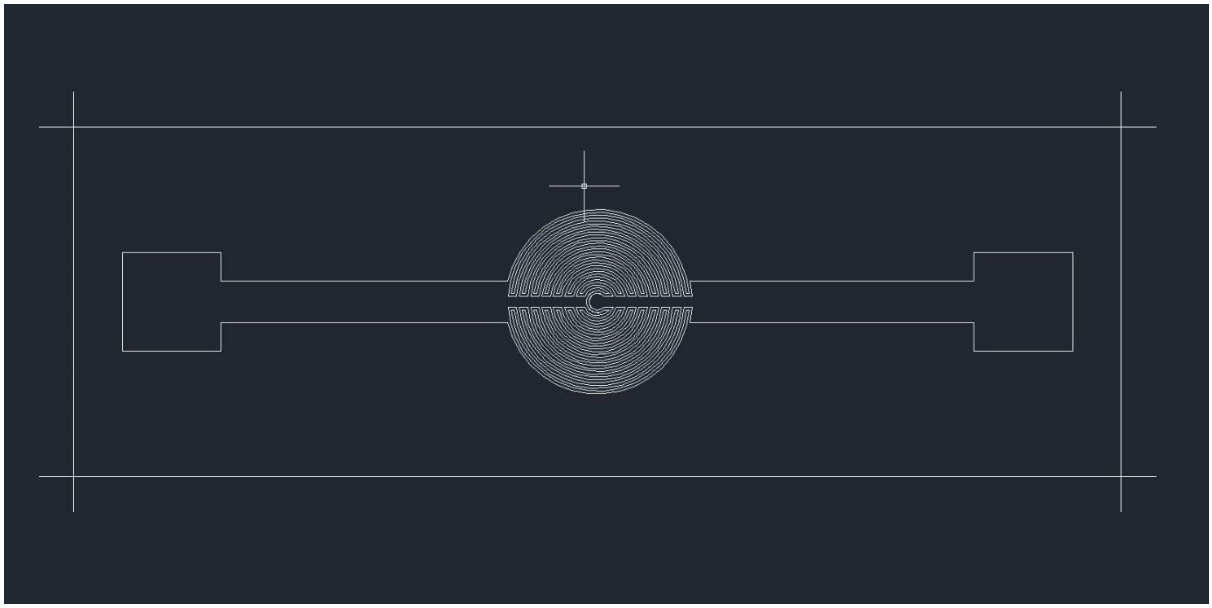

Figure 13 - two array electrode with contact areas

In this slightly zoomed out image shown in Figure 13, it can be seen clearly that the contacts on both side get narrower at least twice in order to form the central sensing area. The widest regions on each extremity of the slide is to enable a large contact region for the metal push-pins to connect to the electrode.

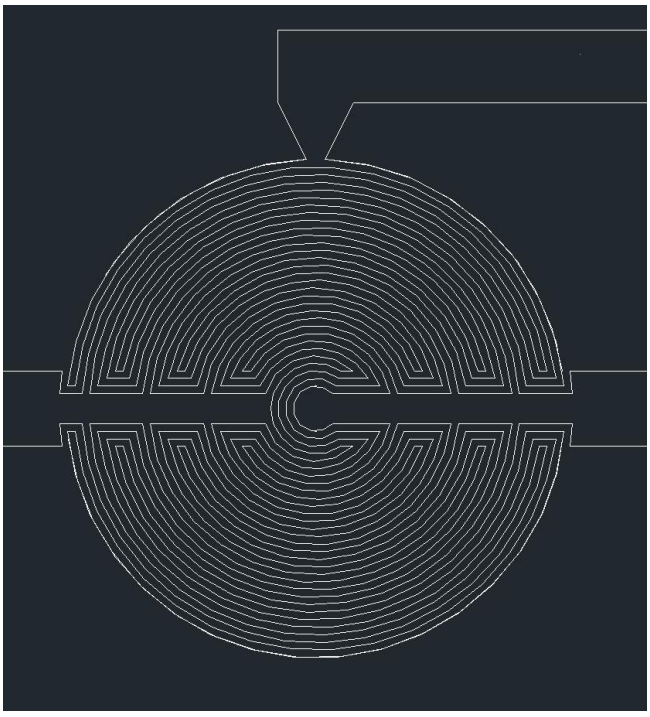

Figure 14 - Image of three array electrode

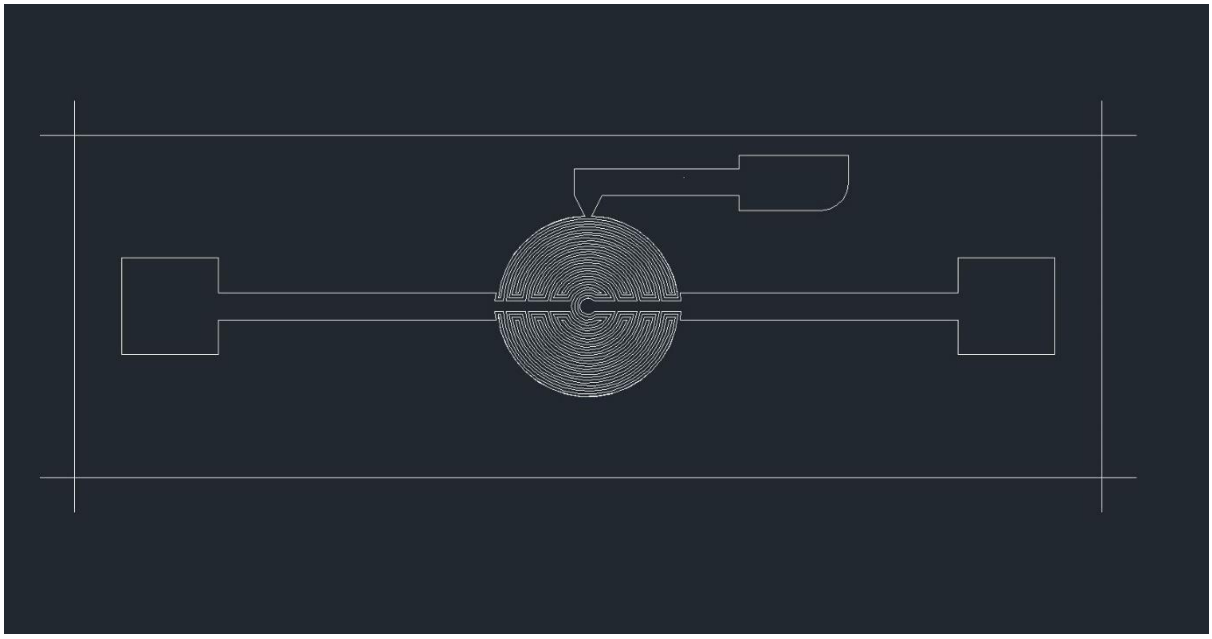

Figure 15 - three array electrode with contacts

Figure 14 and the wider view image of Figure 15 show that the third primary contact region, also known as the auxiliary electrode. This third contact is placed slightly off-centre but also away from the rightmost contact region. This is to ensure that the fields generated or the current flowing through those regions do not counteract with each other, thus a significant space is needed between them to ensure that any disturbances do not occur.

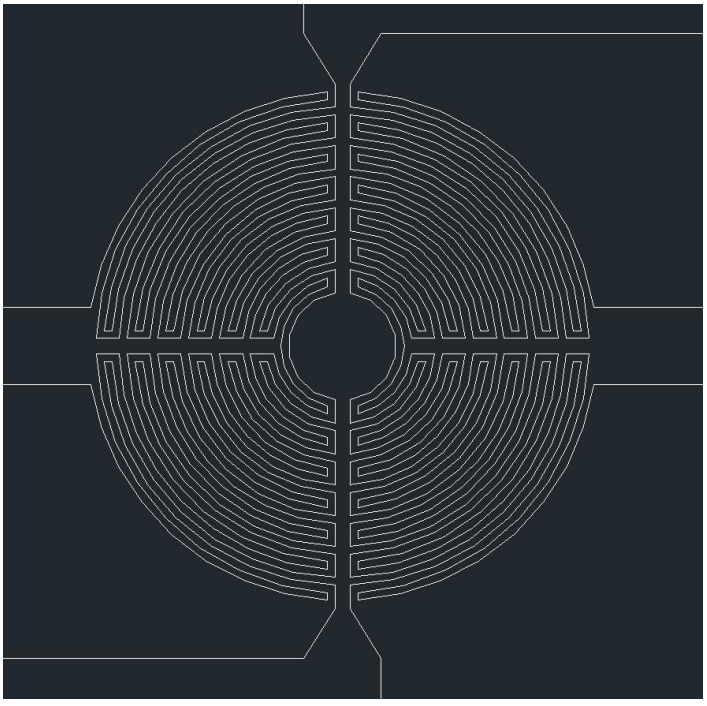

Figure 16 - four array electrode

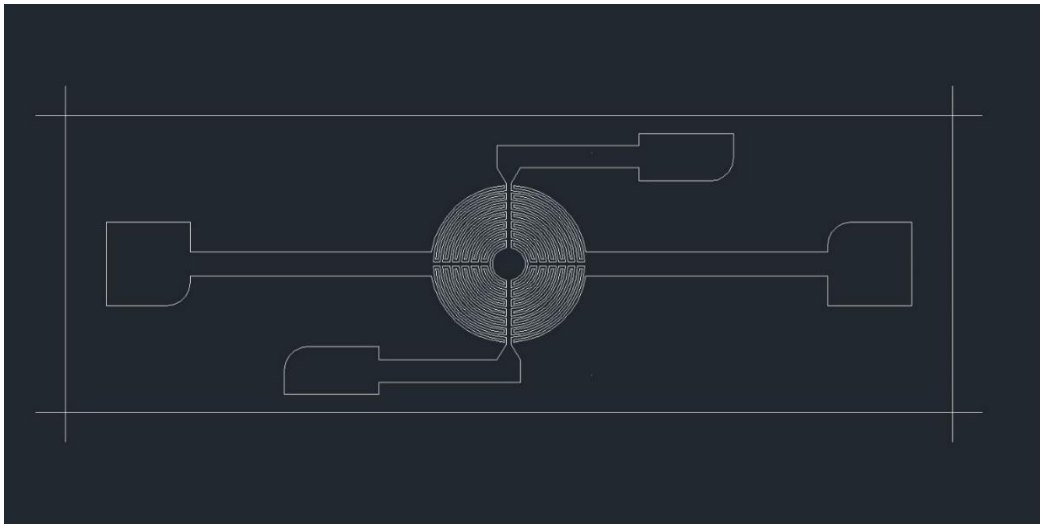

Figure 17- four array electrode with contacts

The four array electrode in Figure 16 and 17 also follows the same design as the three array electrode in design, mirroring the position of the third and fourth contact regions to create an additional contact point. This means that a combination of any two electrodes in a subset may contain a dielectric area as all four arrays are interdigitated in some way.

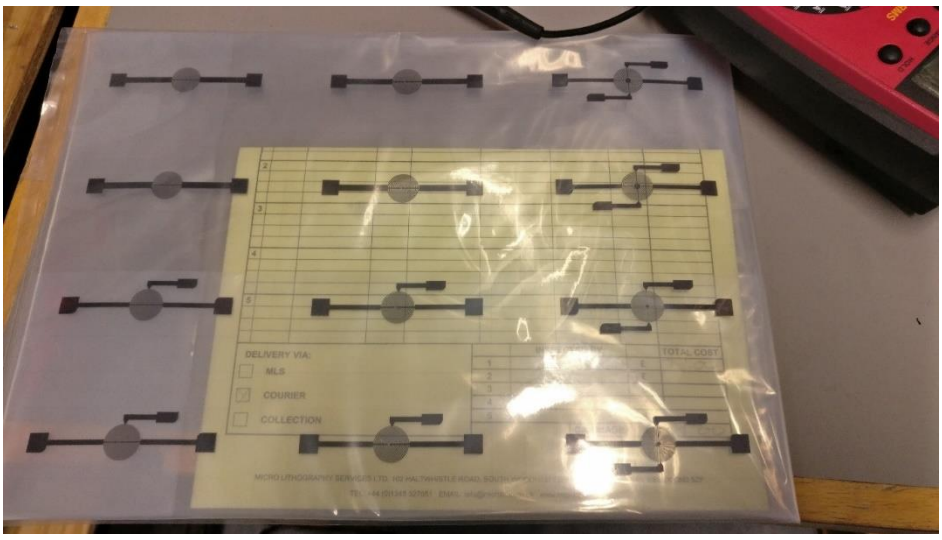

Figure 18 - The completed capacitors as they are printed on acetate paper

The complete capacitors were then sent to be printed on acetate paper. The grid design of the acetate paper meant that it could be cut easily using a pair of scissors to separate the shapes that are intended to be used.

11.6.2 Acetate to glass attachment

The final process in the creation of the mask is placing individual electrode patterns from the printed acetate paper onto individual glass plates. A large plate of 2mm thickness

glass is cut into 100mm by 100 mm squares. This is done at the local glass cutters. The individual acetate electrode patterns are carefully cut following the lines that have been printed on them.
To help align the mask directly onto the centre of the glass plate, guidance lines are drawn in the dimensions of the acetate mask to indicate where the acetate sheets should be placed.
Glue is used to attach the acetate paper onto the glass plate. To do this, a small amount of glue is placed on an unused glass slide and a sharp object is used to apply small dabs of glue onto undrawn areas on the side of the glass, where the pattern would not be affected if smudging occurs. Only a small amount of well placed glue dots are needed to stick the acetate on the glass plate. Using too much will cause glue blobs to expand beneath the acetate and may cross paths with the pattern and influence the outcome of future procedures such as mask aligning and mask pattern deposition.
When placing the acetate onto the glass, a clean pair of tweezers are used as using fingers may attract dirt or grease to the bottom of the acetate mask, in the space between the acetate and glass surface top. The mask is placed face up on the glass plate and firmly spread to avoid air bubbles forming beneath the surface.

11.6.3 Optical Inspection

The mask can then be placed under the optical microscope for inspection. The bottom of the glass plate is first cleaned through vapour degrease before viewed. This is just a precautionary measure to ensure any dirt is not from the glass plate itself.
Since only a few masks were chosen for initial experimentations, only they are viewed under the optical microscope and seem to show reasonable cleanliness.

11.7 Slide Preparation

The electrodes are fabricated on 3 inch by 1 inch microscope slides. The slides must be appropriately prepared before any fabrication can take place. This means that the slides must go through a cleaning process to ensure the surface is free of dirt, grease and other impurities. Depending on the dimensions of the pattern that would be created on the slide, they may be scribed and cut to the appropriate size and shape. However, for the experiments conducted in this study, the full geometry of a microscope slide will be used.
A glass slide that is used as a base for micro or nanofabricated structures are called “substrates”. Aside from glass, other examples of substrates used in nanotechnology include silicon[37], aluminium [38], sapphire [39], germanium [40] and gallium arsenide[41]

11.7.1 Cleaning

Unless scribed or cut first, the cleaning of substrate slides is the first step in the substrate creation process. Thermal deposition or any other means of nanofabrication onto a dirty substrate base will cause many problems for the user later on so it is absolutely paramount for the glass slide to be clean before carrying on with any further processes. A dirty substrate layer will cause any fabricated structures to form over the dirt and grease particles and may either form breakages in the structures or may even cause clumping of photoresist near the dirt particles, causing uneven spread of photoresist.
The most basic cleaning procedure involves cleaning any surfaces with diluted RBS solution and then a 10 minute ultrasonic bath to remove any further dirt.
The required amount of glass slides are placed in air tight bags and filled with RBS solution and diluted with de-ionized water. The surface is agitated slightly by moving the glass slides within the bag gently with the fingers and then the entire bag is placed in a filled ultrasonic bath. It is advised to not overfill the bags with slides as the constant agitation within the bath may cause the glass slides to create friction with one another and develop scratches.
This process can be done as many times as necessary to ensure peak cleanliness. In addition to the substrate, any glass beakers or tweezers can undergo this process of cleaning simultaneously to save time.

11.7.2 Vapour Degrease

Vapour degreasing is a standard cleaning procedure involved in the majority of Nanofabricated structures. As most of the structures created in the clean room consist of micro or nanoscale components, the presence of dirt or grease may affect the functionality or even hinder the creation of these structures.
This process involves heating up solvents to near boiling point to be used in the cleansing of the surfaces of substrates such as glass slides and silicon wafers. The solvents used in the university clean room are Isopropyl Alcohol or IPA and Acetone, sometimes used together one after another. The vapour produced from the boiling of these solvents make contact with the surface of the substrate and condenses as the surface of the substrate tends to be cooler than the heated solvent. The produced vapour then melts or dissolves the impurities on the surface of the substrate.
The glass slides are held over beakers of lightly simmering IPA solvent and then acetone with a pair of tweezers. As the glass are placed at a downward angle over the boiling solvents, the surface of the slide begins to “sweat” causing condensation to run through

the surface and drip to the bottom. This condensation due to the vapours from the solvent will carry any grease particles with them that run through to the bottom of the slide.
The slides are then dried by using a nitrogen gun that displaces any leftover condensation on the surface and can be collected with a clean piece of cleanroom paper. Cleanroom paper are fibreless and therefore will not contaminate the surface of the glass substrates.

11.7.3 Piranha Cleaning

Piranha cleaning is the method of using a mixture of one parts sulphuric acid and hydrogen peroxide to rid surfaces, such as glass, silicon wafers and homemade electronic circuit boards of organic contamination and metals. Alternative ratios of sulphuric acid to hydrogen peroxide may be 7 parts to 3 or 3:1. Piranha cleaning can also be used to clean photoresist residue, though it is advisable to follow photoresist cleaning procedures first else the piranhas etch will form an insoluble organic layer that cannot be removed.
Utmost care must be taken when preparing piranha solution. Ideally the solution must be mixed under an acid hood or laboratory bubble. The handler must be trained in the process of piranha cleaning and students must always be supervised. The user will have to be wearing appropriate gloves and goggles and the fumes must not be breathed in. Any glassware containing the piranha mixture must be pre-heated slightly before the mixture is added to prevent the glass from cracking or breaking entirely.
After the mixture is weighed and prepared, the sample is submerged within the solution and agitated slightly for around 15 minutes then removed carefully with tweezers.

11.8 Photolithography

This subsection delves into the photolithography process of metal evaporation, spin coating using a photoresist, imprinting the electrode mask using the mask aligner, chemical etching and removal of excess photoresist. These steps were done in the department clean room with high powered equipment with thoroughly planned steps and procedures.

11.8.1 Thin Film Metal Evaporation

A thin layer of gold is evaporated on to the surface of the glass slide. However a thin buffer layer of chromium is required between the glass slide and the gold to prevent the gold from peeling away from the glass.
The Bell Jar evaporator is used to deposit 20 nm layer of chromium on to the glass slides

and another 45nm layer of gold on top of that.
The steps to using a bell jar evaporator are as follows

1) The bell jar is pumped down or degassed to a 1μtorr internal pressure
2) The bell jar cover is removed and the samples are placed face down on the wafer holder
3) The metals needed are placed in the “boats” connected to the heating element of the evaporator
4) The bell jar cover and protective metal shielding is placed over the samples
5) The metals are then heated by increasing current supplied to the heating element until white hot.
6) When desired thickness of metal layers have been achieved, the bell jar is left to de-pressurised and the samples are removed.

11.8.2 Spin coating

Positive photoresist, a chemical used in engraving patterns onto a substrate, is thinly applied on to the glass slide by using a device capable of spinning the substrate in place. A positive photoresist is used as the mask patterns used are the desired pattern to be produced on the substrate.
The substrate is placed upon a central platform and a small amount of photoresist liquid is placed evenly throughout the substrate. There must not be any air bubbles during the liquid application as this may cause sputtering and uneven application of photoresist throughout the substrate.
After a few test spins are coordinated, preferably with a glass slide not intended to be used in the project/ a spare glass slide, the desired spin speed is noted. The speed of the spin may change depending on the thickness of the photoresist, as lighter liquid may require a slower spin speed and thicker, more viscous photoresist liquid may need to be spun faster.
All spun-coated substrates are then left to bake in a covered hot plate for around 1 minute at 115 degrees Celsius to harden the adhesion of the photoresist on the surface of the substrate.

11.8.3 Using the Mask Aligner

The mask aligner is a device responsible for projecting the pattern from the mask onto the substrate. This is done by shining ultraviolet onto the substrate, which will dissolve the photoresist not covered by the mask patterns. As the mask is designed specifically for the substrates used in the experiment, the mask can be used as it, as long as the geometrical

shapes are aligned in the centre of the substrates, according to the guidelines printed on the mask.
After the mask aligners warm-up sequence, the mask is placed, print side down, on the substrate and ultraviolet light is exposed on to the surface of the substrate for around 5-7 seconds. The substrates are then submerged in developer solution for around 40 minutes and dried thoroughly.

11.8.4 Chemical Etching

Chemical etching refers to the process of using chemicals to remove excess metals from the substrate. As the process of mask aligning allows the photoresist to conform to the geometry of the mask, the chemicals will etch around the photoresist-protected boundary of the pattern and remove the excess metals around the pattern. As the chemical etching process makes use of possibly hazardous chemical compounds, the measuring, weighing and mixing of these chemicals must be done under a laboratory bubble, where the fumes will not be breathed in, and gloves must be worn at all times.

The chemical etching process must begin in the order of most exposed metal, therefore the gold must first be etched out before the chrome under-layer can be etched. This process cannot be done simultaneously as the etches are not interchangeable and do not mix.
To etch the gold, a mixture of potassium granules, potassium iodide powder and deo-ionized water must be used. The proportions are roughly 83% water, 0.03% iodine granules and 13.77% potassium iodide powder. However as the gold chemical etch is reusable and there were some already in storage from a previous instance it was used, there was no need to make more. In order to etch through the 45nm layer of gold, the substrate needed to be immersed in the solution for around 2 minutes, while being agitated lightly.
After the gold has been etched and the excess chemical etch washed off the surface of the substrate using de-ionized water, the chrome etching process can begin.
To etch chrome, a mixture of DI-water, ceric ammonium nitrate and acetic acid is used. A beaker filled with DI water and part of the acetic acid, around 20% of the total acetic acid used. Then ceric ammonium nitrate solution is added until the mixture has a cloudy appearance, after which the remaining acetic acid is added. The final proportions of the chromium etch is 85% DI-water, 13% ceric ammonium nitrate and 2% acetic acid. The chromium etch chemical mixture has a light pink colour and substrates must be immersed for around 40seconds to 1 minute to fully etch the chromium layer.

11.8.5 Photoresist removal

The removal of photoresist is the final stage of the photolithography process. The substrates are viewed under the microscope to ensure that all the excess chrome and gold have been etched successfully.
The substrates are then immersed into a petri dish containing acetone for a few seconds until the photoresist has been removed. The substrate must then be rinsed, dried and viewed under the microscope to see if there are still any remaining photoresist on the electrode pattern. If there are some remaining photoresist, the substrate can be submerged again in acetone as needed until there are no longer any photoresist remaining. Any photoresist not interrupting the pattern on the substrate can be largely ignored as this will not affect the measurements conducted.
However it is unknown if the presence of photoresist on the electrode will negatively effect the outcome of the experiments. It is even theorized that the photoresist may actually form a protective barrier for the gold electrode, protecting it from dirt and damage.

11.8.6 Storage of Electrodes

The electrodes have now been completed and must be kept clean at all times because these experiments require that the electrodes do not have their surface resistance modified by finger grease, dirt particles and physical damage. The glass slides are kept in a clean sealed container whenever not in use and are never exposed unless they are being used for an experiment.

Figure 19 - The completed electrodes kept in a sealed container

12 Experimentation

Experimentation consist of four studies. Two primary experiments using the nanofabricated electrode and double steel mesh in a gel electrophoresis environment to measure voltage change across the sensing elements as salt solution periodically enters it. The sensors act as capacitors that depending on the concentration of salt solution will alter the dielectric constant in between the interdigitating structure or mesh gap. The presence of charged salt ions causes more charge to transfer between the insulated regions of the sensor thus affecting the voltage across them.
The secondary or supplemental experiment serve as a means to prove or disprove theories that occur as a result from the conclusions made from the primary experiments. The Iodine Visual Experiment is a simple visual experiment using basic concepts whereas the Ionic Transfer Experiment is a more thought-out experiment devised with stronger emphasis on technique and problem solving.
All the procedures and experimental designs are completely novel and original ideas devised for the sole purpose of the experiments that conducted.

12.1 Nanofabricated Electrode Experimentation

The first preliminary experiment was designed to imitate the traditional gel electrophoresis process using a novel miniaturised design. Like current gel electrophoresis setups, there is a central space which is filled with agarose gel and with two metal plates on either side to generate an electrical field. The first difference is that the experimental setup is vertical instead of horizontal therefore the ions are attracted in a downward motion towards the sensor. Another difference is that the presence of ions is detected using electrical measurement instead of visual motion of ionic bands.

12.1.1 Setup and Construction

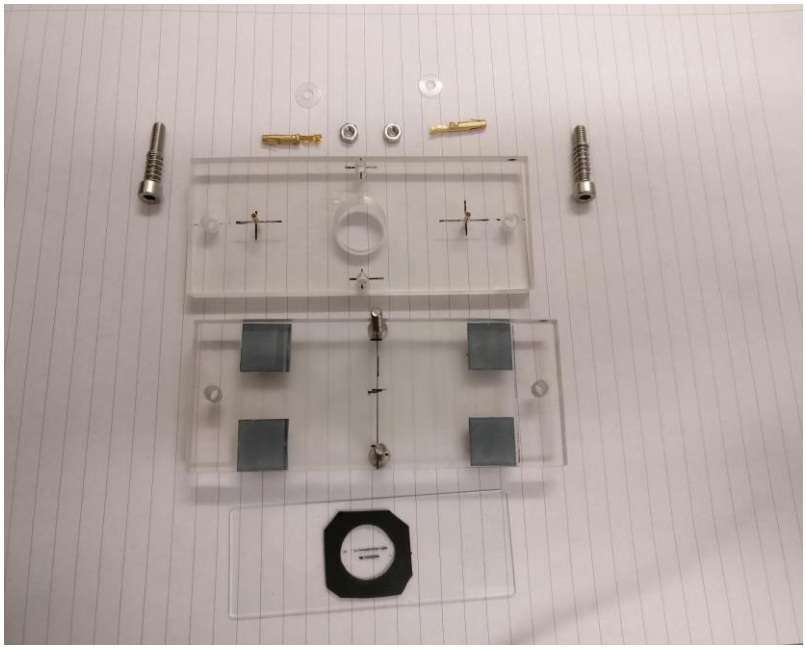

Figure 20- Complete breakdown of the electrode holder

Figure 20 shows the fully deconstructed electrode holder. The two large plastic rectangles are placed atop each other with the glass electrode held in the middle, which will later be replaced with sensor electrodes during experimentation. Lines are drawn to help the user align the electrodes to the centre of the holder. The rubber tubing on the bottom helps create a seal to stop any liquids from escaping the central section. The screws and the washers will help hold the two rectangular pieces hold together though care must be taken to not over-tighten the screws as the glass substrate may crack if excess force is applied. The central hole is around 14mm in diameter and has a depth of 10mm.

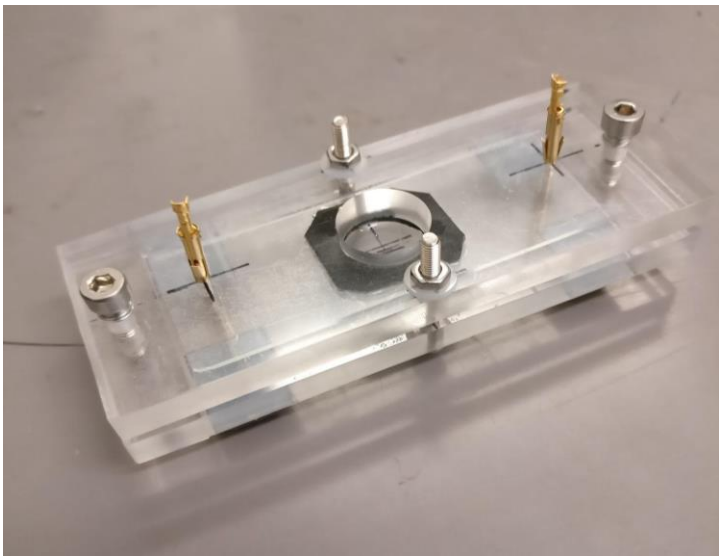

Figure 21- Fully assembeled electrode holder

Figure 21 shows the completed base structure of the sensor holder. The drawing in the centre of the well represents a perfectly aligned central electrode of the glass substrate. The gold connector pins are also attached to show how the connection to the electrodes are made. On the base of the sensor holder are 4 rubber base pads to stop the instrument from slipping, but also provides some elevation, as the bottom electric field plate is situated on the underside of the sensor holder. This prevents the sensor holder from touching the steel insulation box which prevents a short circuit.

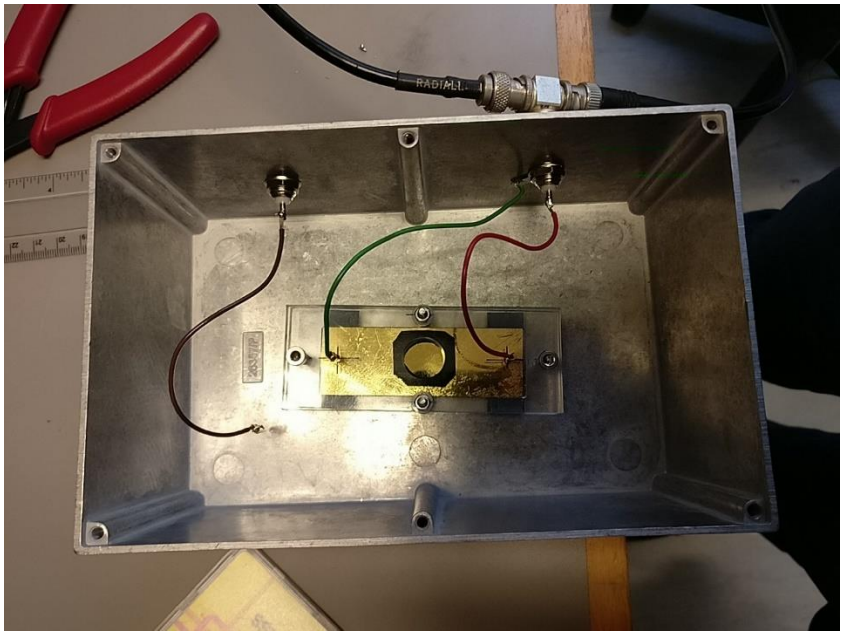

Figure 22 - The sensor within the insulation box

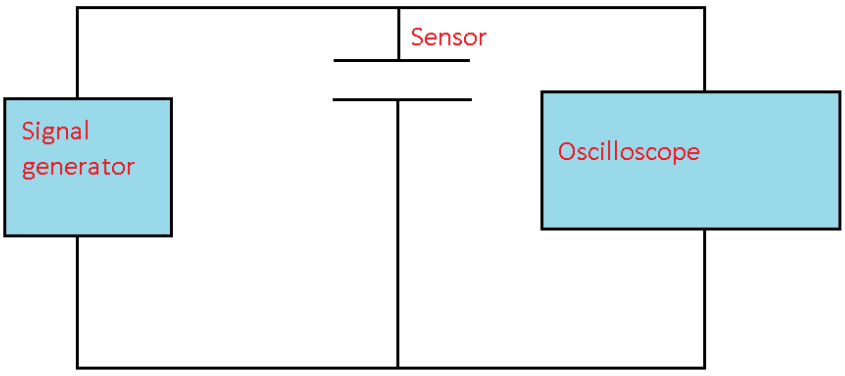

Figure 23 - Schematic diagram of the current sensor holder

Figure 22 shows the top view of the sensor holder within the insulation box and the

connections that are made between the oscilloscope and the two ends of the electrode. The oscilloscope will detect changes that occur across the electrode and will measure peak to peak voltage across the electrodes.

To create the plates used to generate the electrostatic field, two squares are cut from a layer of copper sheet and the sharp edges are treated with wet and dry sandpaper and the corners are rounded. As one of the squares will be a permanent fixture on the bottom of the sensor holder, it is left as is. However the second square will be placed on the top of the sensor holder, a lip is formed by bending one of the edges to about 90 degrees upwards. This allows the user ease of handling of the top plate and can be added or removed from the set up easily. Two small holes are also drilled on either side of each of the plates so they can be inserted on the screw posts of the sensor holder.

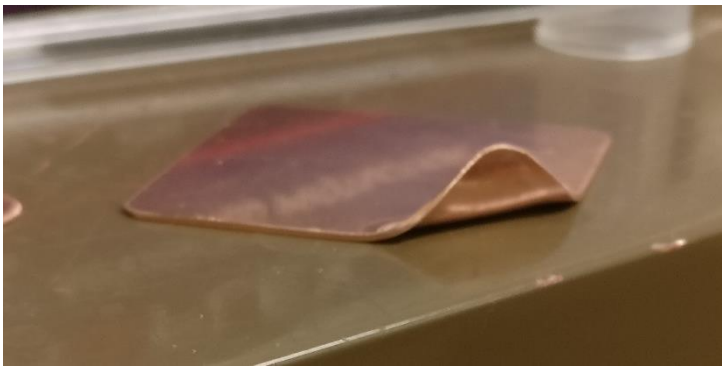

Figure 24 - The bent lip on the copper plate.

Wires can then be soldered onto the plate in order to provide the DC voltage from a battery pack. However, soldering onto copper can be tricky, therefore a small area is first sanded down slightly and a small amount of solder flux is applied to improve the adhesiveness. A table top vice is used to hold the copper plate in place as the copper will heat up during the soldering process. Care is taken when applying the vice as the copper plates may be bent out of shape if too much pressure is applied. The copper plates must be as uniform as possible as an uneven surface may affect the field generated from the plate.

Figure 25 - Excess from the soldering process on the surface of the copper plate

As seen from Figure 25, without the use of solder flux, the solder process can be messy. This is an unwanted effect therefore the solder must first be removed and reapplied thinly to ensure smoother contact on the plate and an even surface area as possible. The wires are colour-coded, so wire with black insulation is applied to the bottom plate and a wire with red insulation on the top to avoid confusion and notify the user of the correct arrangements.

A thin coat of black spray paint is applied on to each plate to create an insulation layer in order to prevent water from creating a short circuit on the plate if there is accidental spillage. As an added benefit, the black also helps the plates look less rugged and more like a professional, neat instrument as the surface of the copper does look slightly dirty.

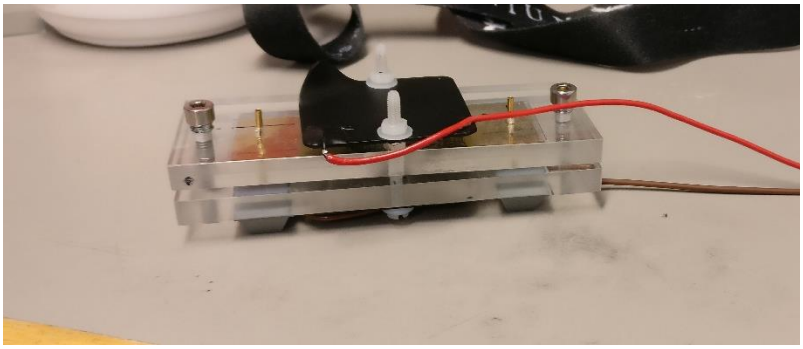

Figure 26 - The completed sensor holder setup

12.1.2 Experimental Considerations

This section is to note several key elements within the experimental procedures that must be viewed at all times. These points are could only be identified after countless

experimental repeats, of which are not included in this document as they contain incomplete or invalid data.

12.1.2.1 Curvature of lip of the agarose gel's well

The liquid sample, that is to be measured, cannot be placed directly on to flat agarose gel. As hardening of the gel occurs, the sides may curl and form dips that might cause the liquid within to run down the sides of the agarose and directly on to the sensor, thus affecting the accuracy of measured results. To fix this, a stopper is designed to provide a cast around the top of the agarose in a shape of a well. This well is designed to prevent runniness of the liquid while still maintaining equal surface area and working distance between the top of the agarose and the sensor electrodes.

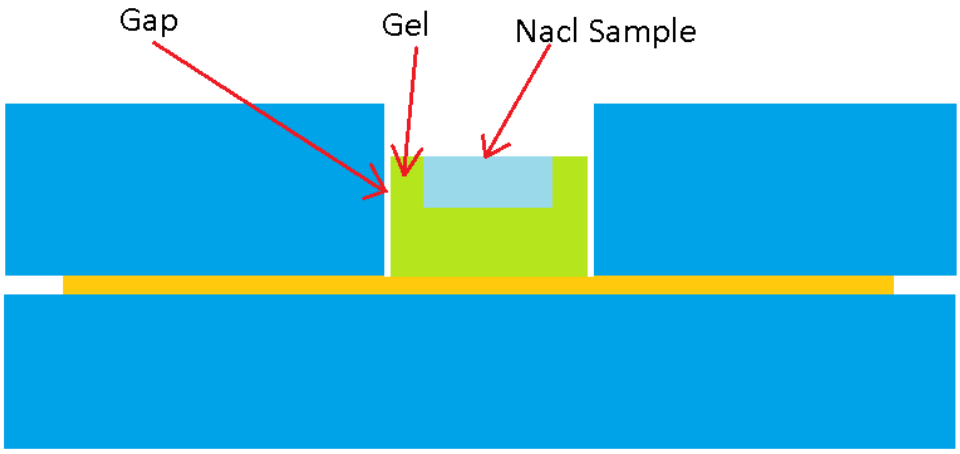

Figure 27 - Cross sectional view of the agarose gel within the sensor holder

A pipette can then be used to carefully place the sample onto the well. A variable that must be constant throughout the experiment is the depth of the well, hence the width of the stopper is designed so that it sits flush on the top of the sensor holder. One factor that must also be taken into account is that when removing the stopper after the agarose has hardened is that the well edges are not damaged. This means that the stopper must be carefully lifted off the top of the sensor holder and the agarose must be fully hardened before doing so.

12.1.2.2 Screening

Before the agarose solution is introduced into the sensor holder, the entire sensor holder must be constructed and placed into the insulation box. There are several reasons for this. Firstly the insulation box provides shielding against external signals and electrical interference that may affect the readings taken. The steel enclosure provides a strong electromagnetic shield against any interferences. Secondly the insulation box may also provide protection against contamination and slight weather effects. Accumulation of dust, sudden gusts of wind and other environmental effects may contaminate the sample or dry out the agarose. This will cause inconsistencies in ion mobility and affect the consistency of measurements.

12.1.2.3 Consistency and control of Experimental Methods

There are several key steps that are taken in ensuring that consistency between experiments is maintained when several cycles are run to ensure there are no repeat measurements necessary.

As the primary mode of measurement is in liquid form, the sample used in all experiments must be of constant volume. With that, the sample introduced into the agarose well at the start of each experiment can either be measured, weighed or inserted in fixed quantities via a combination of the two. In this case, several pipettes of the same make are acquired and the number of drops inserted into the well is kept constant throughout the experiment, unless stated otherwise. In some cases multiple cycles of the same experiment conducted will either consist of 2 or 3 drops per experiment phase. These numbers do not change within each cycle, for example an experiment consisting of 6 cycles will only hold 2 or 3 drops and not a mixture of both.

Another way the experiments are kept consistent is by noting the time agarose takes to fully harden. This is the only variable where there may be external factors beyond control. Current ambient temperature may have an effect on the hardening times of molten agarose solution. Therefore, to minimise inconsistencies, the agarose is heated at a fixed constant temperature, and allowed to cool for a fixed amount of time. Though there may be a way to accommodate ambient temperature change to the hardening rate of agarose, it may be a little too complicated and time consuming to factor in, and therefore is disregarded for the sake of simplicity and convenience. The volume of agarose solution used may also be a factor that affects the consistency of experiments. However the sensor holder is designed in such a way that, provided air bubbles do not exist within the sensing area, the volume of agarose used is always kept consistent. The stopper used in creating the well provides a clear barrier for the agarose and excess is always funnelled out of the top vent and provided the top of the sensor holder is inserted correctly, the depth of the sensing area will always be consistent.

12.1.2.4 Measurement and analysis methods

The sensor is effectively a capacitor and the sample is the dielectric. Sample ions arrive at the sensor and change the dielectric constant of the sensor. As they accumulate, they consequently cause a voltage change across the sensor. The voltage change across sensor is recorded at a predetermined amount of time intervals. This may vary at the beginning and have a more consistent interval rate during the mid or peak points of the experiment. This is because there may be a threshold amount of time for the experiment to fully begin recording any change of voltage. However after the threshold is established, which may also vary from experiment to experiment, a fixed interval rate is established depending on how extreme the changes in voltage are. This peak point interval rate is kept constant throughout the experiment, unless uncontrollable circumstances occur. Several measurement analysis methods are incorporated throughout the course of the study.

The first method is raw voltage input and output which involves comparing direct input and output voltages as time goes on. This simply involves noting down the value of voltage across the oscilloscope directly and no mathematical deduction is really necessary. However, this method assumes that initial output and input voltages must be constant throughout all experiments conducted and therefore may not be ideal in certain circumstances where the initial values are not the same.

A second method can be used to find the voltages relative to the input voltage. This simply involves finding the “gain” or “loss” of voltage at chosen time intervals. This can be done by using the formula

$$voltage\ gain/loss\ = \frac{output\ voltage}{input\ voltage}$$

This then gives the relative voltages which will mean that regardless of the initial voltage readings at the oscilloscope, a constant pattern of voltage change can be used as a marker for the behaviour of experimental systems, assuming there is a linear relationship.

The third and final method can be used to envision voltage “growth patterns”, which is ideal for finding cumulative changes throughout the entire process of one experiment. This differs from the second method as the “relative” method only enables the user to view the ratios of voltage change during the instances of the time interval that is currently being analysed. This third method however allows for the user to see how the patterns have changed over time in a cumulative fashion. There is no benefit of one method over another as the information generated by both these methods are crucial and give two distinct information patterns for the user to decipher and compare with other experiments.

This third method can be done simply by adding the voltage gains or losses over the period of the experiment and continuously as the experiment goes on.

12.1.3 Preliminary Experimentation

The first preliminary study involved using a simplified capacitive sensor instead of the final interdigitated structure i.e. a gold film on a glass slide divided down the centre by an uncoated channel.

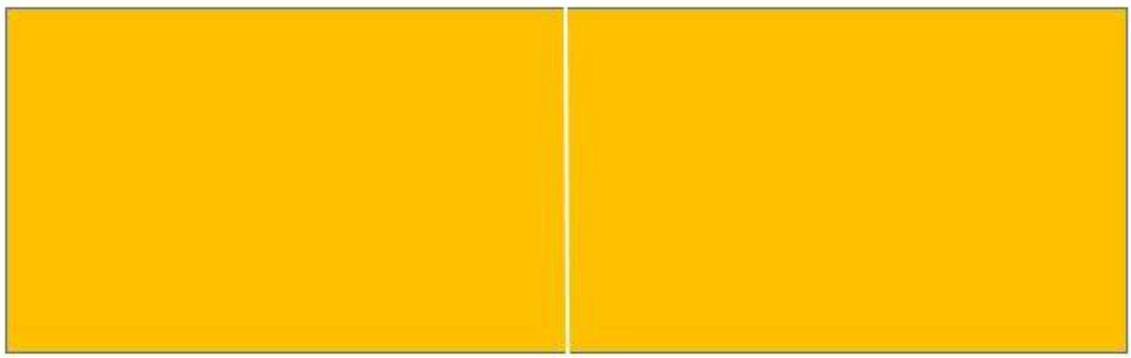

Figure 28 - figure showing the thin layer of gold with a scribed centre

Now that a feasible alternative to the primary experimentation has been established, a study is carried out to determine whether the alternative setup will behave similarly to the interdigitated structure. From past experimentation, it is shown that measuring a change of potential across the substrate will show a drop when an ionic substance is present, but will be unreactive towards non-ionic substances such as de-ionized water.

The glass slide is placed on the holder and a continuous sinusoidal pulse is generated across the two gold areas. At 1V peak to peak and 1000Hz input, the oscilloscope output across the two separated regions.

De-ionized water is then introduced into the sensing area using a pipette and as expected the voltage measured across the regions do not change. However when salt solution of varying concentrations is added, the voltage does begin to drop. This experiment provides a basic pretence for the experiments to come.

This experiment was repeated with 1% agarose gel. The gel was prepared and the well was formed by using the blunt end of a marker pen as a mould for the well. Masking tape was stuck to the end of the marker pen and marks were made along the masking tape so that the depth of the well can be measured. The diameter of the marker was also measured so that the volume of the well indentation caused by the butt of the marker could be measured. The pen was held in place over the hole in the sensor holder using a standing clamp over the centre of the sensor holder.

Molten agarose gel was inserted through the centre of the sensor holder as it enveloped

the marker end, some of the gel was allowed to overfill through the centre. Allowing the gel to overfill slightly would create a rounded lip, preventing any liquids from dripping through the side of the well and directly onto the electrode underneath.
The value of input and output voltage was noted after the gel was given 20 – 30 minutes to harden.
Input Voltage – 1v
Output voltage – 2.2v
The pen was then carefully twisted out from the sensor holder, leaving a well in the middle of the gel in the centre of the sensor holder for the salt solution to be inserted. 10% salt solution was added to the well and the voltage output changes were noted over time. After some time the voltage output measured across the electrode slowly began to drop, and after several hours, the voltage stabilised at around 1.92 volts.

12.1.4 Primary Experimentation A

The primary stage of this experiment studies the influence of electric field on the mobility of salt ions and if the presence of salt ions on the nanofabricated electrodes affects the voltage across the sensor.
The voltage necessary to apply the electric field is generated from a series of 9v batteries placed in series using several 9v battery connectors and the positive end is connected to the copper top plate while the negative end is connected to the bottom copper plate. A voltmeter is used to ensure the voltage is supplied as required.

12.1.4.1 Control Experiment

As a control, an electrode is placed in neutral solution to verify that under non-ionic environments that there will be no changes to the reading across the oscilloscope. The sensor holder is assembled with one of the 2 array electrodes attached and connected to the oscilloscope and the signal generator.
A sinusoidal signal is produced at the input from the signal generator at 1v peak to peak at 1000hz and the oscilloscope is used to measure the corresponding output in between the capacitating electrode arrays.

2 drops of de-ionized water is added onto the sensing area by using a pipette and only a small change of around 20-30mv is observed on the oscilloscope, signifying that a non-ionic substance does not measure a relevant enough change in potential difference across the sensing area.
A small unrecorded amount of salt is added into the beaker of de-ionized water and stirred

until the salt crystals are thoroughly dissolved. This salt solution is then added to the sensing area and the oscilloscope detects a much higher change in potential difference across the sensor.
It can be concluded then that the presence of salt ions in the liquid will change the potential difference across the sensor though it should not be excluded that there is a small change in potential difference when a non-ionic substance such as de-ionized water is present. However, the experimental results can be analysed in a way that will take into account the effect of non-ionic substances on the potential difference.
Another point of note is that the measured voltage of non-ionic substances must be consistent throughout all iterations of the experiment and can be used as an indicator to whether there are external substances are present in the non-ionic reagents used. Simply put, when using a certain non-ionic reagent in multiple iterations of the experiment, whether it be the voltage across the plate or the concentration of salt particles are manipulated, the base non-ionic reagent must be consistently the same in potential difference.

12.1.4.2 Forward voltage salt solution

The purpose of this experiment is to analyse the effect of external electrostatic fields on the motion of ionic substances across a gel by analysing the waveform produced when potential difference of the sensing area is measured over time.
The battery pack used in this experiment consists of a chain of 9v batteries that can be added or removed according to the desired amount of supplied voltage. The batteries are “chained” in series configuration and can be measured with a voltmeter in order to determine whether the actual voltage supplied to the plates on the sensor holder.

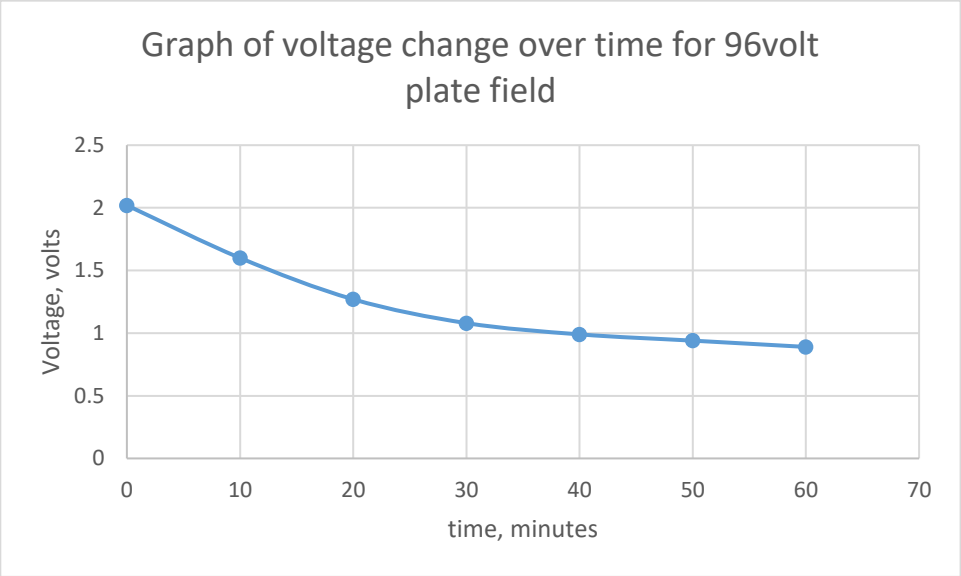

Figure 29 - Graph related to the drop of voltage over time for a plate voltage of 96volts

The graph in Figure 29 above shows a slow exponential reduction of voltage over 60 minute period of time. This reduction in voltage slows down around about 30 minutes is expected to reduce further past the 60 minute mark.

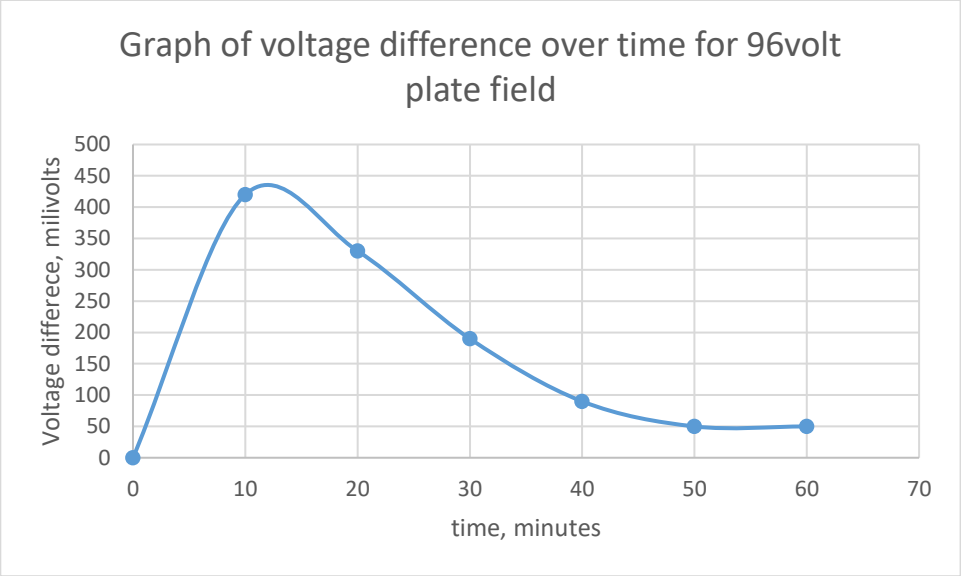

Figure 30 – Graph related to the voltage drop over time for a plate voltage of 96 volts

Figure 30 shows the difference each 10 minute interval has on the change in voltage. The highest voltage difference occurs within the first 10 minutes and decreases exponentially every 10 minutes onward.

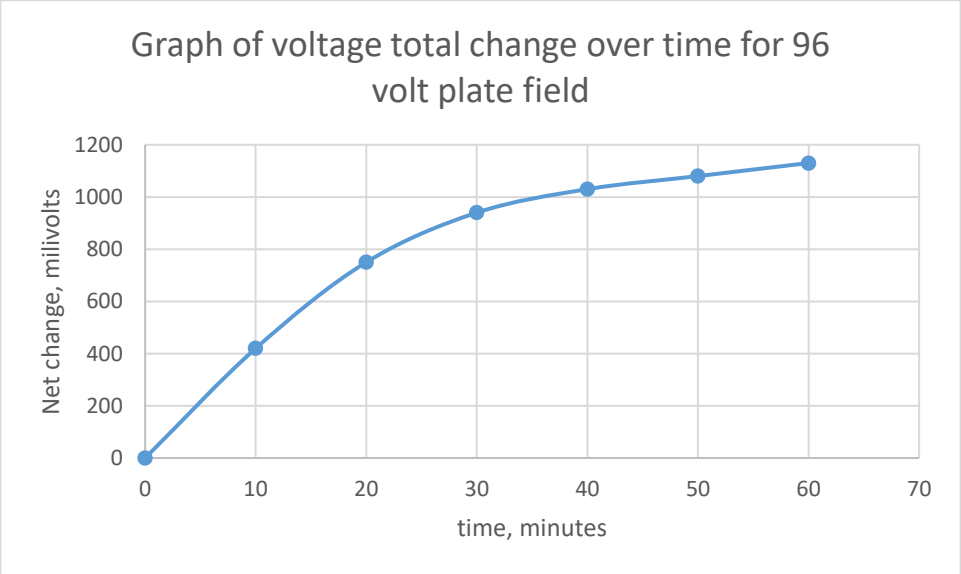

Figure 31 - Graph relating the total change of voltage over time for 96 voltage plates

Figure 31 here shows the cumulative changes of voltage over time throughout the course of the experiment. The there is a total change of 1.13 volts from the beginning of the experiment to the end.

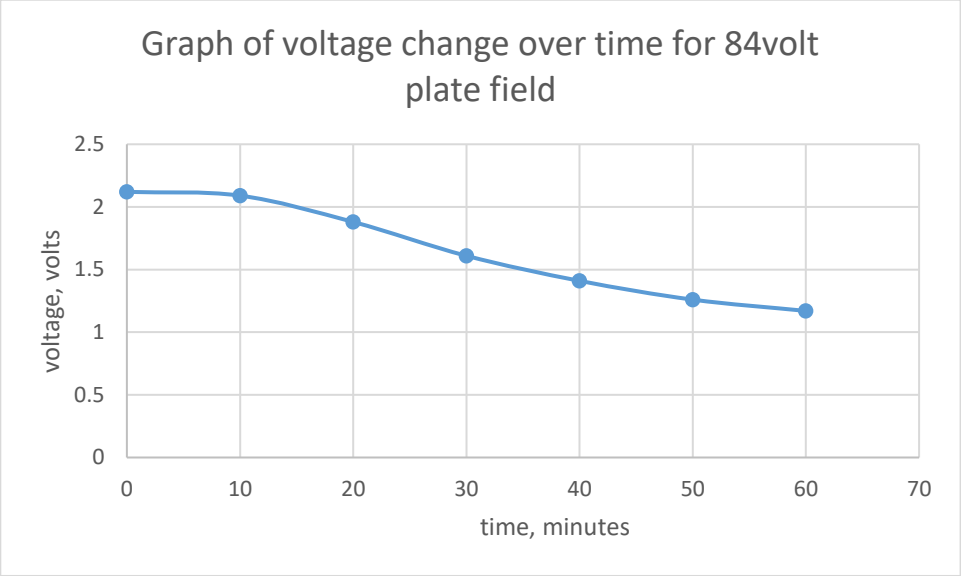

Figure 32 - graph relating to the change of voltage over time for plate voltage of 84 volts

Figure 32 above shows the decrease of voltage over time for the 84 volt plate experiment. It takes around 10 minutes for the initial changes to take place, after which there is a slow sloping drop of voltage. It could be theorized that this would mean the voltage would take a little longer to reach a steady point of decrease, however at 60 minutes, the voltage seems to still be exhibiting a slow exponential decrease.

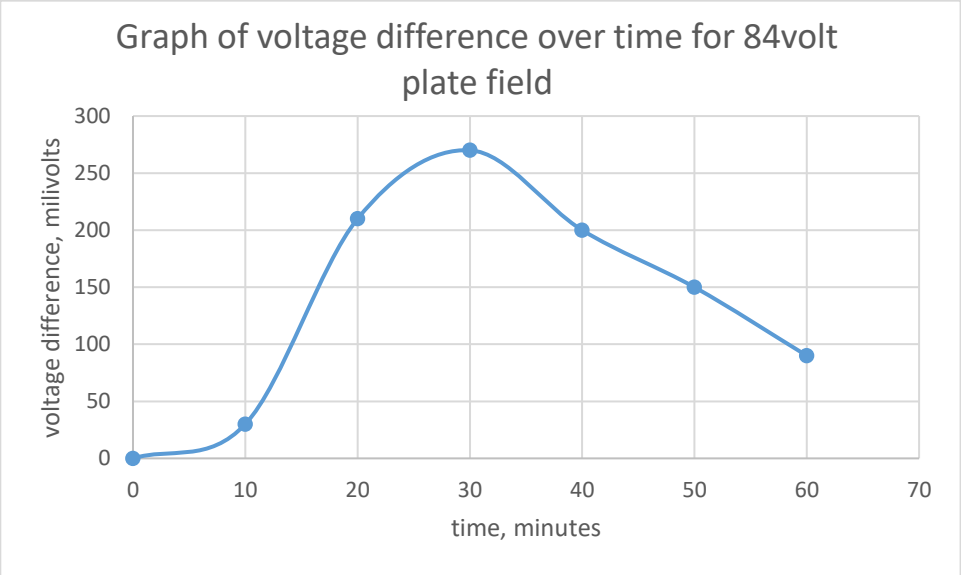

Figure 33 - graph relating to the voltage difference over time for plate voltage of 84 volts

As evidenced here by the graph in Figure 33, there is little voltage difference in the first 10 minutes of the experiment, where between 10 and 30 minutes there is a positive trend in the rate of voltage drop. This trend then decreases after 30 minutes however the slope is still steep at 60 minutes, where it is possible for the voltage to drop further past this point.

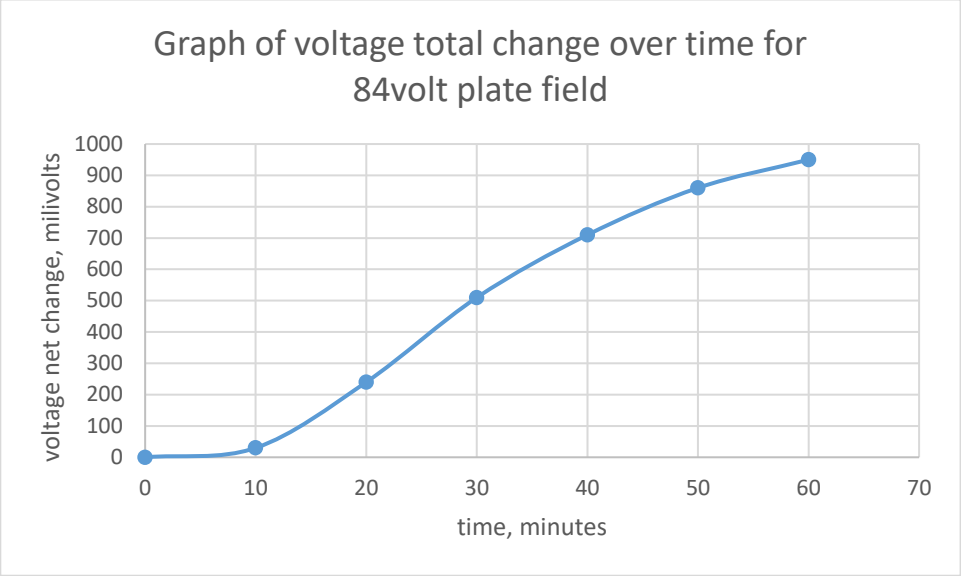

Figure 34 - Graph representing voltage change over time for 84 volt plate voltage

The voltage change graph in Figure 34 shows that in a period of 60 minutes, the total change in voltage is 0.95 volts. This shows that at a lower plate voltage, there is a slower rate of ionic motion compared to the 96 plate voltage experiment. The lower external field strength has not only cause the initial travel time to reduce but also slowed down the rate of motion in the salt ions.

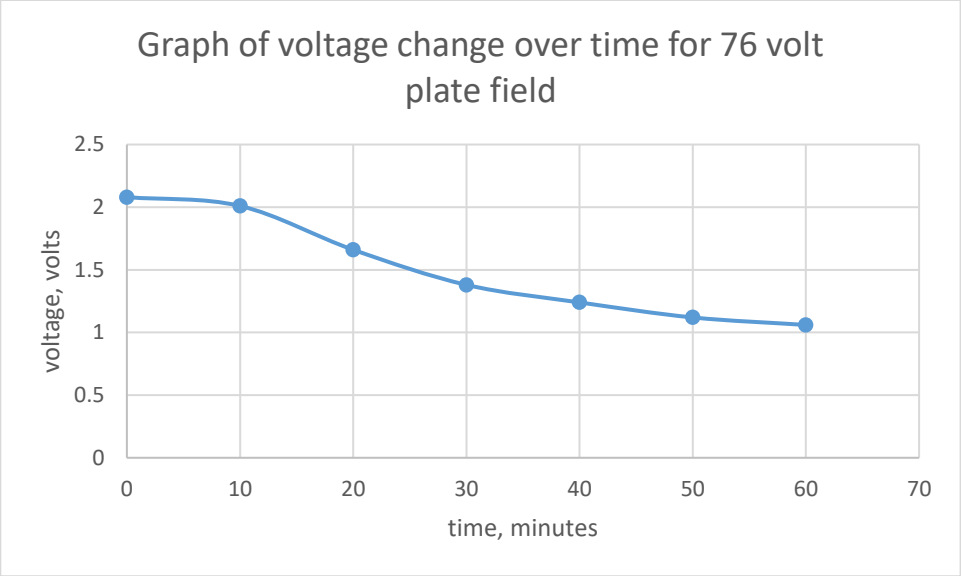

Figure 35 - graph relates to change of voltage over time for 76 volt plate voltage

The graph in Figure 35 showing the voltage change above is similar to the 84 volt plate voltage, having to take 10 minutes before any voltage change is recorded. However, after the initial loss, the exponential slope starts becoming linear around the 50 minute mark, and exhibiting signs showing that the voltage may be constant from 60 minutes onwards.

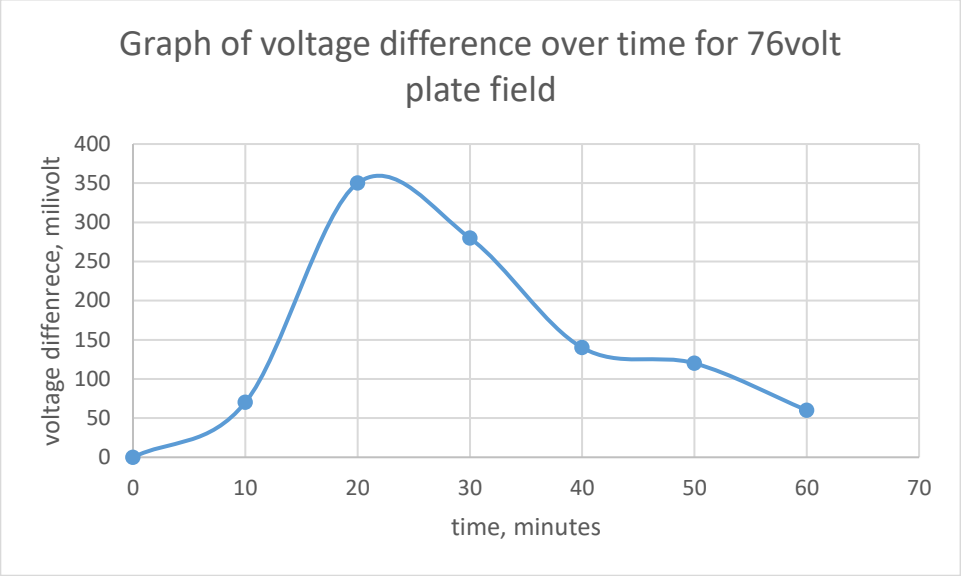

Figure 36 - graph relating to the voltage difference over time for the plate voltage at 76 volts

The graph for voltage difference in Figure 36 shows that the highest change happens between 10 and 20 minutes of the experiment. There is a gradual loss between 30 and 40 minutes with no change between 40 and 50 minutes. The voltage loss from 50 minutes onwards then reaches the point where it is almost as low as 10 minutes, possibly reaching the point where the voltage will not reduce any further.

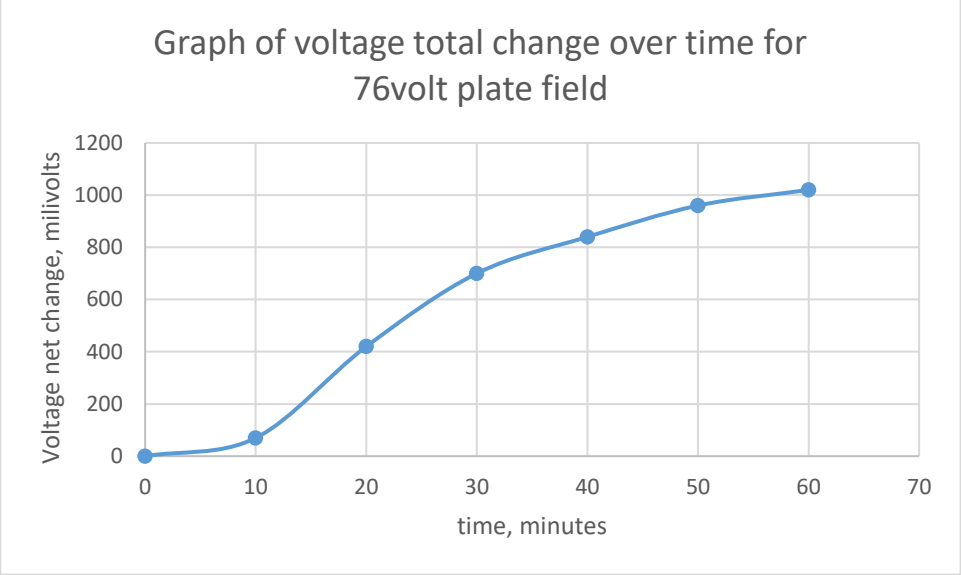

Figure 37 - graph relating to the total change over time for the plate voltage at 76volts

The total voltage reached in this experiment is somehow higher than the 84 voltage plate, showing an increase of 1.02 volts compared to the previous 0.95volt. However the general pattern of the growth of the slope is still the same. The cause of this discrepancy could be due to environmental temperatures affecting the viscosity of the gel. Although for the 84 volt plates, the voltage trend still showed signs of change, whereas the 76 volt plates were reaching the end of its point of change, as evidenced by the gradient of the slope between 50 and 60 minutes of the voltage change graph.

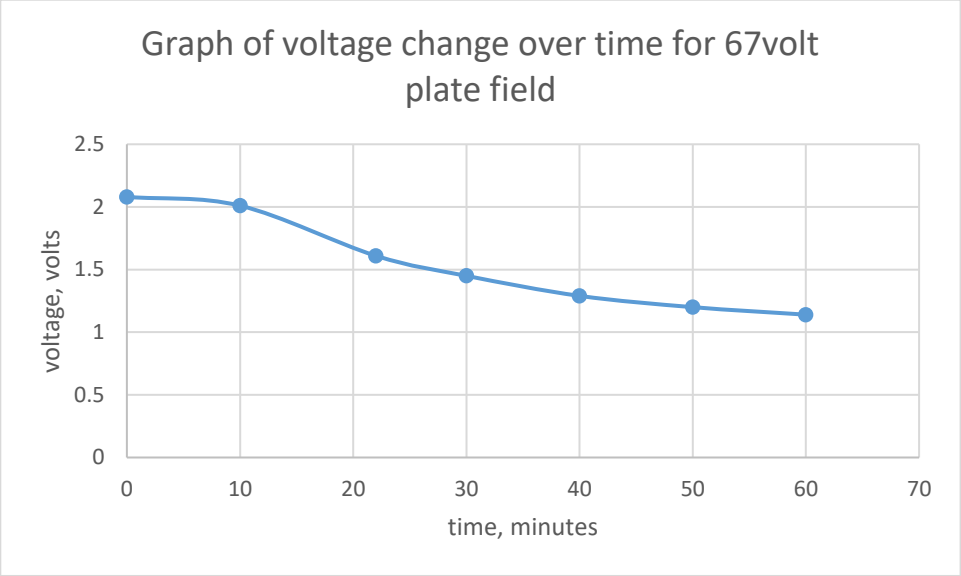

Figure 38 - Graph relating the change of voltage over time for plate voltage of 67volt

Ten minutes were again needed for the ions to reach the sensor electrode for the 67 volt plates. There is a slight strong curve between 10 and 22 minutes and a much shallow curve 30 minutes onward. The change is also much smaller compared to the earlier plate voltage values.

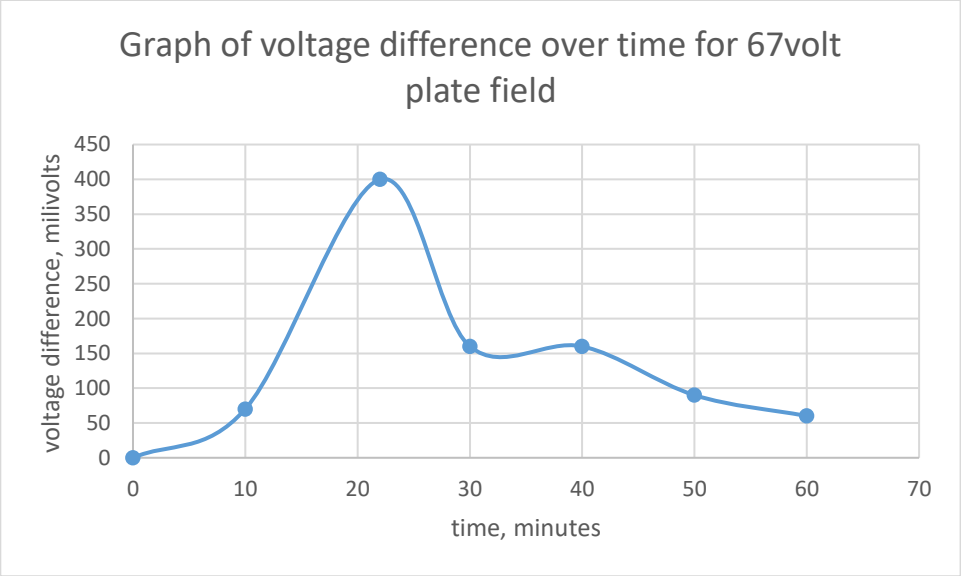

Figure 39 - graph relating to the voltage change over time for plate voltage of 67 volts

The graph in Figure 39 shows that it takes 10 minutes for a 0.075 volt initial change to occur, and the largest change occurring at 22 minutes for around 400 milivolts. The voltage changes reduce between 20 to 40 minutes, recording a change of around 150 militvolts at 30 and 40 minutes. The voltage change then reduces to 100 volts at 50 minutes and around the 50 milivolts at the end of the experiment.

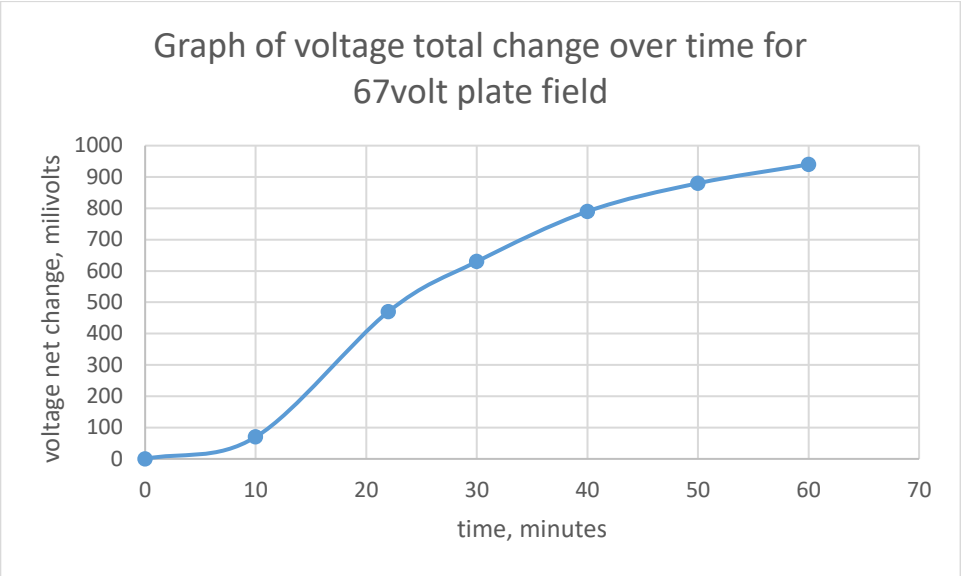

Figure 40 - Graph relating to the total change of voltage for 67 volt plate voltage

The 67 voltage plate reduced the initial measured voltage by 940milivolts in the period of 60 minutes, which was lower than the 87 volt plate voltage measurements. The highest voltage change happens between the 10 and 20 minutes and the trend shares similar qualities to the earlier experiments.

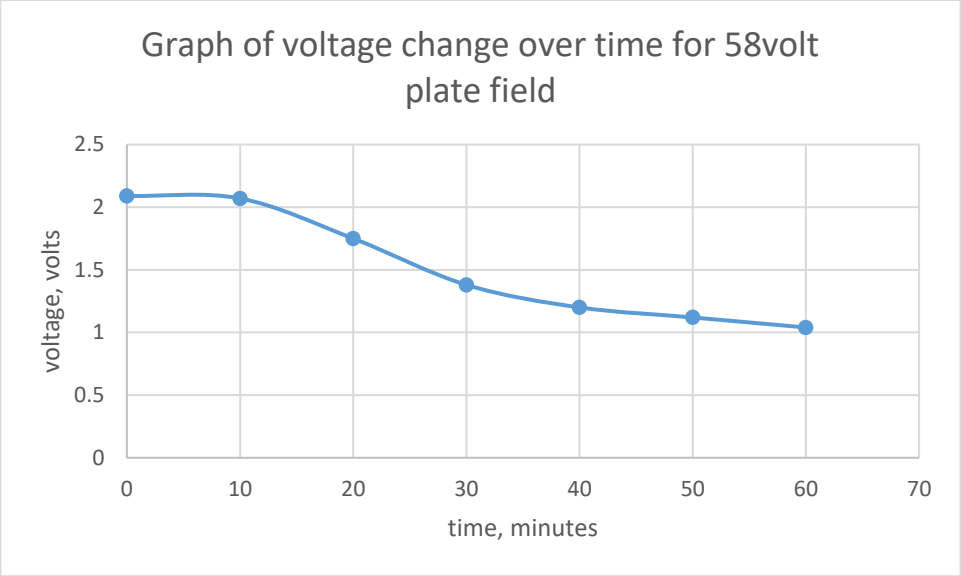

Figure 41 - Graph relating to the change of voltage over time for plate voltage of 58 volts

The main difference in the graph in Figure 41 shows that the voltage change between 10 and 30 volts, which are also the highest gradient of loss throughout the experiment, no longer follows the exponential pattern. The loss of voltage from 30 minutes onwards however has a slow exponential loss until the 60 minute mark. The 10 minute “no loss” stage remains the same as the three previous experiments.

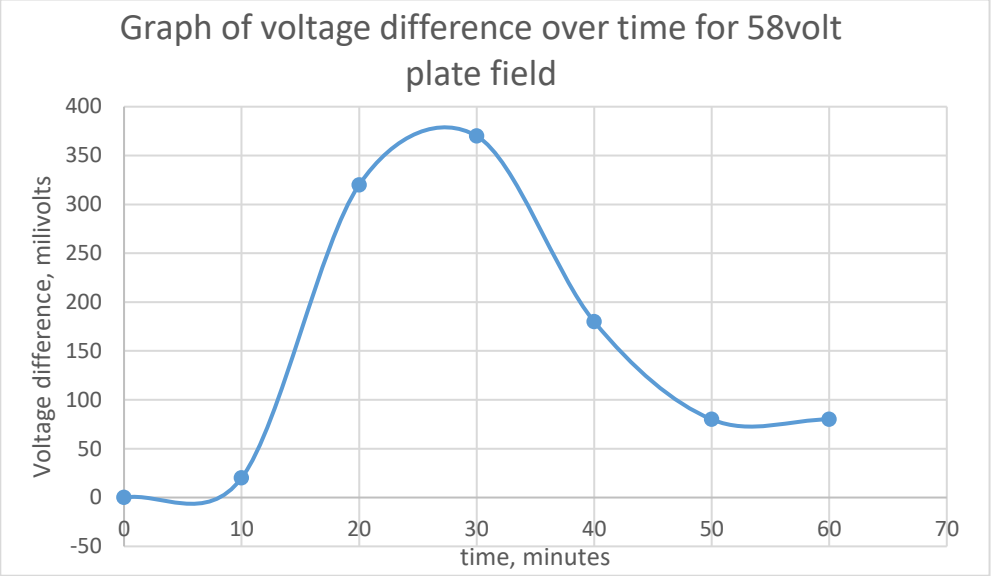

Figure 42 - graph relating to the voltage difference over time for the plate voltage at 58volts

The graph in Figure 42 shows a sharp increase in the rate of voltage reduction between 10 and 30 minutes and also a sharp decrease in the rate of voltage reduction between 30 minutes and 50 minutes, before a somewhat steady voltage reduction pattern is seen after. There are no clear signs that the rate of voltage loss past 60 minutes is present, though it safe to assume either constant decrease or slight reduction.

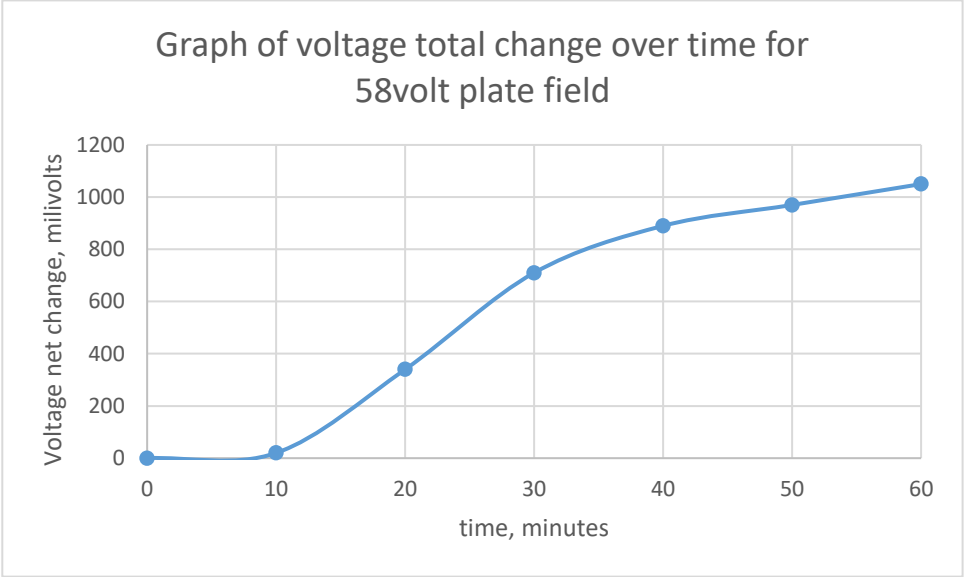

Figure 43 - graph relating to the total change of voltage over time for the plate voltage at 58 volts

The total change for the 58volt plate voltage is the least characteristic of all the experiments done in this phase. As it is higher than most of the other plate voltage measurement readings. The tables below will compare these values in all catagories and a conclusion will be drawn.

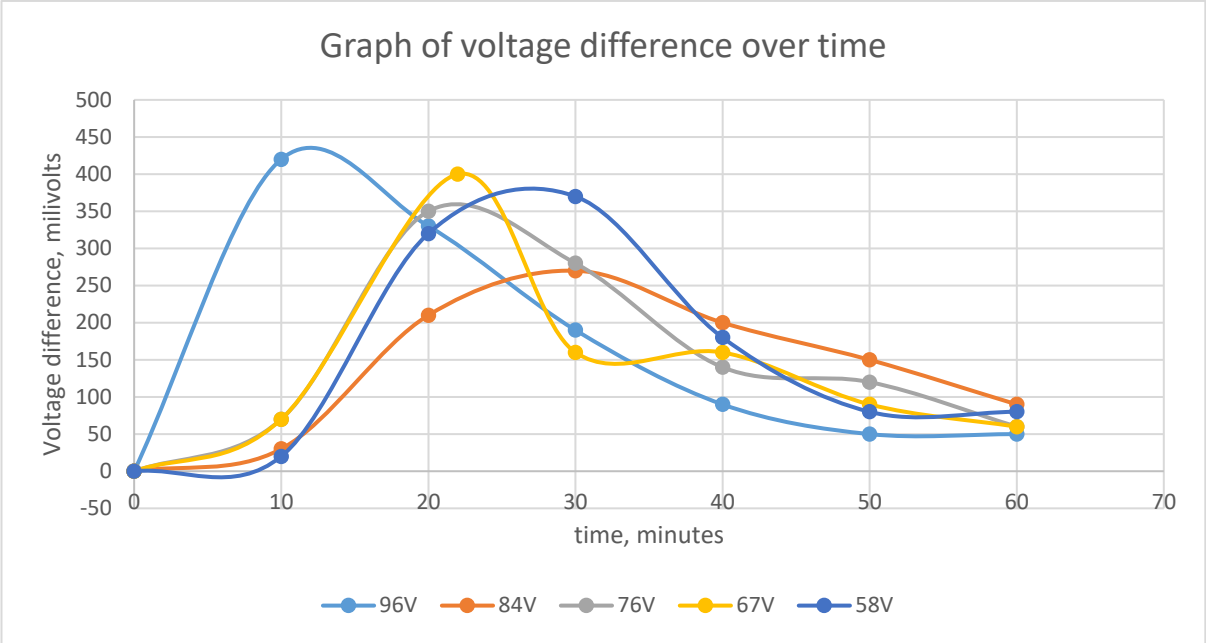

Figure 44 - graph relating the voltage difference over time for all of the plate experiments

The graph in Figure 44 shows all the plate voltage values for voltage difference over time. The differences in the output voltage seem to be very random though all of them follow a similar upward, then downward trend. This could be due to the viscosity of the gels, delay in the starting measurements of the experiment, or the nature of the gel within the sensor holder itself.

The gel within the sensor holder may dry up faster at hotter ambient temperatures, even though a 20 minute dying period is set, some liquid may still remain within the gel. Another contributing factor may also be the amount of salt solution from the pipette being higher or lower in any of the experiments. Presence of air bubbles within the gel structure could also contribute to the inconsistencies recorded in the experiments, as air bubbles may impact the path of travel for the ions from the top of the well to the sensor.

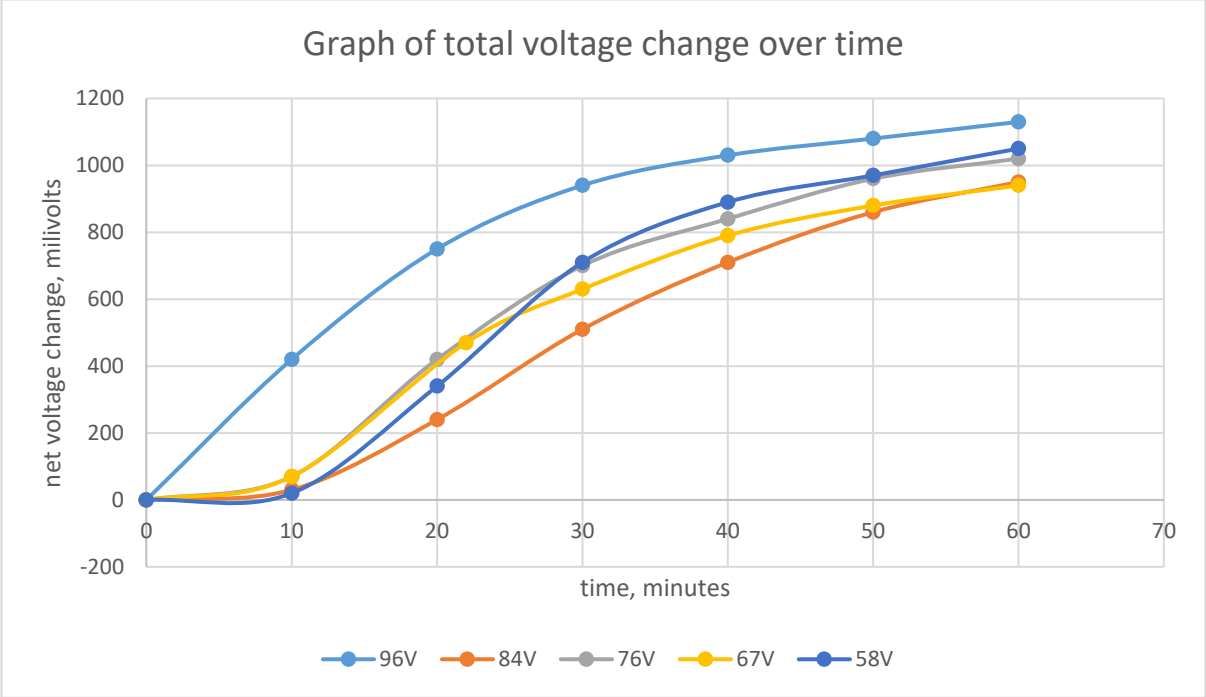

Figure 45 - Graph relating to the total voltage change over time for all plate voltages

The plots in Figure 45 the inconsistent nature of the change of voltage over time for each individual plate voltages. The 58volt plate seems to have measured the second highest total change of voltage over time despite being the lowest plate field strength and 84 volt plate voltage seems to be the lowest on all accounts, such as the lowest rate of voltage decrease, and the lowest total voltage change.

12.1.4.3 Conclusion

To conclude the first primary experiment conducted, the experiment has been largely successful. As salt ions move across the gel, the voltage readings across the sensor will change, reflecting the nature of ion activity as it passes through the well and reach the vicinity of the sensor. However it is unclear whether at this stage, a stronger field will have an effect on the transport of salt ions.

12.1.5 Circuit re-evaluation – Output voltage measurement readjustment

A 1M ohm resistor was added from the signal generator to the electrode. When measuring the output voltage across the electrode, only half of the voltage supplied from the signal generator is measured across the electrode. However, when DI water is added the voltage is reduced to an almost zero value. This has radically increased the sensitivity of the instrument. It is concluded that his is too radical of a change as adding 1% salt

solution shows no effect and it was harder to get an accurate reading. The 1M ohm resistor was replaced with a 100k ohm resistor. Di water again would change the value of the output voltage from 2V output to 1.52V. More advice is necessary to proceed from there on in.

In parallel, a separate experiment was conducted with an alternative circuit design. A 100ohm resistor was placed in series to the electrode. No changes to the system would not be measured across the electrodes, but instead through the 1 ohm resistor.
In an open circuit, the voltage across the resistor would read around 60mv when a 4v AC signal was supplied to the system.
This would mean that the system was producing ;

0.06/100 = 0.0006 or .6mA of current

Adding .5g of DI water to the circuit would give rise to a 180mv voltage across the resistor giving us a

.18/100 = 0.0018 or 1.8 mA of current

Adding a drop of 10% salt solution to the electrode gave an increased the voltage to 1.52 corresponding to a current across the system of

1.52/100 = 0.0152 or 15.2 mA of current

Using this set up it is clear that adding di water and agarose solution would change the current across the system. With the previous set up, it was not possible to account for this change as adding di water and agarose solution did not record a change across the electrode. In conclusion, this circuit alignment suggests that DI water and agarose solution does have an intrinsic affect on the behaviour of the system and should therefore be considered in the final design and as the accuracy of results may be affected.

12.1.6 Primary experiment 2 and Polarity Reversal Experiment

The purpose of this experiment is to study the effect of reversing the polarity of the electrostatic field generated from the plates and the effect on the mobility of ions within the sensing area. This will also be the first experiment under the new voltage measurement method.

In theory, a reverse field should be able to reverse the motion of ions, and help move the ions from the bottom of the sensing area to the top of the gel, near the well. However it is also possible for the ions to be held within an ionic trap formed by the alternating current on the capacitor array or for the negatively charged chloride ions to be attracted to the bottom positively charged plate, thus further increasing the voltage recorded by the oscilloscope.

12.1.6.1 Experimental steps and results

A 90v field was generated using the parallel plates and a 2mm deep well was formed in an agarose solution on top of the electrodes. 2 drops of 10% salt solution was placed in the well and results were taken over time. The graph below shows the change of voltage across the 100ohm resistor over time.

Finally the polarity was reversed and the changes were observed.

Table 1 - Table showing voltage parameters before and after polarity reversal

time, minutes	voltage, volts	change, volts	total change, volts
0	0.48	0	0
15	0.56	0.08	0.08
20	0.61	0.05	0.13
22	0.64	0.03	0.16
24	0.67	0.03	0.19
26	0.7	0.03	0.22
28	0.73	0.03	0.25
30	0.77	0.04	0.29
32	0.81	0.04	0.33
34	0.85	0.04	0.37
36	0.89	0.04	0.41
38	0.93	0.04	0.45
40	0.98	0.05	0.5
42	1.02	0.04	0.54
44	1.06	0.04	0.58
46	1.1	0.04	0.62
48	1.13	0.03	0.65
50	1.16	0.03	0.68
52	1.18	0.02	0.7
54	1.2	0.02	0.72
	Voltage parameters after plate polarity reversal		

time, minutes	voltage, volts	change, volts	total change, volts
5	1.27	0.07	0.79
15	1.36	0.09	0.88
30	1.44	0.08	0.96
45	1.48	0.04	1
55	1.52	0.04	1.04
60	1.52	0	1.04

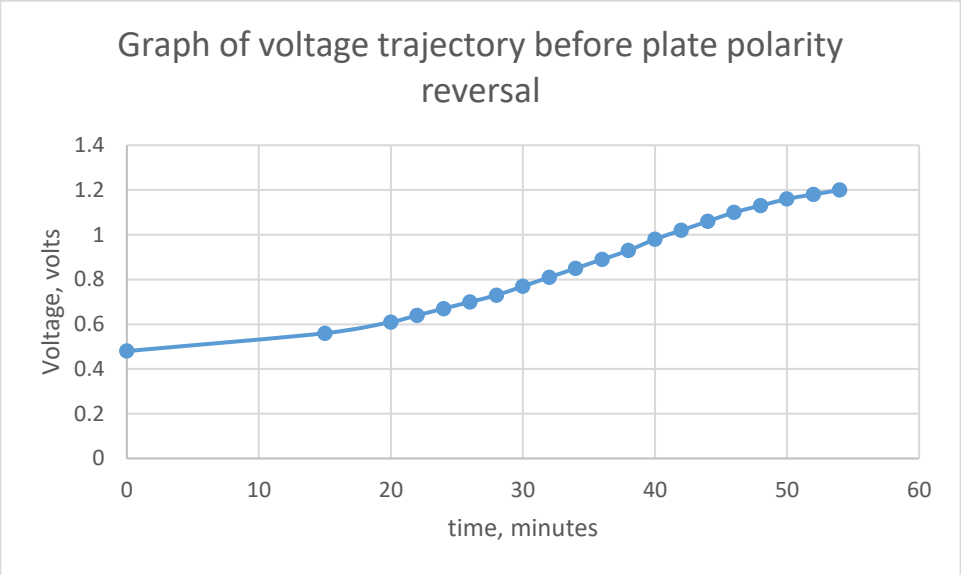

Figure 46 - Graph of change of voltage before the polarity of the plates were reversed

The graph in Figure 46 the value of voltage increasing as the salt ions pass through the gel. This differs from the preliminary experiment as the voltage measured now increases over time as salt passes through on to the sensor rather than decreasing. This is as intended of course and is to “load” the sensor area with ions so that the reversal theory could be tested.

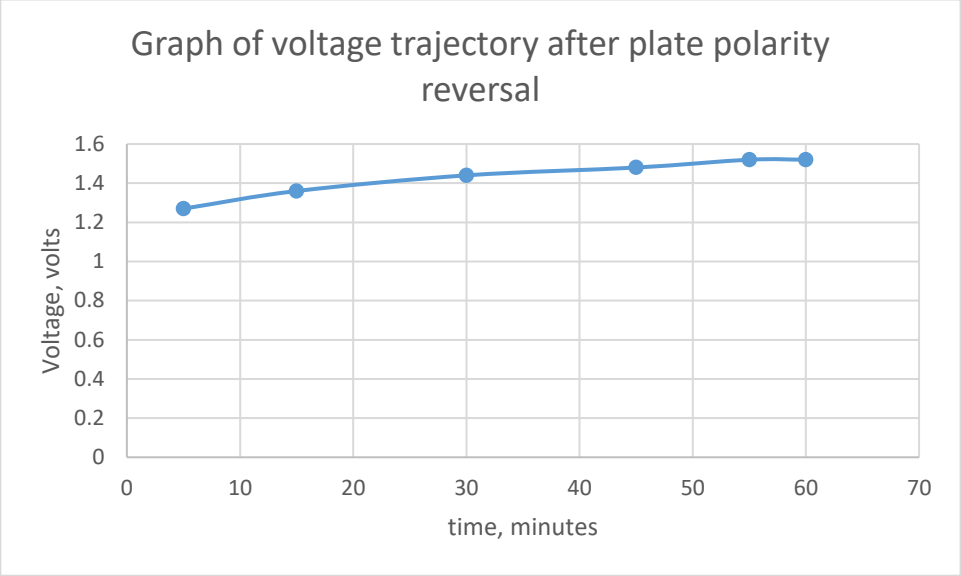

Figure 47 - graph of change of voltage after the polarity of the plates have been reversed

The graph in Figure 47 the voltage output further increasing despite the polarity being reversed. It was hoped that the reverse electrostatic field will cause the salt ions to be pulled away from the sensor and thus the output voltage reading would decrease, however there is no sign of this change at all.

12.1.6.2 Conclusion

It can be concluded that reversing the polarity of the plates do not change the value of voltage reading across the sensor. This could be because the sensor area is already saturated with salt ions, and that the ions in the vicinity of the sensor causes somewhat of an “ion trap”, causing the salt ions to stay within the sensing area.
Another possibility is that the sensor measures the total dielectric properties of the agarose, meaning despite the position of the salt ions within the agarose gel, the reading will still be present. This is different from the initial state of the experiment where the salt ions are only present in the liquid solution within the gel well, hence the difference between the salt present within the gel and the well would be that the ions are pulled from the well into the agarose gel mixture. As the salt ions break through the initial boundary of the well, this theoretically could cause a change of voltage across the sensor.

12.1.7 Circuit re-evaluation 2 – input leads

A lead is placed between the oscilloscope directly to the signal generator using a t-connector. This enables the oscilloscope to measure peak to peak voltage across the output of the electrodes and also input from the signal generator. This step allows for changes in phase difference between the input and output signals to be accounted for.

12.1.8 Primary experiment - Polarity reversal 2

The experiment was conducted again, however this time when the polarity is reversed, the signal generator is turned off to ensure that there will not be an ion trap at the electrode. Two drops of 10% salt solution is used again with a 90volt plate voltage. The AC voltage supplied to the electrode is 1 volt at 1000hz frequency.

Table 2 - Table showing the voltage increase over time for 10% salt solution

Time, minutes	voltage input, volts	voltage output, volts
0	0.987	0.96
10	0.968	1.28
12	0.964	1.46
14	0.964	1.68
16	0.96	1.87
18	0.96	2.02
20	0.96	2.11
22	0.96	2.2
24	0.96	2.26
26	0.96	2.3
28	0.96	2.34
30	0.96	2.38

An interesting point to note is that now that the input voltage is being measured, as the output voltage increases from the introduction of salt ions, the input voltage begins to decrease. Therefore, it is not accurate to assume even if the supplied voltage to the electrode is 1v, this voltage remains constant. A new measurement parameter, “voltage gain” is now used as the primary measured component when conducting experiments. This measured gain can be calculated simply by diving voltage output by voltage input. Table 3 will show these new values.

Table 3 - Table showing gain values at different time intervals

Time, minutes	voltage gain
0	0.972644377
10	1.32231405
12	1.514522822

14	1.742738589
16	1.947916667
18	2.104166667
20	2.197916667
22	2.291666667
24	2.354166667
26	2.395833333
28	2.4375
30	2.479166667

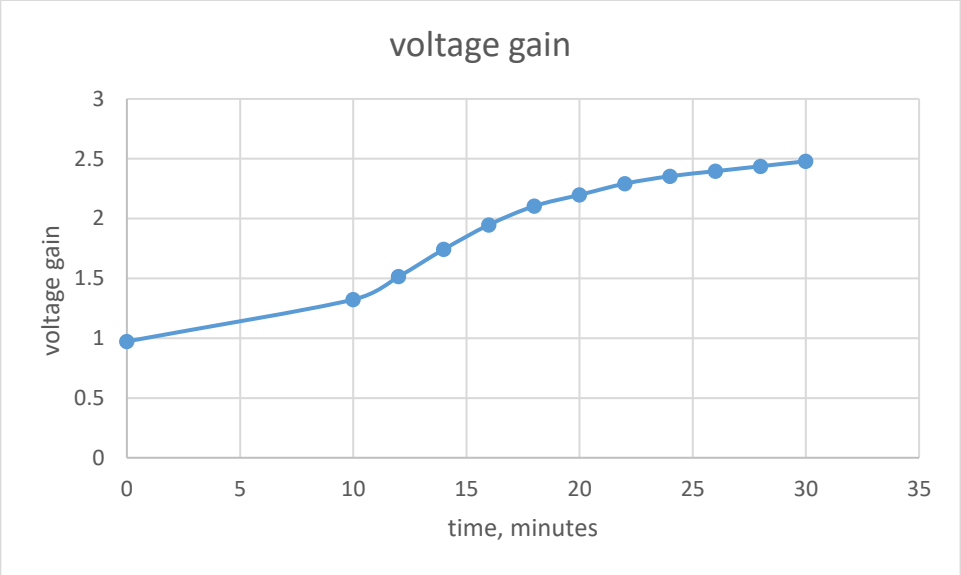

Figure 48 - graph relating to the voltage gain over time

Now that the salt has been “loaded onto the electrode. The Sample is left for some time with the signal generator on the electrode turned off. This will hopefully cause any ions trapped within the electrode to be released and free to move back up towards the well as the polarity is reversed.

The signal generator is turned on for a small amount of time periodically, to measure the changes every few hours as a voltage is needed to make any input or output measurements across the electrode.

12.1.8.1 Results

After around three hours of constant monitoring, it is discovered that the output voltage increases and stabilises, but however does not reduce. This means that the salt ions have either failed to move away from the sensing area or that chloride ions have influenced the reading on the output measurements. Without visual aid, there are no clear conclusions that can be made aside from some speculation.

12.1.9 Section Conclusion

For this segment, the experimental setup has been able to measure changes in voltage caused by the introduction of salt particles. Though the varying of plate voltage should technically have a linear relationship on the rate of travel on salt ions, it is shown that the motion is somewhat random. This could be due to the external influences as discussed in the relevant experimental conclusion above.
The polarity reversal experiment has failed to read a reverse trend in the output voltage measurement reading. A visual aid could be useful in diagnosing the events that occur after the polarity is reversed, however this requires a high powered microscope to view individual ions. Dyed ions could also be used, however this would still require a high resolution display and a powerful camera or microscope. However it could be theorized that by reversing the polarity of the plate, considering salt contains Na and Cl ions, this would mean that the overall affect could be the same.

12.2 Ionic transfer experiment

This experiment mimics the change of internal dielectric properties by introducing DI water periodically to a cell that already contains a liquid with foreign conductive substances. Additionally, this experiment also sets out to determine whether the electrostatic field that is produced by the signal generator on the electrodes suspend the salt ions within its vicinity. The purpose is to ensure that the readings taken when concentrations change are accurate within the cell as having suspended ions when more or less dielectric material is added may influence the measurements taken. A slow stream of deionized water is introduced into a cell containing 10% salt solution. The stream is introduced in a controlled manner to simulate a gradual change in salt concentration as a faster flow may forcefully carry salt particles, whereas a slower rate will ensure the salt particles will be slowly removed from the cell allowing whatever processes that occur closer to the electrodes to still occur.

12.2.1 Experimental Setup and Construction

The sensor holder is first set up by placing the electrodes within it and adding 10 drops of 10% salt solution onto the opening. The top of the sensor holder must be screwed in securely as the salt solution within it must not leak through any potential gaps within the cell as this will adversely affect the outcome of the experiment. The initial parameters are set from the signal generator at 1volt peak to peak AC signal and a frequency of 1000Hz. The output is then measured at this initial stage to be 3.0 volts.

The setup of the experiment requires two beakers, one containing DI water which would flow into the cell and the second would receive excess water that would overflow from the cell. A two port stopper would be placed tightly above the cell which would house the pipes from both beakers and to prevent any leakage from the cell. A pipe will first be placed between the stopper and the “receiver” beaker and the pipe from the DI water would have a clamp placed securely on it. A syringe is used to create a siphon and the clamp would be tightened until desired flowrate is achieved, which would then be fitted into the stopper.

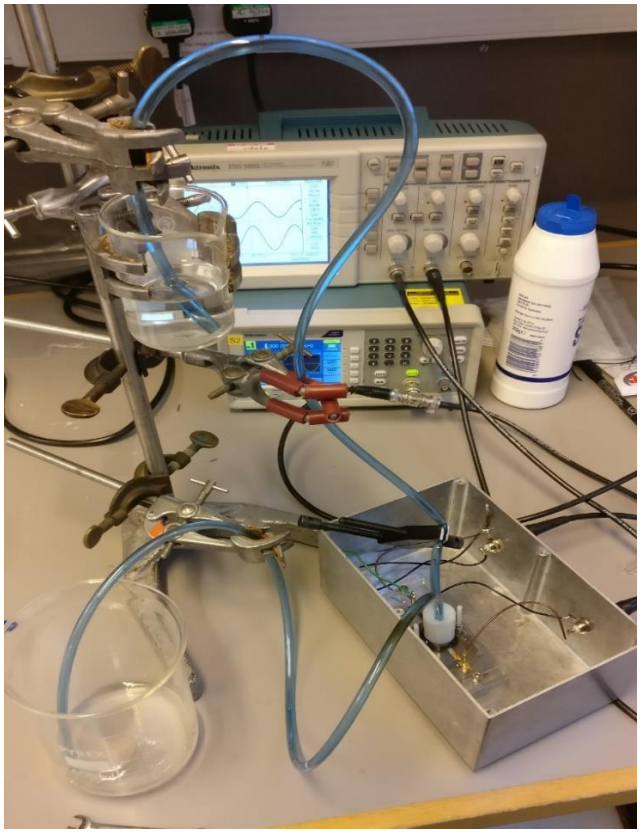

Figure 49 - image shows the full setup of the ionic transfer experiment

12.2.2 Experimental Predictions

Through the supply of uncharged de-ionized water, the zone of saturation should slowly begin to lose charged ions as the liquid within the sensing area starts to overflow and a fresh supply of de-ionized water is introduced.
This would mean that as less conductive liquid enters the sensing area, this will alter the dielectric properties within and the voltage readings measured will alter accordingly. This would mean that at the start of the experiment, the value of voltage across the sensor will be high and as the sensing area slowly fills with water, the voltage will begin to drop steadily until a value close to zero will be reached.

12.2.3 Problems faced during experimentation

One of the main issues surrounding this setup is ensuring a slow enough water flow through the tubing. Several vices were used to tighten restrict the water flow at different sections of the tubing. Since the tube is transparent, the water flow could be calibrated by sight easily before being introduced into the setup.
Attaching the tubing onto the setup may cause some water to flow out of the setup and across to the wires, paper towel is kept nearby so that this excess water could be removed quickly.
The amount of water used to obtain the lowest possible voltage across the sensor means that the beaker must be refilled constantly to ensure a constant supply of DI water. If the water runs out before it has been refilled, this will form air bubbles that will slow down the process of the experiment. When an air bubble is formed, the experiment must either be restarted, which is a long and tedious process, or the timer must be stopped and the water must be forced down the tube using a wire so that the air bubble can be removed.

12.2.4 Procedure

The electrode is placed within the sensor holder and a few drops of 10% salt solution is added onto the sensing area, enough to cover the entire sensing region, the value for output voltage is recorded, this is the initial output voltage value.
The sensor holder is secured within the metal box enclosure and a beaker is filled with DI water. Two vices are securely attached around different sections of a tubing and placed in the beaker. A syringe is used to draw water from the tube, creating a siphon and the tightness of the vices are manipulated until desired flowrate of DI water is achieved.
The tubing is placed into the nylon round stopper and inserted carefully into the lip of the sensing area. A second tube is inserted into the second hold within the rubber stopper and the other end is placed into an empty beaker, this will cause excess water from the sensing area to draw out into the beaker. As water is introduced into the sensing area, the changes of voltage is recorded over time.

12.2.5 Experimental results

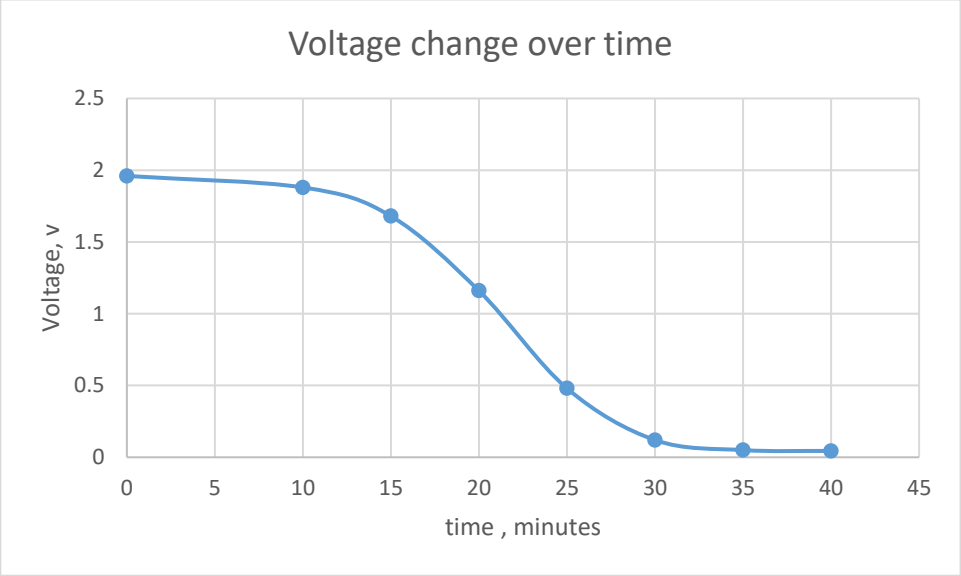

Figure 50 - Graph representing the voltage change over time for the ionic transfer experiment

The graph in Figure 50 shows the initial voltage at the output decreasing over time. For about 15 minutes, the water from the first beaker will start to flow through the tube and into the sensing area. The decrease of voltage in voltage occurs when the concentration of salt solution begins to reduce as the solution becomes more diluted and the number of salt ions start to decrease as the water excess water flows out of the sensing area. The lowest possible value reached for this experiment is 40milivolts. This value is then compared to the voltage output when there is only DI water in the sensing area. After the completion of the experiment, the electrodes are cleaned and DI water is added into the sensing area and the voltage is measured across it. The value recorded is 28 milivolts, which is only slightly less than the measured value across the electrodes in the ionic flow experiment.

12.2.6 Section Conclusion

It can be concluded that since the voltage reduction from the slow dilution of the salt solution reaches close to the value of the output voltage when only DI water is present, an ionic trap is not formed when the sensor electrode is active. The experiment has succeeded in measuring a voltage close to the actual value of DI water only. The slow introduction of fresh DI water means that the salt solution is not flushed quickly through the exit tube meaning that if an ionic trap were to form, the salt ions will still be suspended within the electrode. It is not the case however as the value of output voltage reached a low minimum point thus proving the absence of an ionic trap.

12.3 Supplemental Experiment - Visual iodine characterisation

To study the motion of the travel of charged particles, a visual experiment may be able to provide a more reliable representation of the occurrences within the cell. However due to the compact nature of the sensor holder an alternative setup has been devised which would provide the user with a clearer view of the experimental process.
Iodine is used in this experiment as it has a dark red/brown colour which would clearly indicate the position of the particles. As iodine exists in crystal form and store-bought iodine solution is usually in Potassium Iodide form, to fully isolate Iodine particles, iodine crystals are submerged in water over night, and the brownish-red precipitate is collected to be used in analysis

12.3.1 Setup and Construction

An unmeasured amount of iodine crystals were placed in a beaker of de-ionized water to allow for the iodine molecules to freely travel within the water. At first, there was very little change, however through slight agitation and with time, the de-ionized water slowly started to change colour. Iodine crystals did not dissolve thoroughly within the liquid, however the crystals do break down slightly and cause some discolouration within the liquid.
Two 1ml vials were half filled with molten 1% agarose solution and left to cool until the gel has fully hardened. A few drops of equal parts iodine water was placed in each vial until a visible meniscus is formed on the top of each vial. The vials are then covered with an air tight stopper to avoid spillage, stop the iodine from evaporating and the agarose from over-hardening.
At the initial stage, an image is taken of both vials with a camera, so that comparisons may be made. The first of the two vials are placed in between two copper plates and the second is used as a control. 96 volts were measured from using ten 9 volt batteries in series and attached to the copper plates.

12.3.2 Experimental considerations and minor details

There are a few things to consider for this experiment as Iodine is considered mildly harmful. During the course of the experiment, extraction, transport and manipulation of iodine crystals and liquids are handled with tweezers, gloves and spatula. Measurement and initial dilution of iodine crystals are done within the clean room, under a laboratory

safety bubble as iodine fumes are considered an inhalation hazard. The California Department of Justice from the Bureau of Forensic Sciences Senior Industrial Hygienist, Mark Cameron states ; “Iodine vapor(sic) is intensely irritating to mucous membranes and adversely affects the upper and lower respiratory system” and he further explains that inhalation of iodine vapour may lead to chest and throat complications and cause headaches [42]. Contact with iodine may also cause irritation, burns and will also be absorbed through the skin therefore inhalation and skin contact must be avoided.
When agarose is filled, both vials must contain the same amount of solution and the meniscus levels must have the same curvature as to ensure that the levels of iodine travel can be accurately compared. This can be done by avoiding air bubbles through slow insertion of molten agarose into the vial and accurately measuring agarose solution either by measuring weight or volume. The meniscus levels may still vary either way, therefore when using a pipette or syringe to insert the agarose, the solution must be filled straight to the bottom of the vial and any contact with the sides of the vial must be avoided. This has to be done carefully as the vials are rather narrow. Contact with the sides of the vial may cause the agarose to stick to the vial and slowly flow to the bottom, either prolonging the filling period or causing weight and volume measurement inaccuracies if hardened while still attached to the sides. A more reliable method of “measuring” meniscus levels is by placing both vials close to each other on a flat surface and comparing the levels by eye. This may be the best method however air bubbles will have some adverse effects on the consistency of the experiment, if present.
The two vials must be tightly sealed after agarose and iodine solution is added. In fact, it is advised that iodine must be inserted in to the vial almost immediately after the agarose hardens as to prevent a number of different scenarios.

- Drying out of the agarose solution
- Iodine evaporation and subsequent release of harmful fumes
- Spills and accidents

All of the above points contribute to a few additional problems such as anomalies in the rate of flow of ions and health and safety concerns.

12.3.3 Experimental Predictions

It is predicted that the external electrostatic fields would either cause the attraction or expulsion of Iodine ions. In the oxidation state for Iodine, in which the state for the loss of electrons occur, the ions are identified as Iodides and holds a negative charge, with the symbol being I^-. With this being the case, the positive plate is placed on the bottom of the vial in order to attract the negatively charge ions. As the iodine is brown in colour, the ionic motion is expected to be visible to the naked eye, as compared to salt ions, which are

colourless. Thus, when compared to the control, the vial with the external field is expected to have a band lower than that of the control, signifying that the external field has assisted in the motion of the ions through the agarose solution.
Another prediction would be that the band of colour formed by the electrostatically assisted vial would be faint as a result of the higher acceleration and spread of the ions. The unassisted vial would be less spread out and have a thicker band of colour as the acceleration of ions would be slower or even non-existent, depending on if there is any motion at all through the agarose.

12.3.4 Experimental results and observations

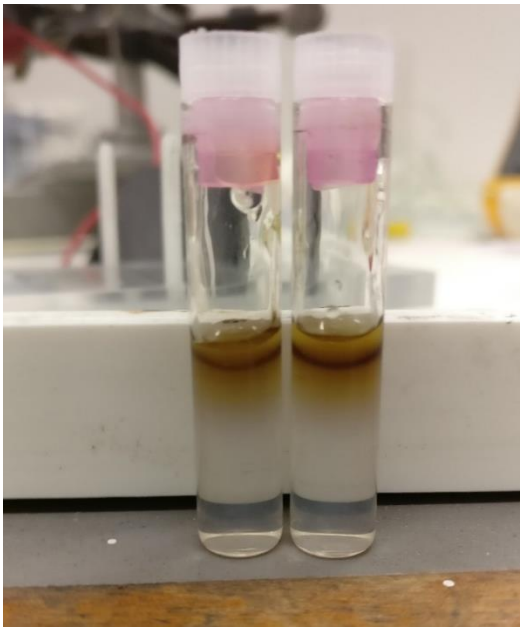

Figure 51 - Image of the iodine samples before experimentation

An image shown in Figure 51 is taken prior to subjecting the vial to the electrostatic field. The picture is taken against a white background to clearly indicate that the miniscus levels of both vials for the iodine are roughly equal. One of the vials is placed in between the two copper plates and subjected to 96volts. After 24 hours, the vials are observed.

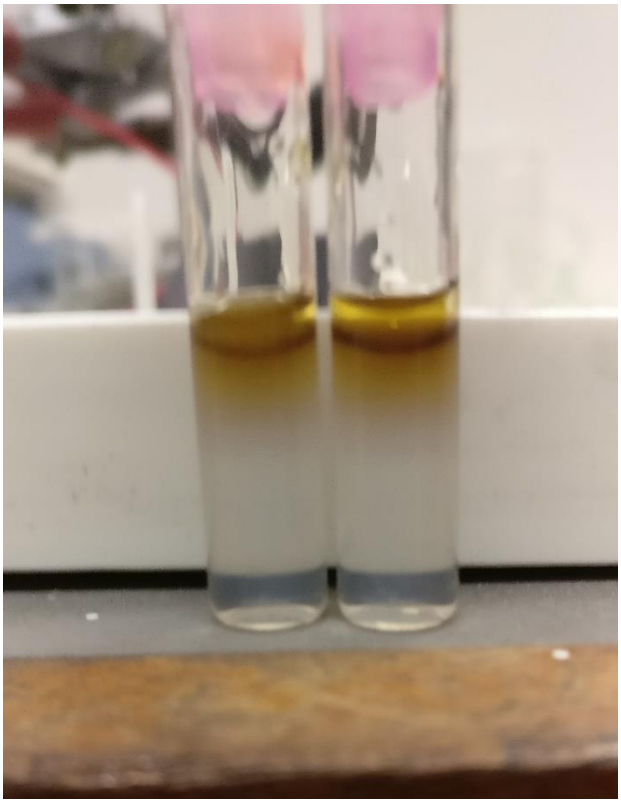

Figure 52 - the two vials after 24 hours

The vial on the left was placed in between the 96 volt plates and the only visual difference is the slight thinning of the iodine band. It was hoped that there would be a clearer indication of movement of the brown iodine particles by showing that the band of iodine particles being further apart from each other.

12.3.5 Section Conclusion

In this section, two vials containing agarose and iodine crystal solutions were used to visualise the motion of coloured iodine solution through agarose gel. One vial was left without any plate voltage across it, whereas another was placed in between two 96volt copper plates. The experiment was left for a period of time and images were taken before and after a 24 hour period.

It is unclear whether the slight discolouration was caused by the presence of the plates. It could be concluded that the iodine particles moved away from the meniscus at the top of the gel layer however the initial pictures show that the meniscus band was not as thick to begin with.

The distance between the plates here is quite far therefore it could be theorized that the electric field generated would not be strong enough to repulse the iodine molecules through the gel. A stronger field could technically have been able to do this.

12.4 Double Mesh experiments

The purpose of the double mesh experiment is to determine whether the electrostatic fields that are formed between two parallel plates form an “electron trap”, causing ionic particles to be stuck within the plates. Furthermore, the double mesh experiment will consist of a perforated mesh that will allow for ions to travel through the sensor, with hopes that when the ions that have travelled past the mesh will collect at the bottom of the sensor and voltage readings will steadily decline as all available ions disperse through the sensing area.

An experiment will be devised first by using stainless steel mesh as a preliminary study to determine the viability of the experiment and then the steel mesh will be gold plated in order to conform to the continuity of past experiments. The experiment will also study the effect of higher concentrations of ions and the effect on the measurements recorded.

12.4.1 Setup and Construction

The main sensing element in the Double Mesh experiment consist of 2 sheets of stainless steel that is cut into equal sized plates, with small perforations that allow for ions to pass through but also mimics the capacitive detection method as seen in earlier experiments. A polythene sheet is placed in between the two metal plates to prevent direct contact and potential short circuit, however a small circular hole is cut in the middle to allow for the liquids within the experiment to fill the entire working area.

The working area of the cell are two cylinder shaped plastic pieces with a central hole on the top and bottom. To prevent unnecessary leaking, the bottom cylinder is not drilled the whole way through when measured substances are added. A parallel “side fill hole” is added on the bottom plate so that gels can be added to the cell and to prevent bubbles from forming which will adversely affect the accuracy of measurements and prevent linear ionic motion. Runnier liquids may also be inserted this way via syringe and leaking will not occur provided the syringe remains attached to the side fill hole or a plug can be used to cover the hole if a top fill method is preferred. Additional holes drilled onto the cylinders, mesh and polythene as required so that the pieces screwed together to form the complete setup.

Finally a top cap for the setup is created using round nylon 66 bar with shaped protrusions to help form the well in which aqueous solutions may be dropped into. This is fitted to the top of the setup before the introduction of agarose solution so that when inserted, the agarose solution will harden to the shape of the protrusions. A smaller hole is also drilled on to the top of the cap and fitted with a tube so that the excess agarose does not spill from the setup and cause a mess.

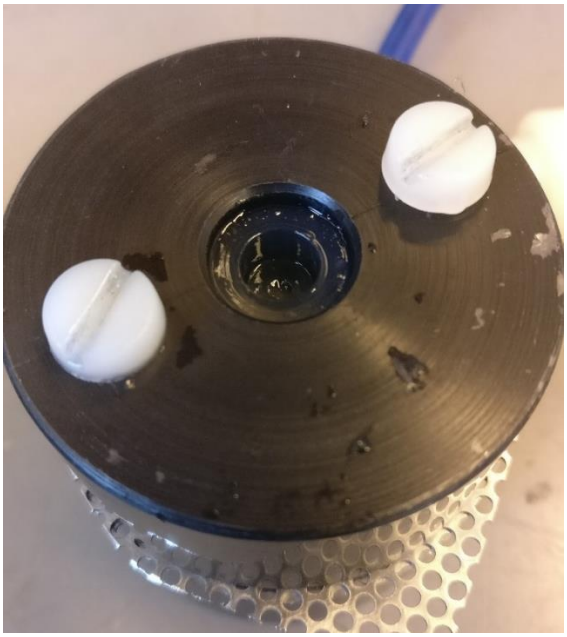

Figure 53 - image of the "well" caused by the nylon stopper indentation.

Figure 53 represents the “well” that is caused by the nylon stopper. The salt solution used for the experiment will be placed within it, though only a small amount is placed to ensure the well does not overfill.

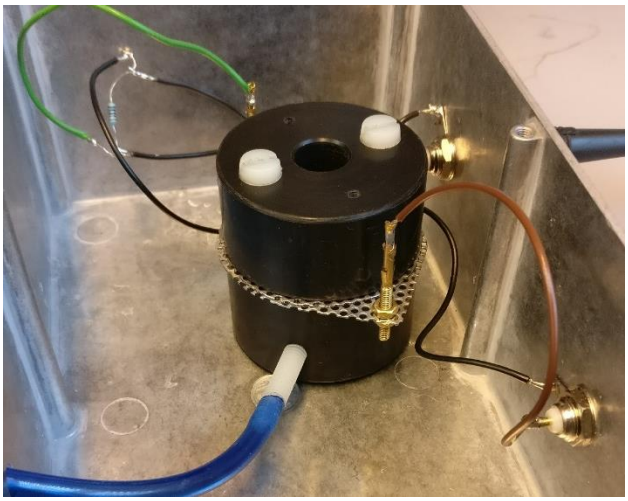

Figure 54 - the complete double mesh setup within the metal enclosure

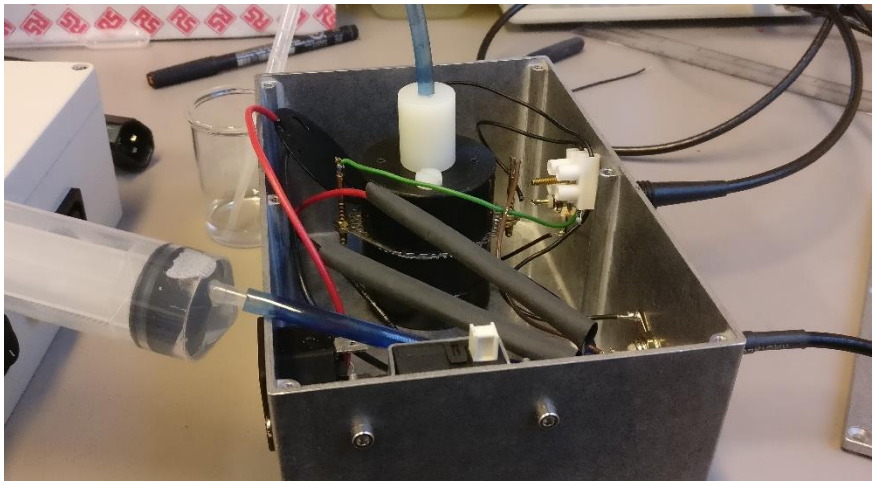

Figure 55 - the process of injecting agarose

Figure 55 shows the placement of the syringe when the agarose is injected into the double mesh cylinder construct. The top stopper can be seen above the top of the cylinder, which is where the excess agarose will flow out from.

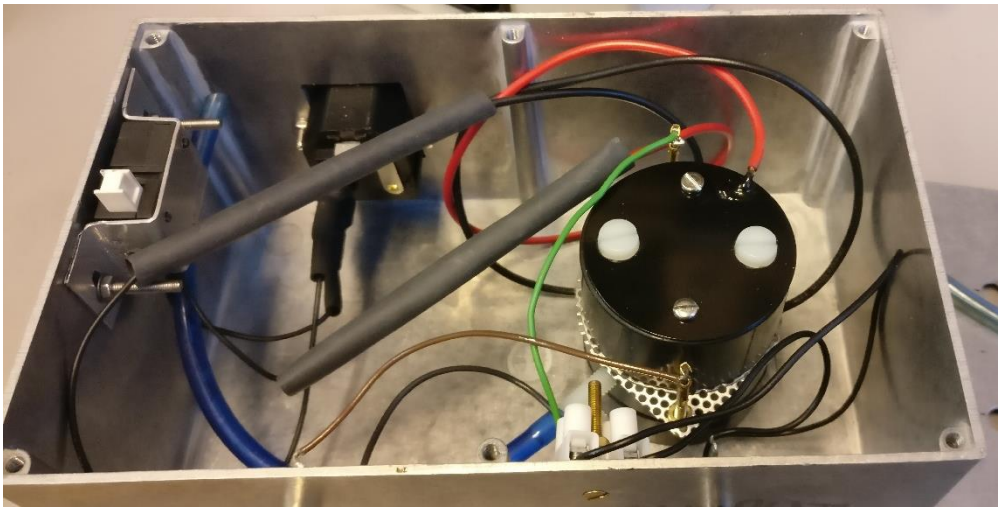

Figure 56 - the end phase of the construction, before experimental measurements begin

Figure 56 shows the top voltage plate attached onto the top cylinder and the connections that are made. The green wire represents the output voltage to the oscilloscope. The red wire provides the positive plate voltage.

12.4.2 Experimental Considerations

Due to the size of the plastic cylinders, the effective distance between the copper plates have now been increased considerably. This presents several new variables if past experiments were to be replicated. An increase in distance between the plates coincides with a loss of force acting on ions and an increase of distance for the ions to flow which ultimately will increase the time for the experiment to run one complete cycle. Whether these changes are linear or have a compounding negative effect will have to be analysed

in preliminary experimentation. A simple solution is to increase the voltage supplied to the copper plates. This means that an excess of 200volts may be needed to increase the efficiency of the experiment. Using these many 9v batteries however may cause some health and safety concerns and therefore the battery pack may have to modified to account for these extreme conditions.

The meshes are made out of stainless steel and when cut contain many sharp edges. To prevent the possibility of injury, the stainless steel plates are cut to fit the shape of the of plastic cylinders to limit the protrusion and exposure of jagged edges. Wet and dry is also used to smooth out the sharpest edges and prevent damage to the polythene sheets and the handler. A small lip on either side of the plate is left on opposite ends of the two plates to form the contacts needed for measurements to be made.

As the plates are made of stainless steel, directly soldering on leads would be difficult. There are two possible solutions devised for the connectors. The first would be to attach crocodile clips onto the mesh directly. This does cause a slight inconvenience however as the crocodile clip cables would have to have a 100ohm resistor soldered in series between the setup and the signal generator and third wire would have to be soldered in to make a parallel connection to the input of the oscilloscope, so measurements can be taken. This is an unnecessary step as the previous setup already these features built in to it. Therefore it would be a better idea to simply drill a hole into the very sides of the mesh and place the connector clips used previously and integrate these two setups. That way the sample enclosure can be used to run both experiments interchangeably, saving time and resources in the process while maintaining some versatility.

12.4.3 Plastic cylinder and steel mesh/polythene sheet sandwich assembly

Before the assembly of parts, the solutions involved are first measured and mixed as per usual as the agarose requires time to form and ensure that the battery packs are assembled and ready to use.

The polythene sheet is placed in between the two stainless steel plates while ensuring correct alignment of the three holes. The plate orientation can be altered so that the mesh shape is purposely misaligned in order to control the size of the gaps between them, this also simultaneously increases the volume of individual holes per area for the mesh couple. The top plastic cylinder is then placed above the mesh and the screws are inserted in the two side holes to hold the mesh/polythene sheet sandwich so that the bottom plastic section can be fit without having to worry about accidentally misaligning them. The screw posts are tightened up to complete the setup.

12.4.4 Measurement and analysis techniques

In this assembly, the ionic substances pass through the gel due to the electrostatic field applied from the parallel plates. The mesh plays the part of two parallel electrodes with the agarose acting as the dielectric separation layer between the two meshes. This is similar to the ionic transfer experiment however instead of being a horizontal measurement, the measurement is done in a vertical alignment.

12.4.5 Procedure

Agarose solution at 1% concentration is prepared and heated up at 120-150 degrees on the hot plate. While waiting for the agarose particles to fully integrate into the solution, the plastic and steel mesh is assembled as discussed in the earlier section. The salt solution needed for the experiment is also prepared during this time.

After the agarose solution has been fully formed, the mixture is stirred slightly to incorporate fully.

All the connections from the input and output of the oscilloscope are connected to the meshes and the plates are attached to the battery pack. The top stopper is added on to the top hole of the plastic cylinder and secured evenly.

A large syringe is used to collect some of the agarose mixture and the mixture is carefully injected into the hole in the bottom of the plastic enclosure. The agarose mixture is allowed to flow through the setup until the mixture passes through the tubing of the top stopper. If the agarose level starts to drop visibly back down the tubing, more agarose from the syringe is added until there is no more visibly movement. The injection process must be done slowly and carefully to avoid air bubbles from forming within the setup. The syringe must also be left in the tube during the hardening process to ensure the agarose does not flow out of the setup through the bottom entrance hole.

The agarose solution is then left to harden and settle for 20-25 minutes in which after the top stopper can be removed and cleaned and the syringe can either be cleaned or discarded depending on how many times the syringe has been used or how much agarose residue has hardened within the syringe. Additional agarose must not be added in after the gel has hardened as this may disintegrate the gel already within the setup. The gel must also be fully harden before the top stopper is removed as this will cause the agarose well to not keep its shape.

Salt solution is added onto the well formed by using a pipette. Two drops are sufficient to cover around 50% of the well volume. Adding too little may impede the speed of the experiment, adding too much may cause the liquid to seep through to the top of the well and directly onto the mesh through the sides of the agarose enclosure.

The top and bottom plates can then be screwed firmly onto the setup and the timer be started immediately. Measurements of the initial values are taken first and at time intervals thereafter.

After the experiments have been completed, the experimental setup must be cleaned thoroughly. To clean the setup, remove the plastic cylinder from the sensor holder and disconnect all the batteries. Remove the plates from the top and the bottom of the cylinder and remove the oscilloscope connections. The cylinder screws are then all removed and separated into all it's base parts, the cylinder top and bottom and the two meshes.

The hardened agarose within the cylinder top and be easily removed by patting firmly onto the palm of the hand and discarded. The cylinder top is then cleaned with soapy water and placed on some paper towels. A syringe is filled with clean water and then inserted onto the entrance point of the bottom cylinder piece. Pressing hard into the syringe will cause the gel to expel from the bottom cylinder piece and must be done where the hole from the cylinder is facing a sink. This is to avoid any of the gel from causing a mess on the laboratory floor. The excess remains of the gel in the cylinder can then be washed out using water from the faucet or running water from the syringe repeatedly. Soap and water is again used to clean the entire base after all of the gel has been removed. A paper towel is then used to wipe the inside of the hole and the cylinder is placed on a separate paper towel to dry completely.

A pair of rubber gloves is needed to clean the two steel meshes. Running water is first used to wash any gel that remains on the mesh and soapy water is used to clean the meshes. If there are gel remains within the crevices of the mesh, compressed air with a narrow nozzle attachment is used to clear out these crevices or a pair of tweezers can be used carefully, as to avoid scratching the mesh, to remove any of the remaining gel. Finally the centre of the mesh is cleaning by using IPA and excess IPA is cleared from the mesh using compressed air.

The top stopper can also be cleaned by using a syringe with soapy water to remove excess gel, and the soapy water flushed repeatedly with clean water and left to dry. The polythene sheet is cleaned with simply with soapy water and rinse with clean water before being left to dry on a paper towel.

After drying completely, the meshes are placed in a clean ziplock bag, and the cylinders are kept separately. All the screws, nuts and bolts are also placed in a separate bag so they are not lost.

12.4.6 Preliminary Experiment 1 - Setup familiarization

The purpose of this experiment is to familiarize the user with the new setup and to put established experimental procedures into practice.

The parameters for the first experiment are;

- 1 % agarose solution
- 10% salt solution
- 1khz sensor input at 1volt peak to peak
- 95.6 volt plate voltage

Before the agarose was added, the voltage output across the two meshes were;

- 1 volt mesh input
- 40mv mesh output

After the agarose was added these voltages then changed to;

- 968mv mesh input
- 1.38v mesh output

The start time of the experiment was at 12:17PM and the table of results are as follows.

Table 4 - table showing the first hour of experimentation for the double mesh experiment

Time (minutes	Input (volts)	Output (volts)	voltage difference
0	0.968	1.38	0.412
20	0.968	1.38	0.412
30	0.968	1.35	0.382
40	0.968	1.37	0.402
50	0.968	1.38	0.412
60	0.968	1.37	0.402

Table 4 shows the first hour of experimentation. As noted, there were no considerable changes throughout this hour and this behaviour was very much not the expected outcome of the experiment.

From that point onwards, an additional 3 drops of 10% salt solution was added and the experiment was resumed. The results following this change is shown below.

Table 5 - table showing the changes in voltage after 3 drops of salt solution were added

time (minutes)	input (volts)	output (volts)	difference	total change
0	0.968	1.38	0.412	0
10	0.968	1.41	0.442	0.03
20	0.968	1.43	0.462	0.05
30	0.968	1.45	0.482	0.07
40	0.968	1.47	0.502	0.09
50	0.968	1.51	0.542	0.13

60	0.96	1.54	0.58	0.168
70	0.96	1.58	0.62	0.208
80	0.96	1.62	0.66	0.248
90	0.96	1.66	0.7	0.288
100	0.96	1.7	0.74	0.328
110	0.96	1.74	0.78	0.368
120	0.96	1.78	0.82	0.408
130	0.952	1.82	0.868	0.456

The data here now shows the corresponding values of change over time for the mesh setup. One point to note that the values of voltage at the output should not be measuring above 1volt as the input supplied to the meshes are only 1 volt. It is unknown as to why this has caused the output values to be higher than the input value though it may be due to some of the settings on the oscilloscope that have changed the scale of the output readings.

The graphs for the experiment can be seen below.

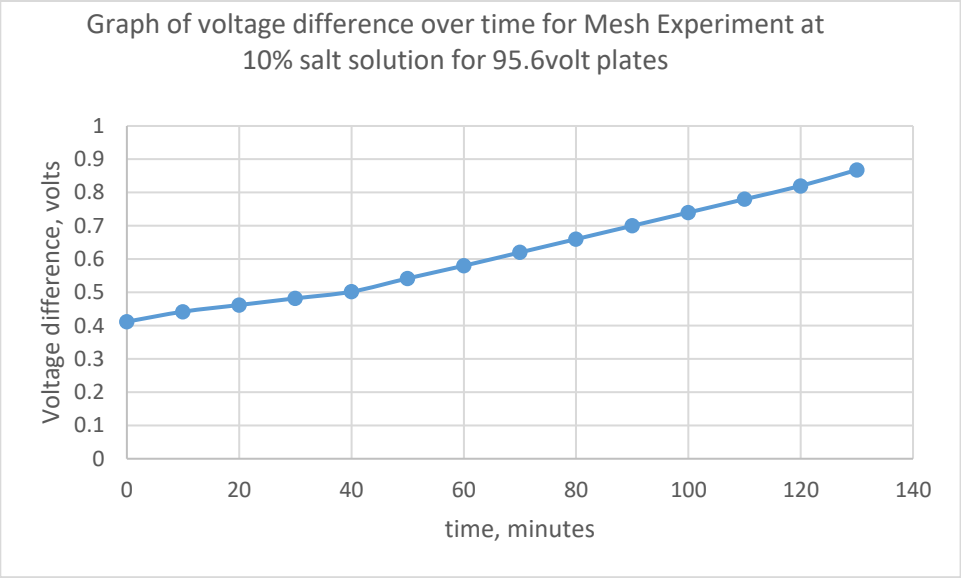

Figure 57 - Graph relates to the voltage difference over time for the double mesh experiment

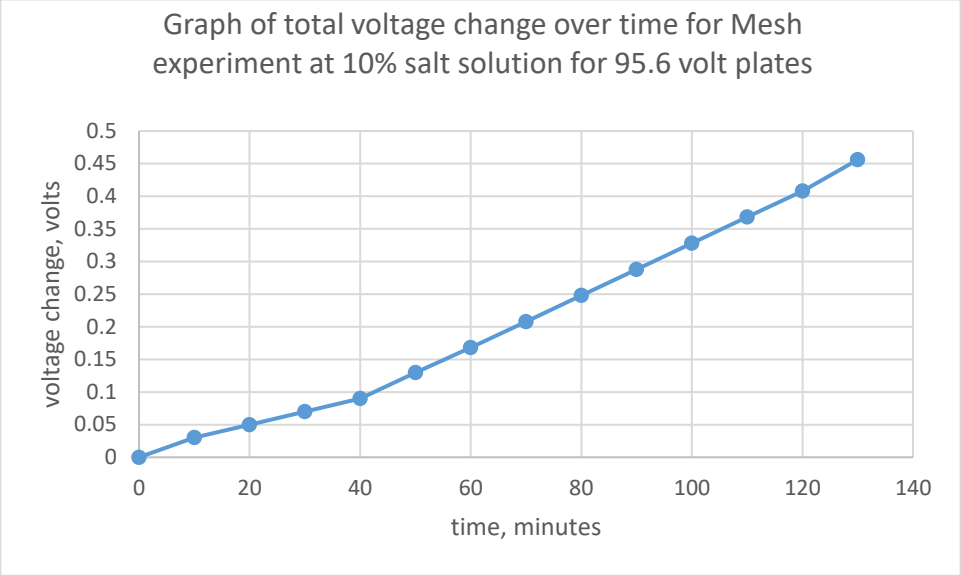

Figure 58 - Graph relating to the total voltage change over time for the double mesh experiment

Both graphs in Figures 57 and 58 show the steady rate of increase in voltage output over time for the double mesh experiment after 3 additional drops of salt solution was added into the agarose well.

12.4.7 Preliminary Experiment 2

Preliminary experiment 2 is to measure the output changes across the mesh without the presence of plate voltage. The experimental procedure is unchanged.

The parameters for this experiment are

- 1 % agarose solution
- 10% salt solution
- 1khz sensor input at 1volt peak to peak
- 0 volt plate voltage

Table 6 - table showing the double mesh experiment without external electric field

time	input voltage	output voltage	voltage gain
0	0.948	0.175	0.184599156
20	0.948	0.175	0.184599156
30	0.948	0.175	0.184599156
40	0.948	0.175	0.184599156
50	0.948	0.175	0.184599156
66	0.944	0.199	0.210805085
73	0.928	0.209	0.225215517

83	0.928	0.219	0.235991379
90	0.924	0.228	0.246753247

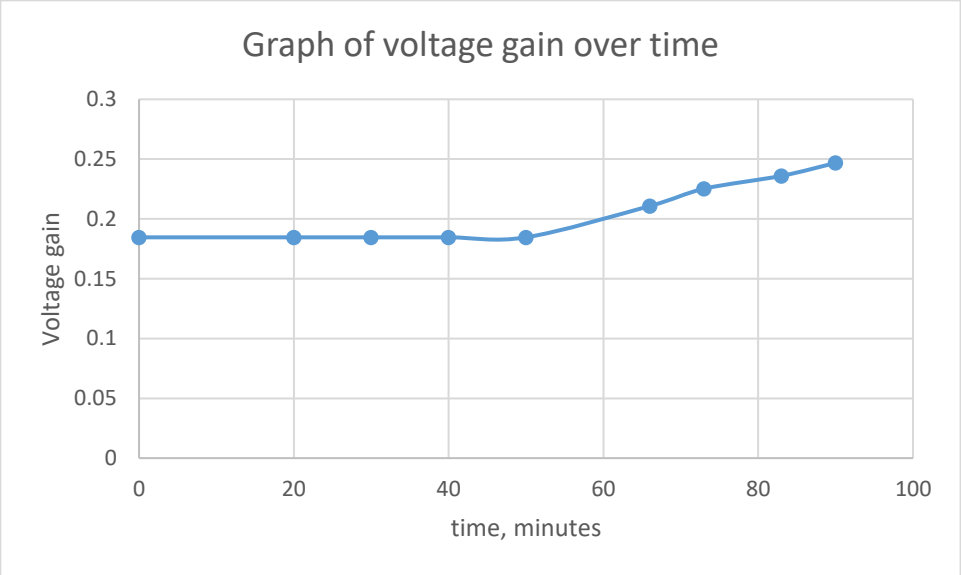

Figure 59 - graph showing the increase of output voltage over time

The graph in Figure 59 shows in the absence of a plate voltage, it will take around 40 minutes for a change to be measured across the meshes.

12.4.8 Experiment modification

This section underlines the steps that are taken to modify the current experimental setup to improve the performance, accuracy and speed of the experimental procedures. A battery box is designed to safely house 200volts supply voltage used to generate a field across the copper plates. Silicone sheets are used to create an airtight seal to prevent moisture loss in the experiment and to prevent the agarose from drying out. The meshes are gold-plated to provide consistency with the capacitive electrode loops and the top cylinder is reduced in size to shorten the initial transit time of the salt ions towards the mesh.

12.4.8.1 The battery box

Since the scale of the experiment has been increased dramatically, the voltage supplied from the initial battery pack no longer supplies adequate voltage across the plates, this is caused by the wider gap between the positive and negative plates. To account for this increase work area, a specialised battery pack is constructed to provide the necessary voltage across the plates that will generate a far larger electrostatic field.
However, having a large supply voltage also means some strict health and safety

measures must be taken.
A plan is drawn to first ensure that the battery pack will contain measures to prevent hurting the user. Therefore the entire battery chain will be contained within an insulated box. Holes are drilled within the box to contain sockets needed for the entry of IEC power cables.

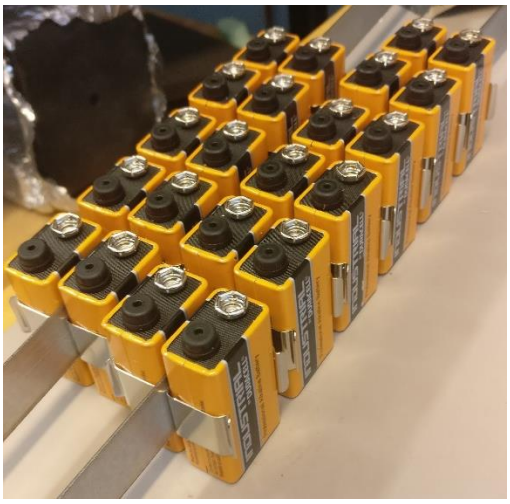

Figure 60 - image of the constructed battery cage

Figure 60 shows the total amount of new batteries used in the modified battery pack. The steel brackets will hold the batteries firmly in place to stop them from thrashing around in the box when being transported. The batteries can be removed as needed from each bracket through careful movement of the prongs that hold them in place. If roughly handled, the prongs could scratch the surface of the batteries and cause damage. However, there really is no need to move the batteries around from the bracket after final placements have been made as voltage manipulation can be done without removing batteries from the brackets.

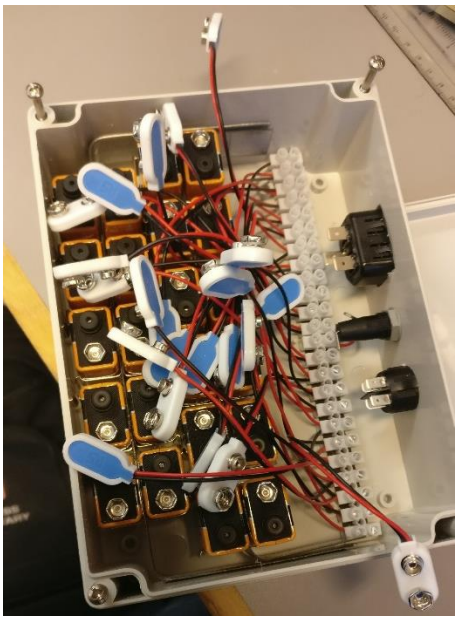

Figure 61 - image of the battery cage fitted into the battery modification box

Figure 61 shows the battery brackets having been bent to fit to the shape of the battery enclosure and placed within it. Several 9v battery connectors are then placed in a series of 6mm brackets and placed along the side of the box. this will help the battery box supply variable voltages needed to the experimental setup. Also seen in the image is the position of the switch, a fuse and the power cable input connector.

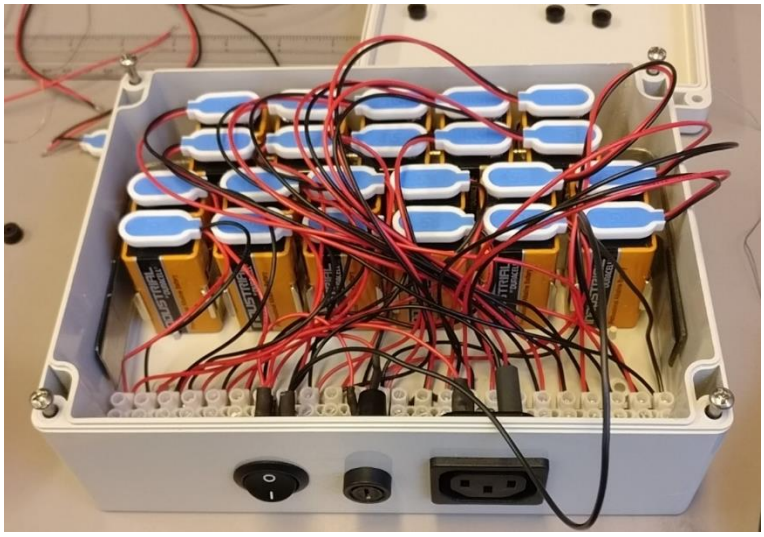

Figure 62 - Image of completed battery pack before the wires were cut to fit

Figure 62 shows the completed attachment of all 9 volt battery connectors in series as well as connections made between the battery and the switch, fuse and power cable connector input. The loose wires are trimmed as necessary and tucked neatly within the

enclosure to prevent wires from loosely hanging out from the box.
If necessary, the connection from the end of the battery line can be moved anywhere in between the series of battery connections to control the voltage output supplied by the battery box. Though not the most ideal way of controlling the output voltage, this is the most convenient as it does not require external components or additional electrical switching. For the purpose of the laboratory experiments run, this setup should be sufficient.
Interlock switches are added in both the sensor enclosure and the battery box as a safety measure. This is to prevent a connection from being made if any of the lids of both boxes are not firmly secure.

Figure 63 - Image of the sealed power supply box used to provide the copper plates with voltage

Figure 63 shows the completed box with the cover screwed onto the box. Warning stickers are printed and stuck onto the box as a safety measure to prevent those unfamiliar with the battery box from handling it.

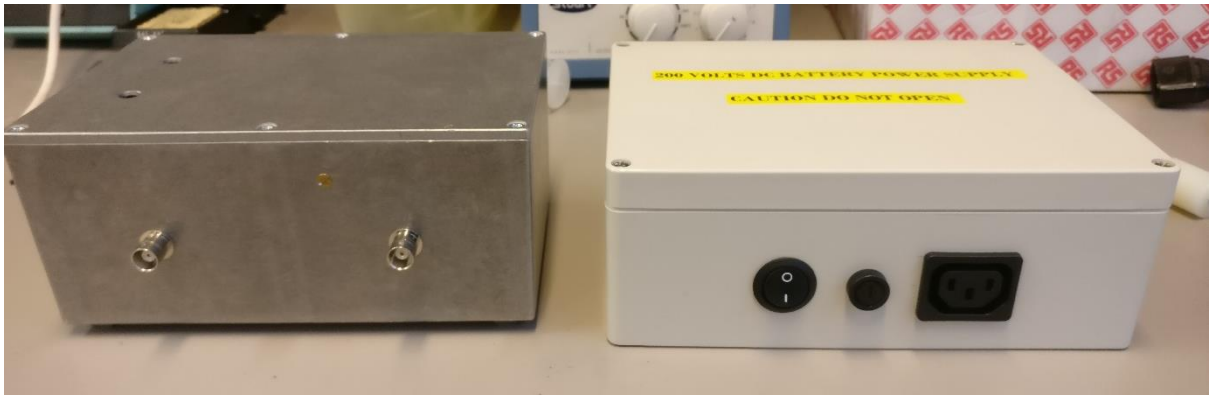

Figure 64 - Image showing the comparison between the battery box (right) and the sensor enclosure (left)

12.4.8.2 Silicone Sheets

To fix the sealing problem from the original setup, the polythene sheet is no longer used in upcoming experimental procedures. In its place, silicone sheets are used as an alternative. One sheet is placed in between the two meshes to act as a separation layer. Two other sheets are used on either side of the mesh, in between the first mesh and the top cylinder and another between the bottom mesh and the bottom cylinder. based on the placement of these silicone sheets a large central hole and two side holes are drilled onto all three silicone sheets to accommodate the screws that hold the setup in place and also as a means for the gel to pass through the entire set up.
The silicone sheet also act to prevent moisture loss within the setup. Additionally another silicone sheet will be used after the agarose has hardened and placed between the top voltage plate and the top cylinder piece. Only two small holes needed to be drilled on either side of the silicone sheet, which are needed as the screws are inserted through the top plate into the top cylinder.

12.4.8.3 Gold plating

The meshes are also brought into the clean room to have a thin layer of gold deposited on top. This is to ensure some continuity in the experimental procedures as gold is also used to create the electrodes in earlier experiments. A thin 20 nanometer layer of chromium is used as a base layer for the steel mesh and a 40 nanometer layer of gold is deposited on top of that.

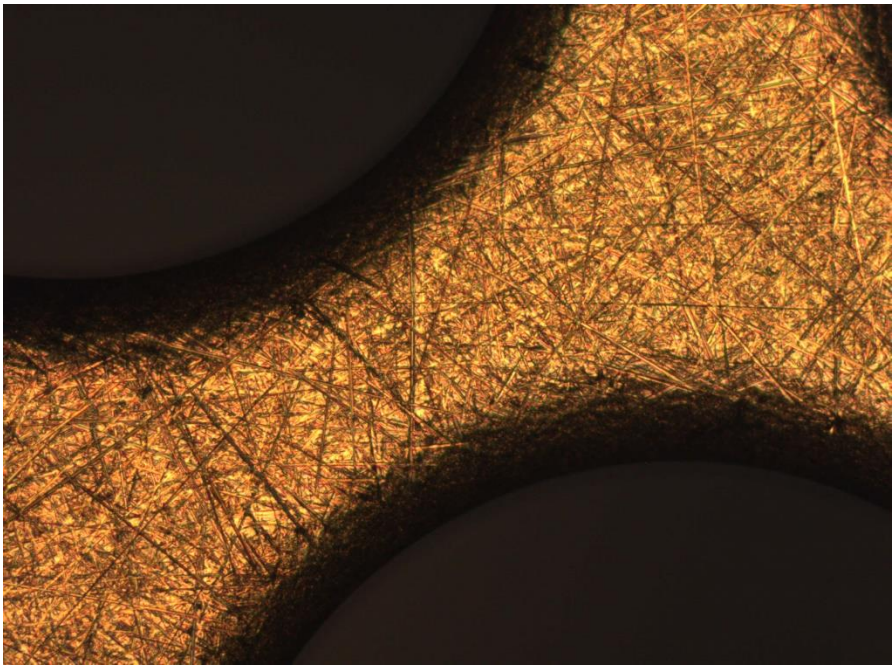

Figure 65 - Image showing the gold deposition on the steel mesh

Figure 65 shows the deposition of gold on the burred section of the steel mesh. The steel mesh is constructed in such a way that there is a flat section and a burred section like the one seen above. There are some visual scratches on the matches, but this is probably due to the manufacture, shipping and handling of the mesh. The gold has been deposited on to the recesses of all the scratches, therefore the behaviour of the mesh should still remain the same.

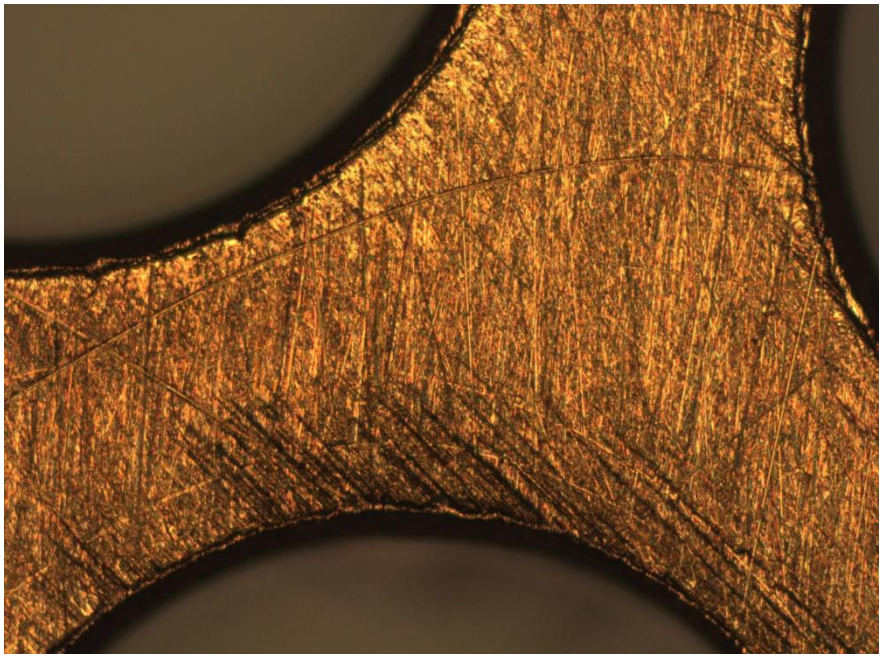

Figure 66 - Gold deposition on the steel mesh

Figure 66 shows the flat section of the steel mesh with the gold deposition. Both sides have to be put into the bell jar evaporator therefore the process must be done for each side.

12.4.8.4 Top Layer Cylinder Thickness Reduction

The final modification done to the experimental setup is the slight reduction in the thickness of the top plastic cylinder. This has been done to reduce the start time of the experiment by affectively reducing the “distance” the salt ions have to travel to reach the steel mesh array. Doing this also reduces the gap between the Electrostatic field plates thus increasing the field strength in the experimental area.

The top cap is also shaven slightly to accomodate this change, reducing the distance between the top of the cylinder hole and the start of the agarose well. This is so that the well does not start too low into the sensing area and that there is a reasonable distance between the well and the mesh.

The bottom cylinder is virtually untouched as there needs to be some space for within the bottom section of the experiment so that the salt ions can “collect”.

Figure 67 - image shows the completed double golden meshes within the two plastic cylinders

Figure 67 shows the shortened top cylinder. The central hole is where the agarose will come up to when molten agarose solution is injected through the blue tubing at the bottom. The nylon stopper will attach to the top of the cylinder and the agarose will form around it, causing the shape of the salt solution insertion well to form.

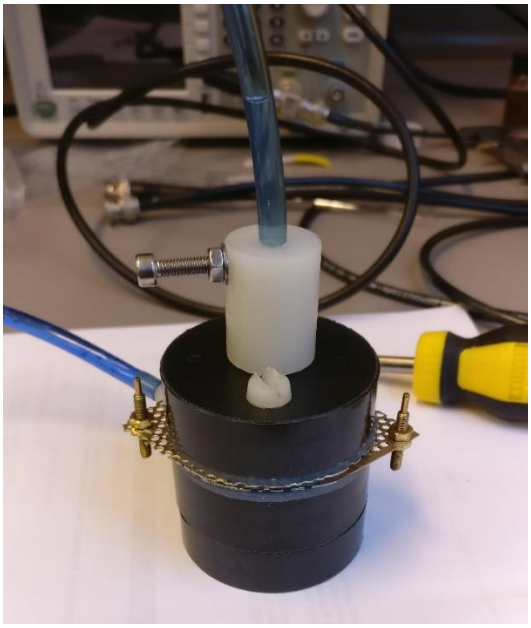

Figure 68 - the mesh setup with the nylon stopper.

Figure 68 shows the excess flow of the agarose out of the top of the stopper. This can be used as an indication for when the setup is completely filled with agarose. The top stopper can be pulled out and a well will be formed on the top of the hardened agarose.

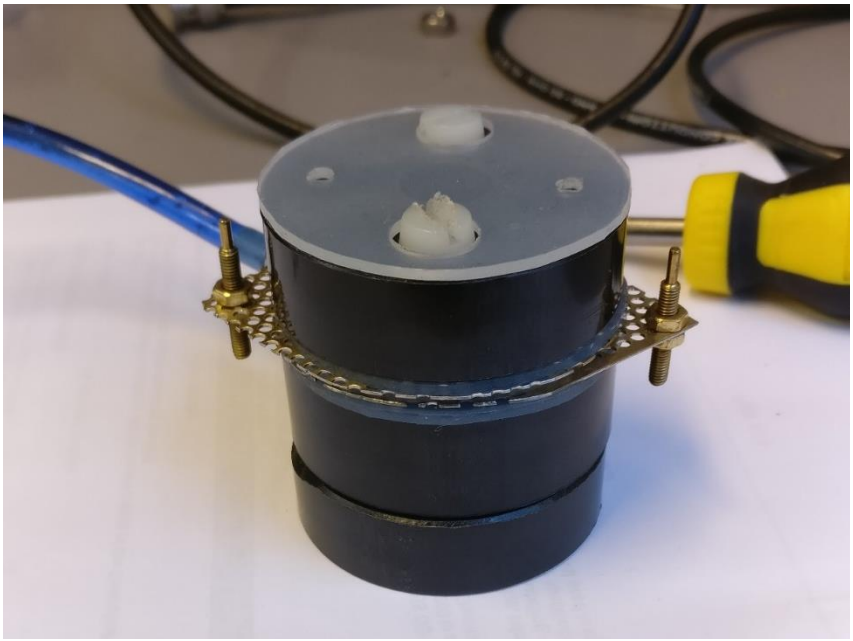

Figure 69 - image of the reduced size cylinders and silicone sheets

Figure 69 shows the positions of the silicone sheets that act as separation layer for the mesh and also to prevent the moisture of the gels from drying out. The copper plate will be placed above the top silicone sheet and a screw can be attached to hold both in place.

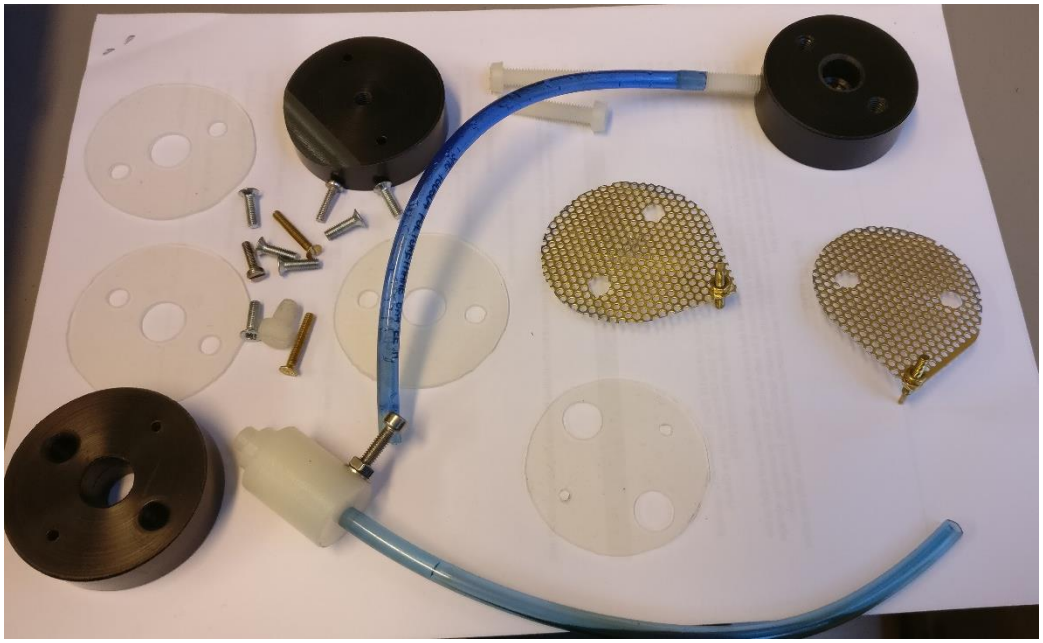

Figure 70 - image showing the complete breakdown of parts

12.4.9 Primary Experimentation – Double Mesh Gel Electrophoresis

The procedure for this experiment is the same as in the preliminary experiment for Double Mesh gel electrophoresis in the section earlier. All experiments conducted with have individual sections and a collective conclusion. This section of the experiment is to study the effect of varying salt concentration on the voltage over time for 200volt plate voltage and plateless conditions.

12.4.9.1 Control experiment – Neutral conditions

This experiment is conducted using the gold double mesh with no salt water or plate voltage attached to the system. The purpose of this experiment is to characterise the passive operating conditions of the instrument and to verify that in absence of ionic samples, the output voltage measured will not change.
The experimental setup is first constructed and the agarose solution at 1% is prepared. Before injecting the agarose solution, a measurement is made by just measuring the value of the output voltage in air.

12.4.9.1.1 Results and observations

At 1000hz, 1 volt sensor input voltage, air itself is measured to be 4milivolts. Molten agarose is injected and this value changes to 968milivolt sensor input and 110milivolt

sensor output. As the agarose hardens, more measurements are taken

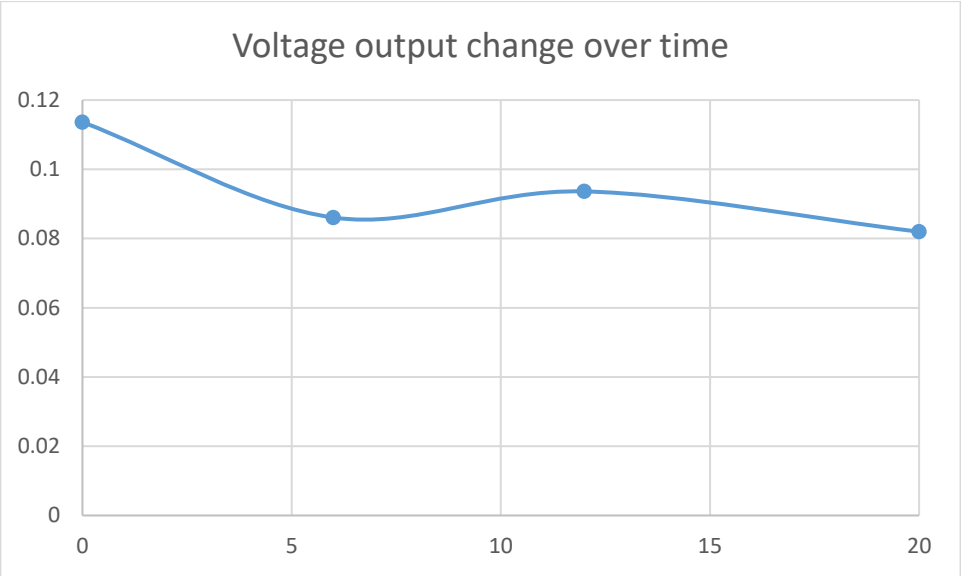

Figure 71 - graph relates to the change of voltage over time for the agarose

The graph in Figure 71 shows that as the agarose hardens from its molten form and begins to cool, there is a high initial voltage recorded at the output, as time goes on, and the agarose cools and solidifies to its gel state, this value drops.

This is an important figure to note as the final value of agarose can be used as a starting point for experimental procedures to begin. This value can also be used to determine when the agarose has fully formed into the gel.

DI water is then added onto the well of the agarose to determine whether di water will affect the change in output voltage. After 2 hours, there was no recorded change in the output voltage.

The copper plates were attached onto the setup at 200v volts and the output change is further monitored and there was no change in the output for another 2 hours.

The weight of the setup is measured to determine if there was a loss of moisture in the setup overnight.

The next day, the output voltage still remained the same however the mass of the setup has been reduced by 0,2 grams.

12.4.9.2 Conclusion

To conclude this phase of the experiment, air and agarose both record a change or some characteristic output voltage value. This reading may differ from experiment to experiment depending on the ambient temperature slight deviations on the concentration measurements of the agarose mixture. However, the initial value can be retroactively accounted for by manipulating the analysis methods using either voltage gain between output and input or simply the deduction of output from input, whichever is more

convenient. This can only be the case if one method is used throughout all other experiments in its class. Moving forward, only the gain is used quotient is used in following experiments to ensure consistency.

12.4.9.3 The effect of electrostatic field on salt solution

The purpose of this experiment is to determine the change of output voltage over time for varying concentration of salt solutions. Each of the experiments were done individually and run for a period of 2 hours. Voltage measurements were taken regularly at 5-minute intervals.

The experiment is then left for approximately 24 hours to determine if the salt solution passes through the mesh and reads a lower reading than the night before, in essence correlating to the earlier hypothesis that the voltage would reduce as the salt ions collect at the bottom of the plastic cylinder.

There are 5 different values for salt percentages that were chosen for this experiment. A higher value of 30% salt solution was initially chosen as one of these values, however there were still salt crystals present within the solution even after a long period of stirring. This is not ideal as other experiments conducted with salt solution that was fully dissolved before being placed in the agarose well.

12.4.9.3.1 Results and Analysis

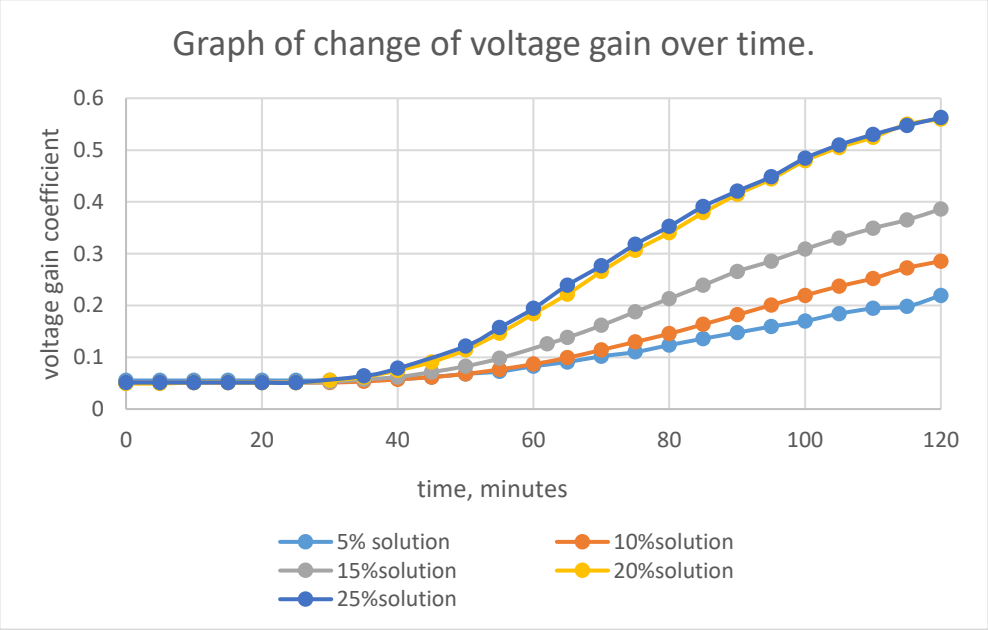

Figure 72 - Graph relates to the change of voltage over time for varying salt solution concentrations

The graph in Figure 72 above relates to the change of voltage gain over time for varying salt solutions without the presence of an external electric field. This means that the salt

solution relies purely on diffusion and gravity to pass through the agarose gel and onto the sensor.
As predicted, the results show that the higher concentration salt solutions read a much a higher voltage overall on the sensor output.

Analysis - As the higher amount of salt ions per-volume of solution means that the dielectric constant within the capacitive sensor will increase thus allowing for more charge to flow across the sensor and increasing the overall current throughout the circuit.
Since the oscilloscope measures voltage at the resistor, which is always constant, an overall increase of circuit current means a higher voltage at the resistor.
An alternative analysis

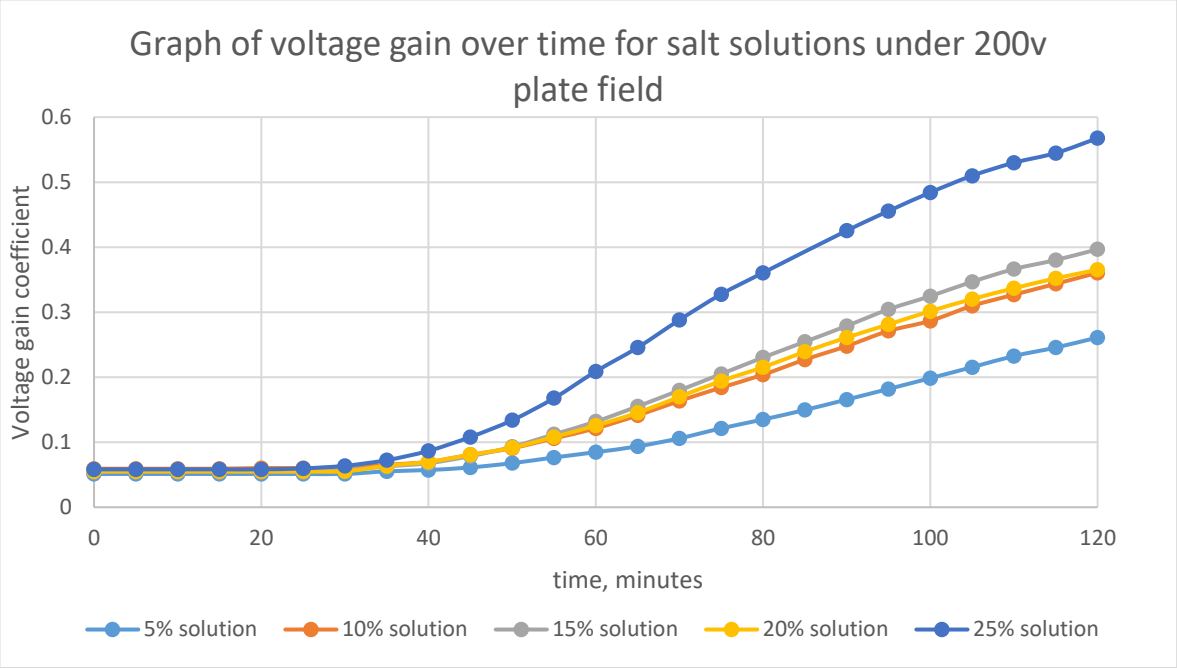

Figure 73 - Graph relating to the change of voltage gain over time for varying salt solutions under 200v plate field.

The graph in Figure 73 shows a similar growth pattern for the salt solutions under 200v plate voltage. This may seem uncharacteristic at first, but looking closely at the details of the graph will show that the transit time has slightly reduced. For example, for the 25% salt solution is shown that at 20 minutes, without the plate, the output voltage is 51milivolt and under 200v plate field, the output voltage is at 58milivolts. This table will be shown in the appendices. This is not as high as would be expected however this could also be due the plate field possibly not being strong enough to really effect the motion of ions.

Analysis - the graph shows a closer spread for mid-concentration salt solutions and the low and high concentration salt solution remaining relatively the same. This could mean

that even under the strong electrostatic field, the motion of ions only exhibit a small or negligible change in transition time. The experiment in section 11.1 shows a more sensitive reaction towards the field due to the much smaller scale of the experiment and the lower distance of the plates, regardless of the strength of the Electric field.
An argument could be made that table salt consist of Na and Cl ions, both of opposite polarities, meaning that the molecular bond formed between these ions will hold them together. As the plate provides a one directional electric field, one ion will be repulsed by the field and the other will be attracted by it, meaning that this could cause the motion of the salt ions moving through the gel to be effected

The experiments above were also used to view the changes of voltage after a 24 hour period, and for all experiments, the output voltages do not reduce. This could mean that the sensor measures the overall mass charge ratio of the agarose solution rather than within a small “sensing region” within the experimental setup.

12.4.10 Section Conclusion

A successful double mesh capacitive sensor setup was used to detect the flow of salt ions through a gel. The construct was an original design based on a rough sketch idea and was built into a functional sensor made within a workshop. The design allowed for agarose solution to be injected on the bottom of two sandwiched plastic cylinders that have been hollowed out. Between the two cylinders, the two meshes are placed with a small gap in between them. This gap was originally formed with a polythene sheet, but was later replaced with thicker silicone sheets. The same silicone sheets were also used to seal moisture within the setup to stop the agarose gel from drying over time. Using a nylon stopper, a well could be formed by placing it on top of the opening on the cylinder and salt solution could be placed within the well with a pipette. Two copper plates could be placed on the top and bottom of the cylinder and a voltage could be supplied to the plates and form an electrostatic field between them.
Two preliminary experiments were conducted to familiarize with the construction and experimental procedures involved with the setup. The preliminary experiment was also to determine that the output sensor voltage would not change under the presence of DI water, or if there was indeed a change, this change would be different from salt ions, which they were as presence of salt ions would mean a much higher voltage across the mesh.
The sensor has managed to detect a change of voltage across the meshes at varying salt concentrations and verify that for each concentration, the voltage gain response graph over time will be different. Though for the 200v plates, the 20% solution seemed to be

lower than the 15% solution, this is only a slight inconsistency as the other results showed an increasing voltage growth and final voltage measurement reading.

13 Improvements

For the experiments using Nanofabricated Electrodes, the experimentation general went well with very few improvements needed. Most of the issues faced during experimentation were merely from needing to restart the experiment several times due to failure in measuring output voltage due to possible cleanliness issues or imperfections in the gel agarose structure such as formation of air bubbles. However it would have been beneficial to have conducted experiments with other ionic substances such as Methylene blue, as the colour would be a useful visual tool in detecting the motion of electrons in the plate polarity reversal section.

The iodine visual experiment could ultimately be improved by using a much larger electrostatic field by using a higher voltage across the plates. However this would mean a specialised setup for the experiment itself as the vials could not fit within the plastic cylinder. This would be very time consuming to create.

The double mesh experiment could benefit from several more reruns, though the time consuming nature of the experiment meant that time was very limited. The setup of the experiment takes a long time as there are many parts that need to be put together. Cleaning and drying of the experimental setup also takes time as there are small holes that cannot be dried with paper towels.

An overall improvement would be to provide automation in the collection of voltage readings throughout all the experiments. This would mean that experiments could be conducted for a longer amount of time, generating a far wider series of results. This could be done by using Labview software for data analysis.

14 Conclusion

Gel electrophoresis is a useful method of analysing macromolecule samples for in the fields of chemistry and medicine. However the miniaturisation of gel electrophoresis apparatus could prove useful as a space and cost saving alternative. Electronic measurement of biological samples is an ever expanding field and therefore could provide a suitable alternative to fluorescent display in current electrophoresis technology. Combining both miniaturisation and using electronic measurement to improve a well established method of clinical diagnostic is not an easy task, therefore careful planning and creativity is required to design, test and implement a possibly novel analytical device. Using state of the art equipment, a capacitor with micro scale interdigitating loops were fabricated through photolithography. A suitable on-board sensing unit would then be built to accommodate this capacitor to allow for electronic measurement to take place. The collective device was successfully used as a sensor to detect the changes of voltage through the slow transition of ionic particles through an agarose gel layer by using an Electrostatic field. This field was produced using repurposed copper plates along with a battery pack supplying anywhere from 9 -90 volt using a series of 9-volt batteries. This battery pack would later be modified to provide an excess of 200volts.

Output voltage of salt solution was measured at a number of electric field strengths with a varying degree of consistency and reversing the plate voltage did not manage to reverse the readings across the electrode. The circuit would also be improved by introducing a 100ohm resistor to be taken as the new measuring point and also voltage input was monitored in further experiments.

An experiment was successfully conducted by measuring the voltage output across the same sensor that was pre-saturated with salt solution. The salt solution was diluted slowly over time by using a slow drip-flow method of introducing DI water and over time, the voltage across the sensor would reduce as the salt solution decreased in concentration. A voltage reading close to zero was recorded, meaning that a theory suggesting that an ionic trap could have been formed was disproven successfully.

The iodine visual experiment was inconclusive in providing enough of a visual representation of the electrostatic fields effects on the motion of iodine particles. This could be due to the large separation layer of the 1ml vials used requiring a larger electric field to support a higher transition time difference between both the investigated vial and the controlled vial.

The double mesh experiment showed high promise by not only increasing transition time under the presence of high electric field but showing variance in terms of salt concentration. Though one of the salt concentrations used showed poor results, the others were successful in portraying an increasing relation to transit time and overall higher voltage reading for increased concentrations. The final output voltages did not

show a decreasing trend of output voltage however leading to the conclusion that the sensor was still sensitive enough to measure salt ions after they pass through the mesh. To conclude this document, the methods used were highly effective in distinguishing salt concentrations with some minor inconsistencies. The sensor is able to measure voltage change with increase salt ion saturation however the salt must be fully expelled from the gel before a drop of voltage can be detected, as evidenced by the ionic flow experiment. With some minor changes, altering dielectric activity within a capacitor is a fundamentally feasible method of analysis and should be considered when miniaturising larger scale, visually driven diagnostics and detection devices.

15 Appendices

15.1 Photolithography images

These images were taken using the built-in camera of an optical microscope showing impurities within the electrodes. The samples were thoroughly cleaned and only perfect electrodes were used in experimentation.

The dimensions and details for each samples are given below;

- sample 1 and 2 are 100µm thickness and has 2 contacts
- sample 3 and 4 are 200µm thickness and has 2 contacts
- sample 5 and 6 are 200µm thickness and has 3 contacts
- sample 7 and 8 are 100µm thickness and has 3 contacts

15.1.1 Sample 1

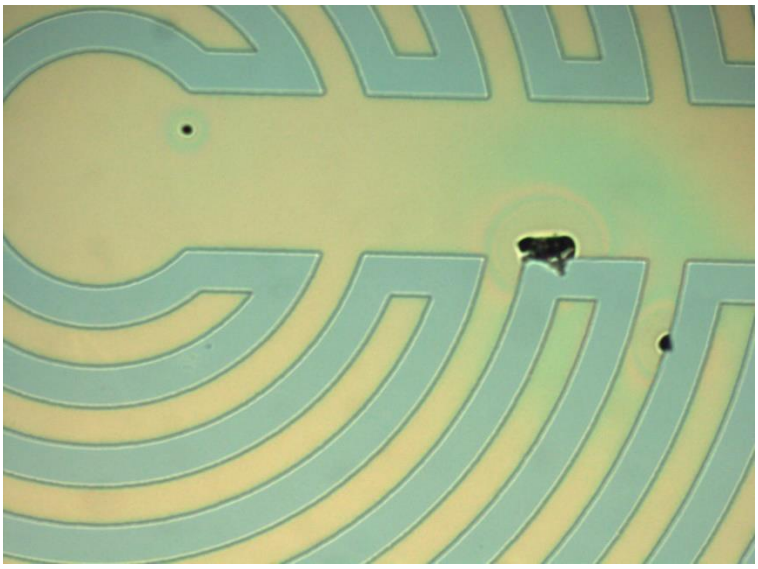

Figure 74 - image of dirt on the loop for sample 1

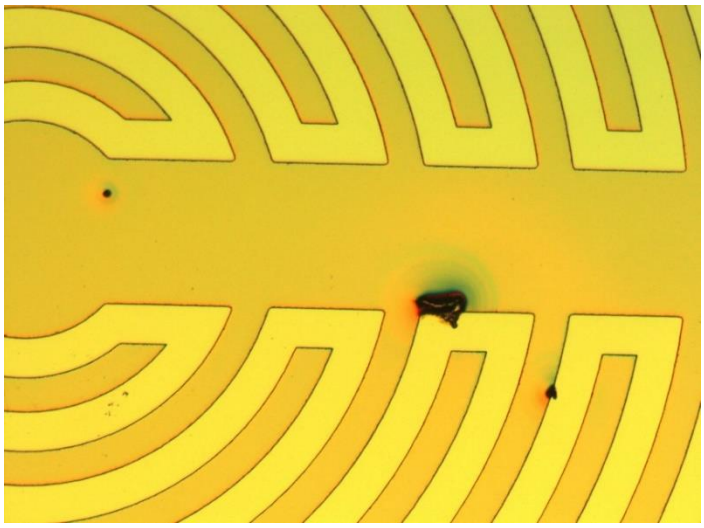

Figure 75 - image of dirt on sample 1

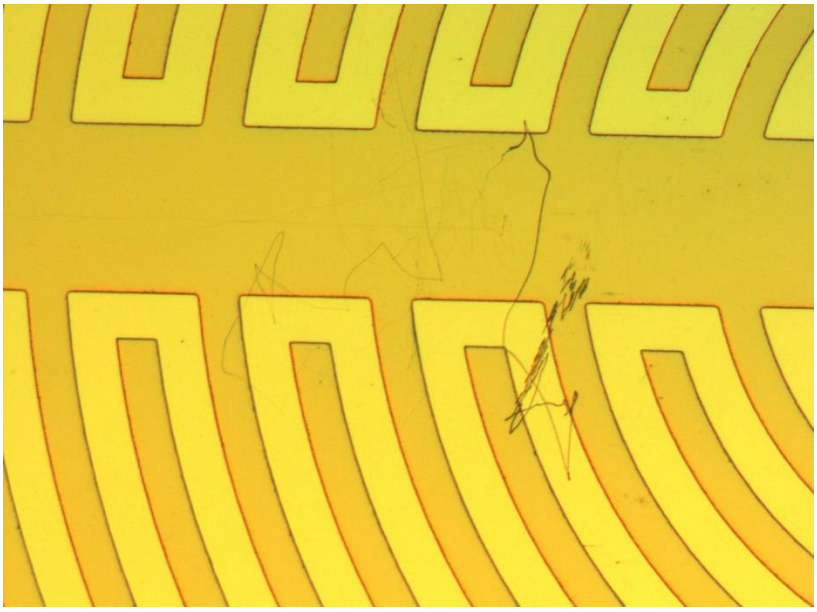

Figure 76 - scratches on sample 1

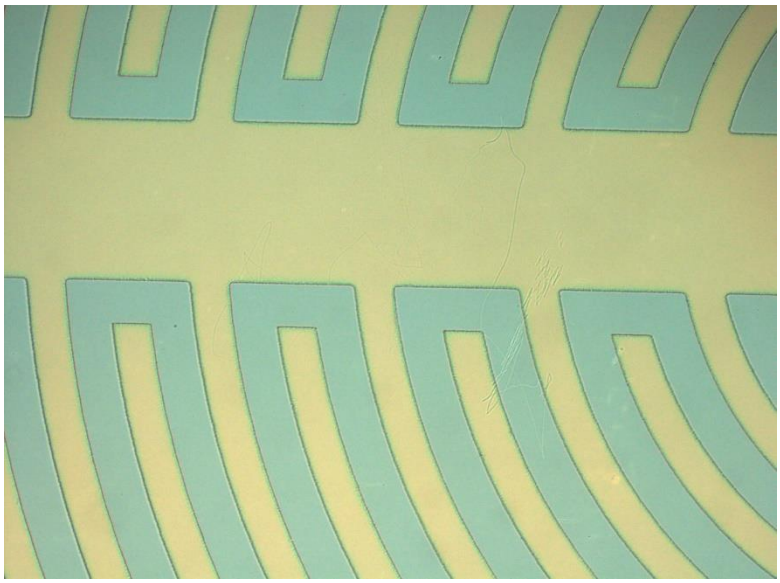

Figure 77 - scratches on sample 1

15.1.2 Sample 2

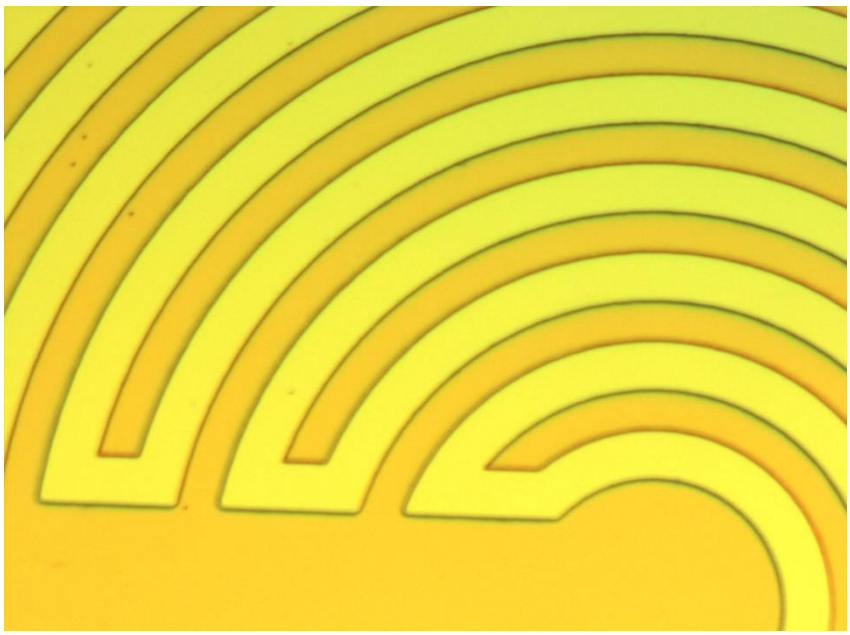

Figure 78 - Image showing the loop interdigitation on sample 2

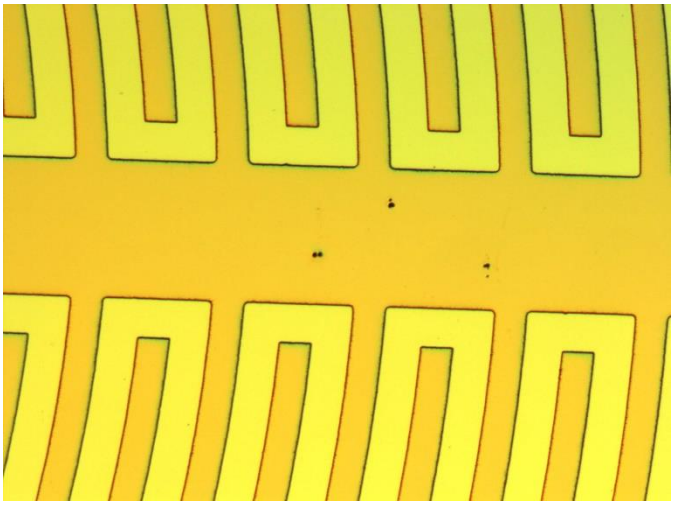

Figure 79 - image showing some drit on sample 2

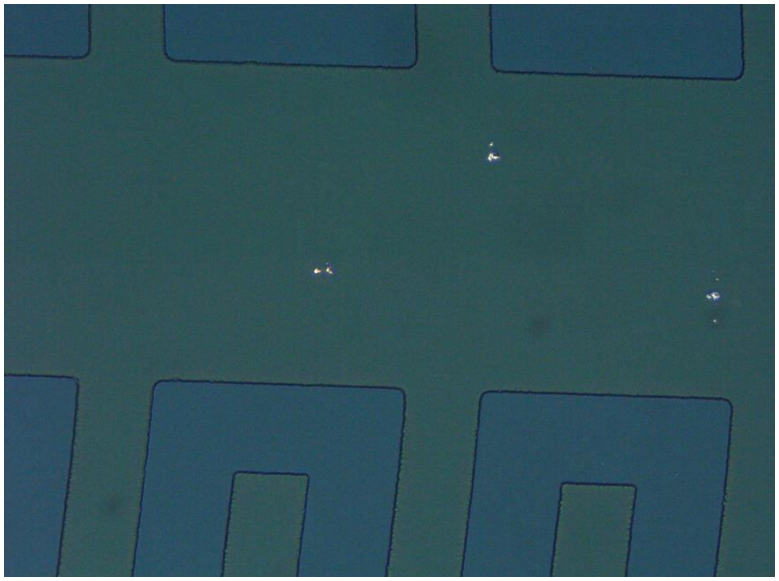

Figure 80 - image showing some peeling on sample 2

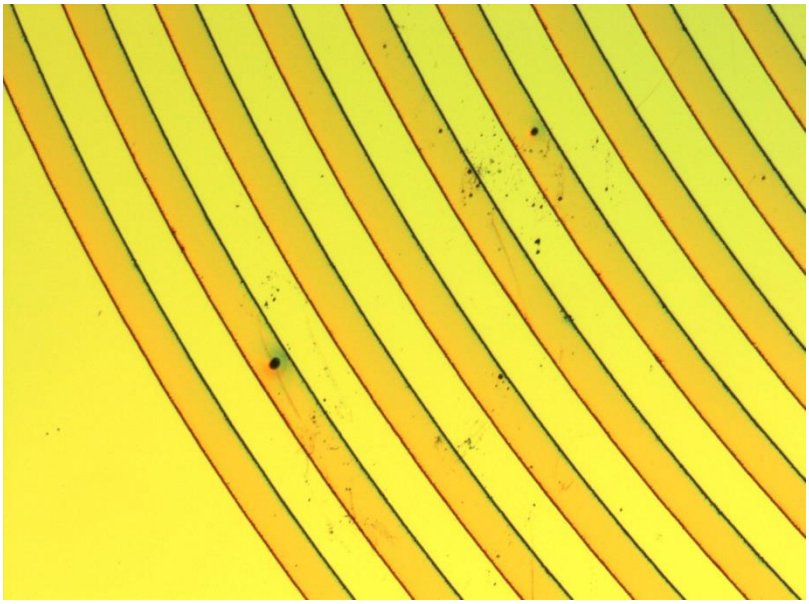

Figure 81 - image showing some dirt on sample 2

15.1.3 Sample 3

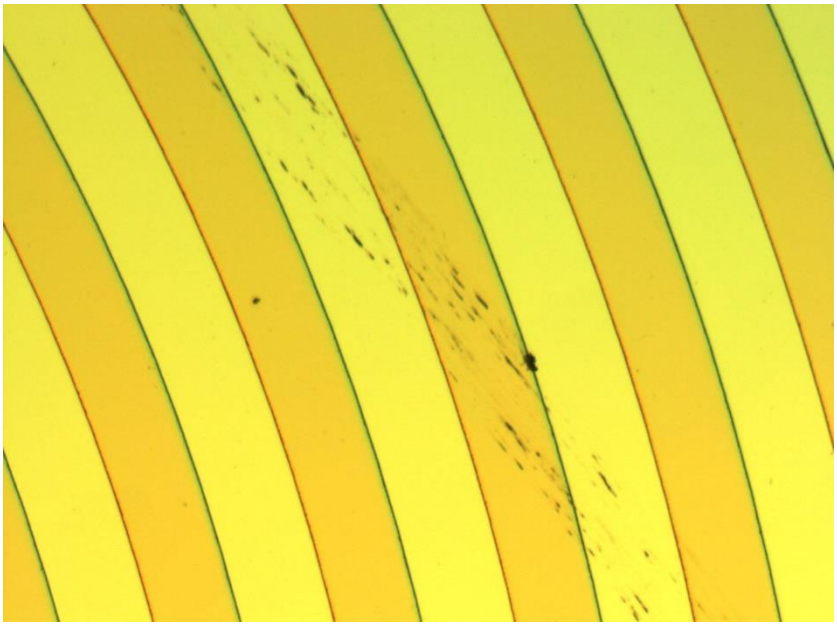

Figure 82 - image showing some dirt and scratches on sample 3

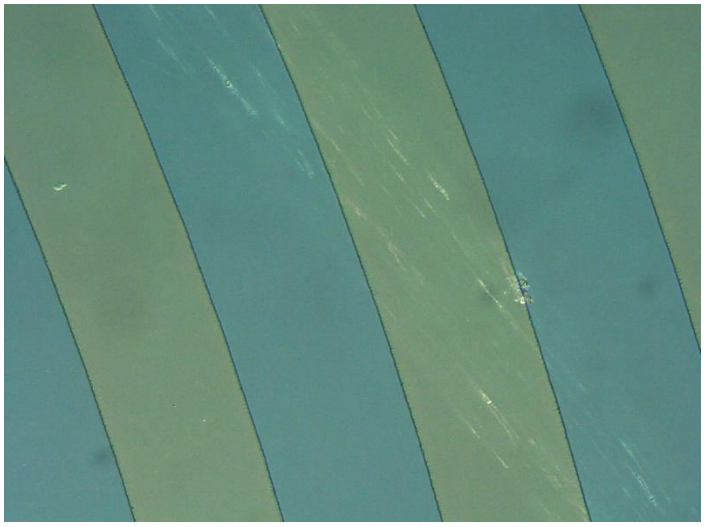

Figure 83 - image showing negative light version of the scratches and dirt on sample 3

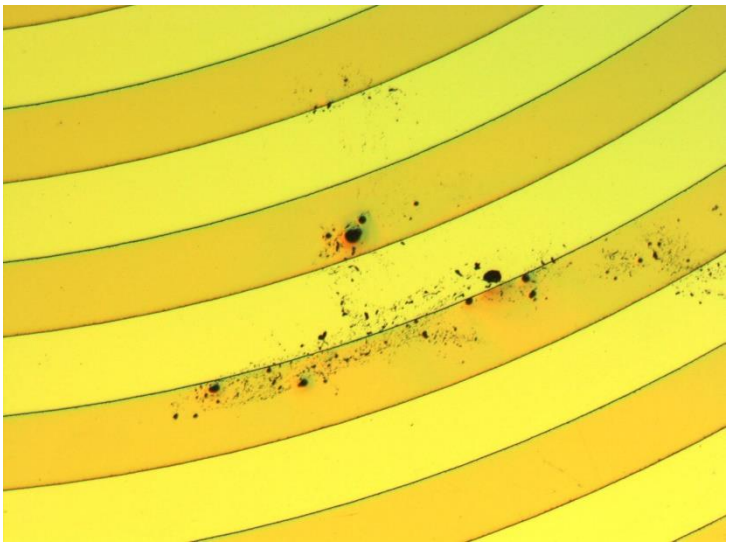

Figure 84 - Image showing dirt on sample 3

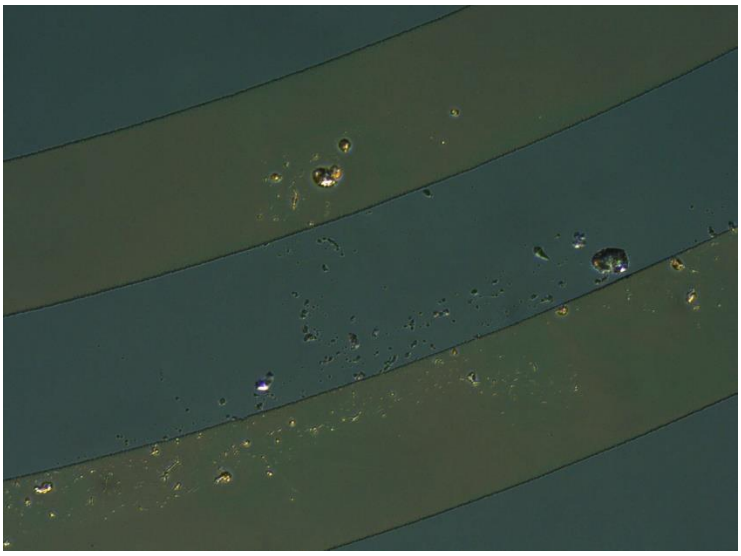

Figure 85 - the reverse light image of the dirt on sample 3

15.1.4 Sample 4

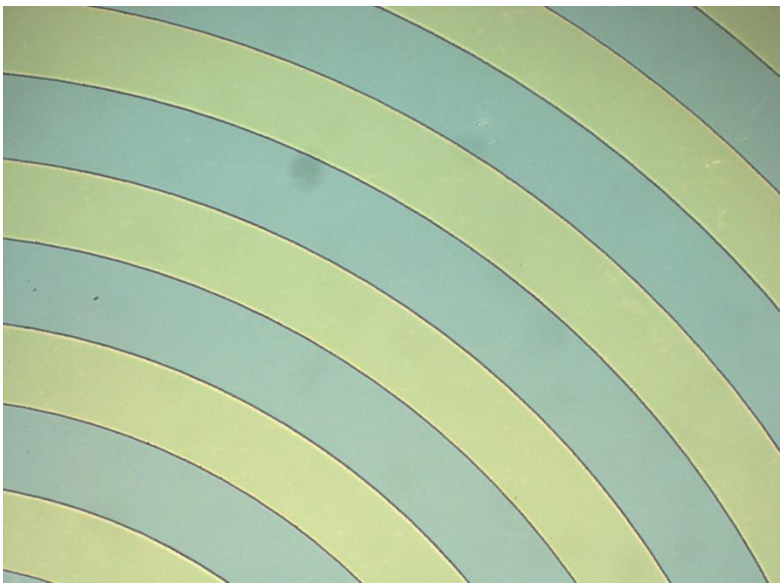

Figure 86 - image shows the loops on sample 4

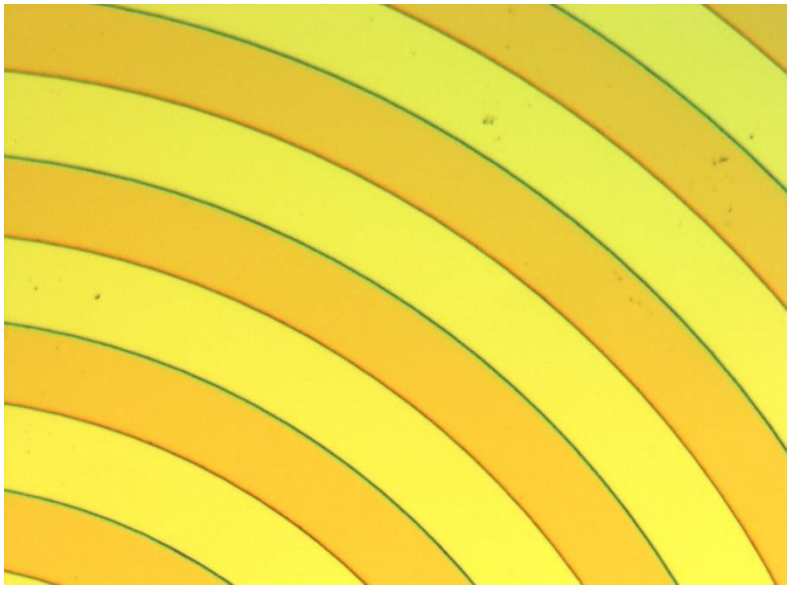

Figure 87 - image shows the same image but under brighter light

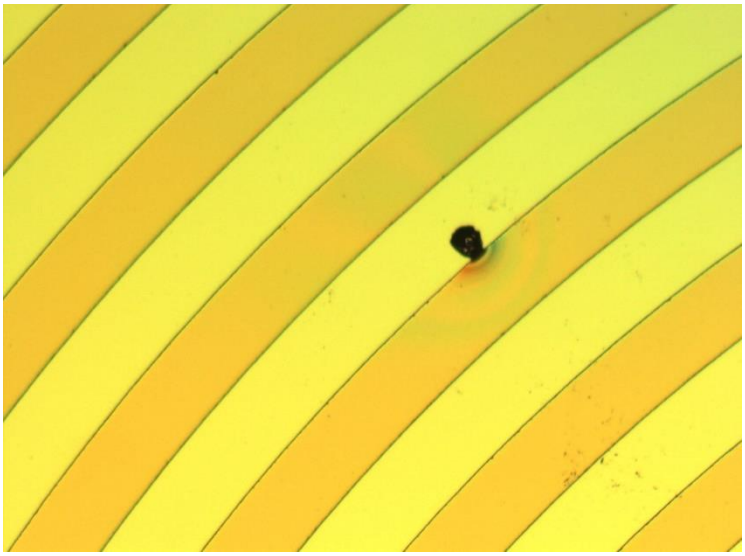

Figure 88 - image showing some dirt on sample 4

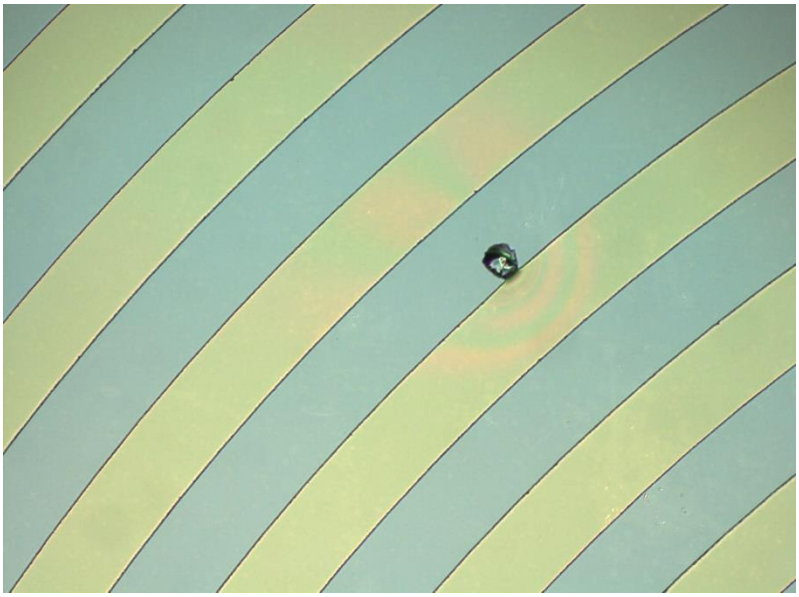

Figure 89 - image showing some dirt on sample 4

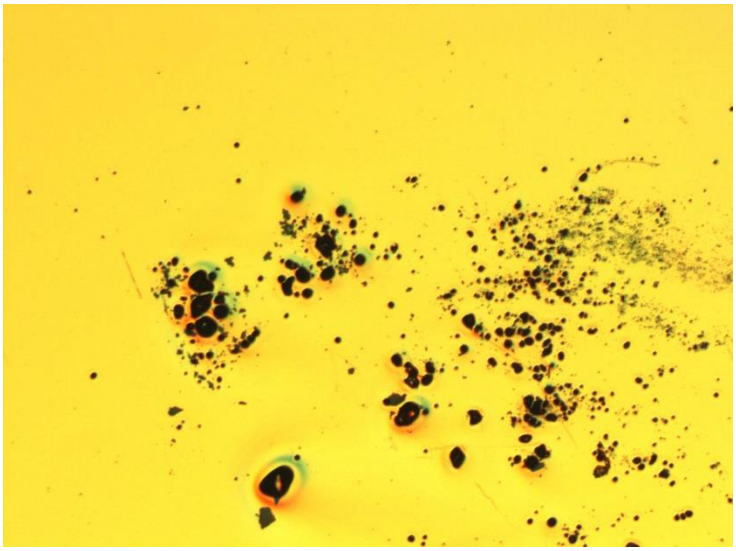

Figure 90 - image shows some dirt on the contacts at sample 4

15.1.5 Sample 5

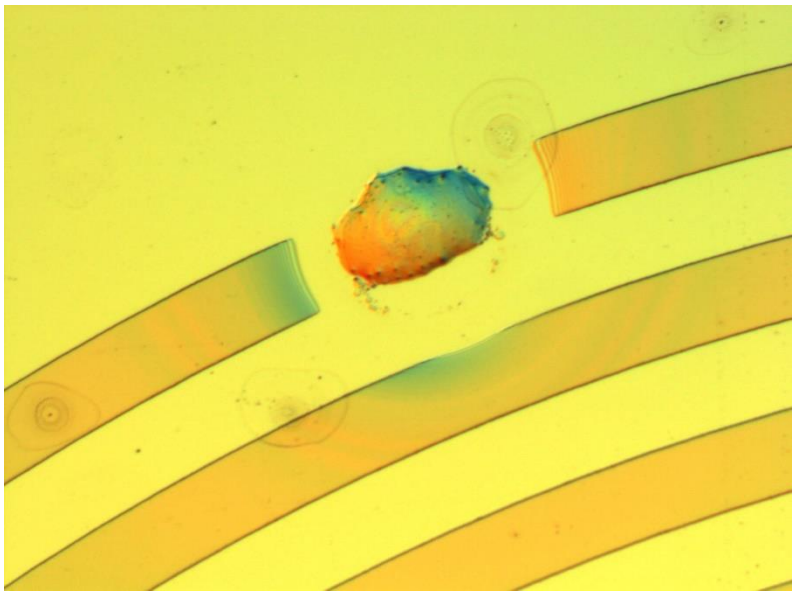

Figure 91 - image showing the broken connection on sample 5 due to dirt

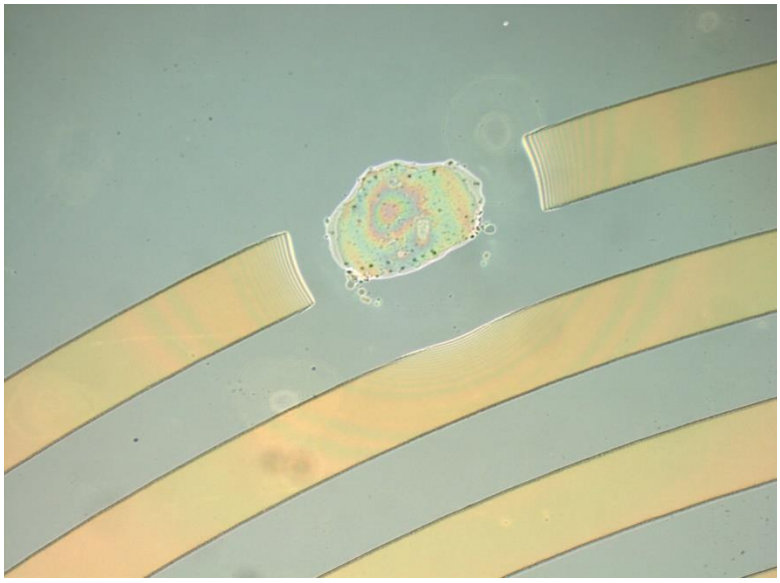

Figure 92 - image shows the same broken connection under reverse light

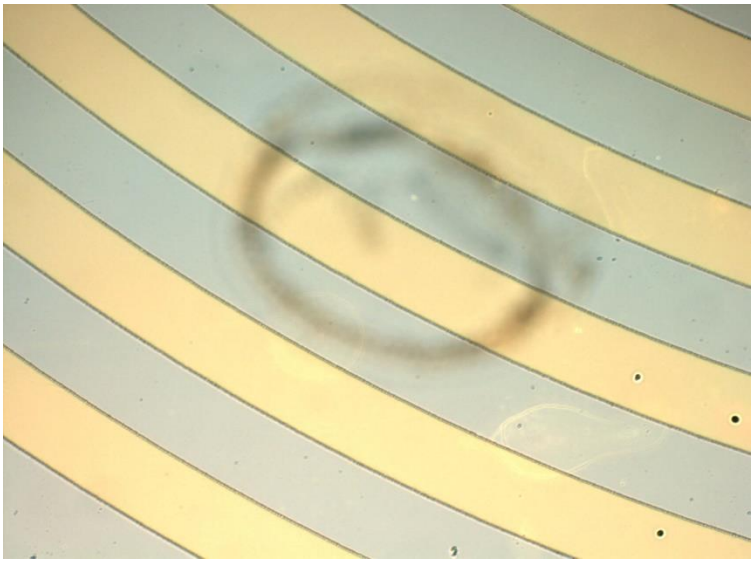

Figure 93 - image shows some smudging on sample 5

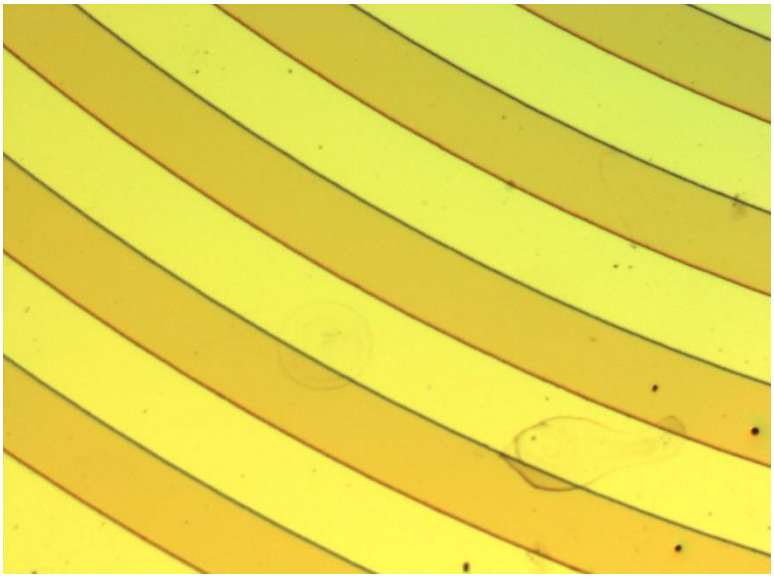

Figure 94 - image showing some smudges and dirt on sample 5

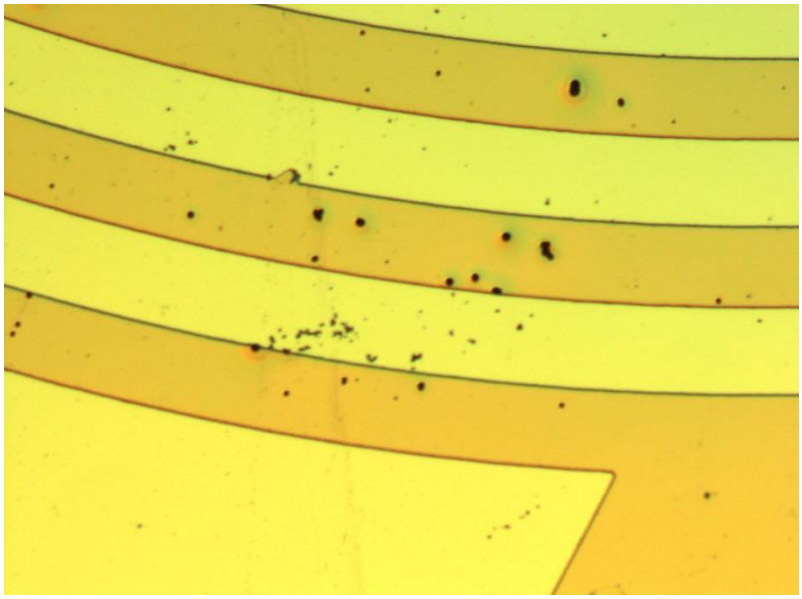

Figure 95 - image showing dirt on sample 5

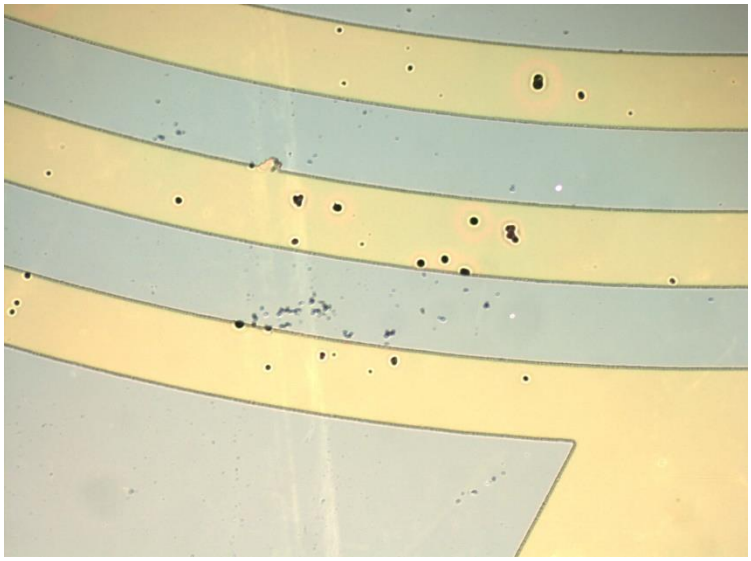

Figure 96 - image showing the same dirt under reverse light

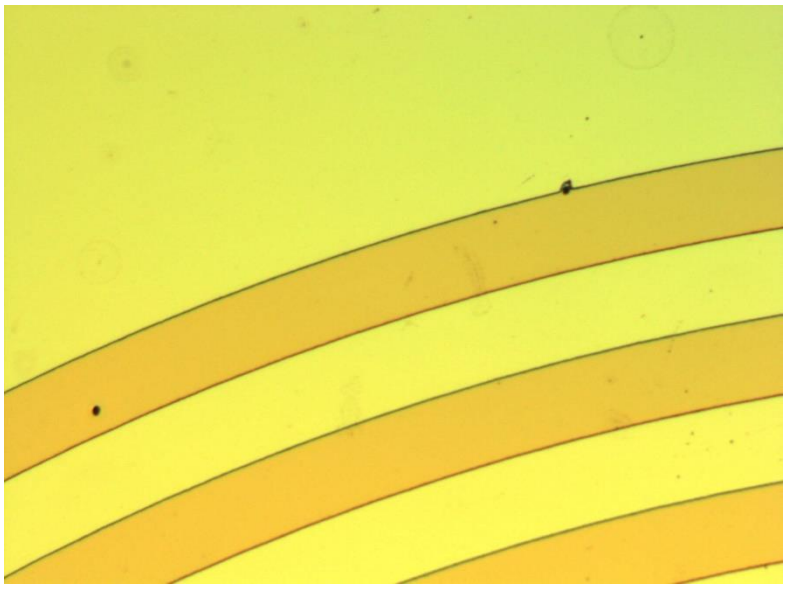

Figure 97 - image showing some dirt on sample 5

15.1.6 Sample 6

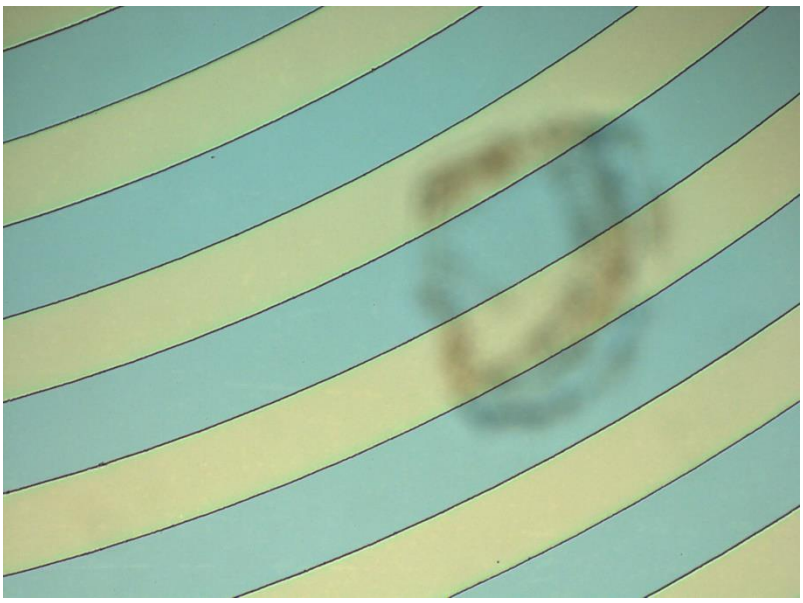

Figure 98 - image showing some smudging on the glass substrate for sample 6

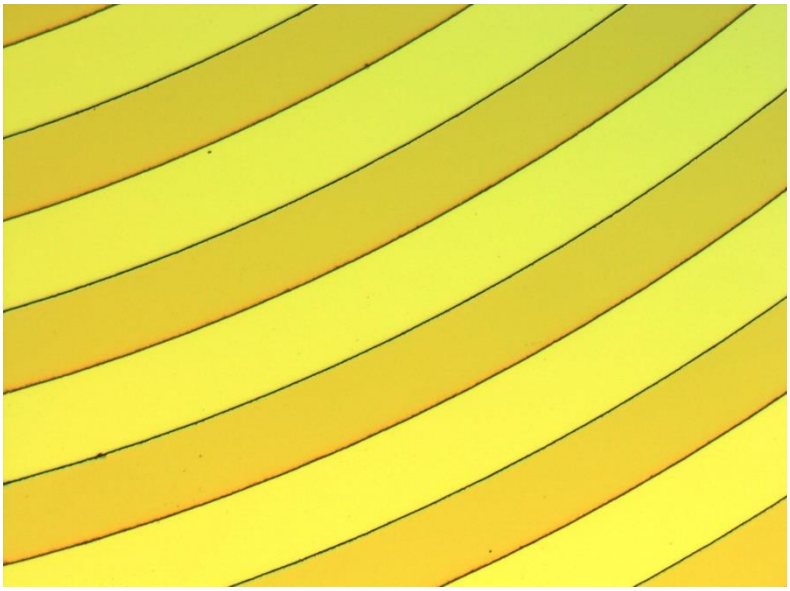

Figure 99 - the reverse image showing that the smudge does not effect the loops

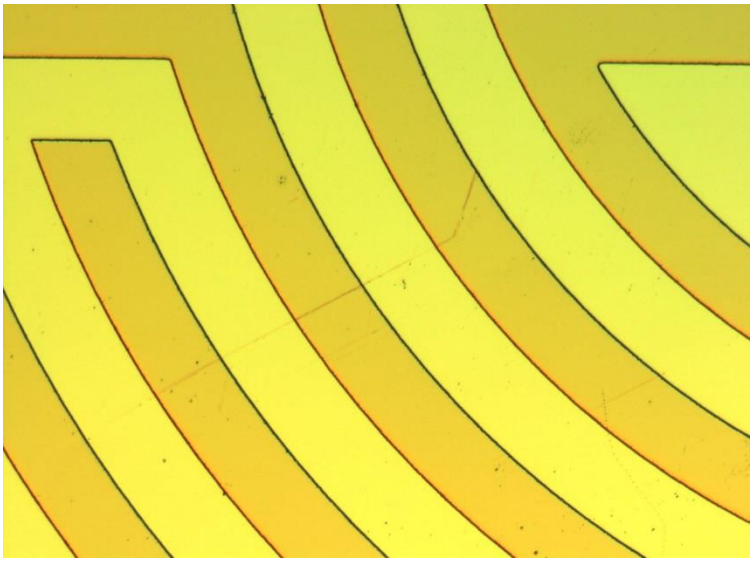

Figure 100 - some light scratching on sample 6

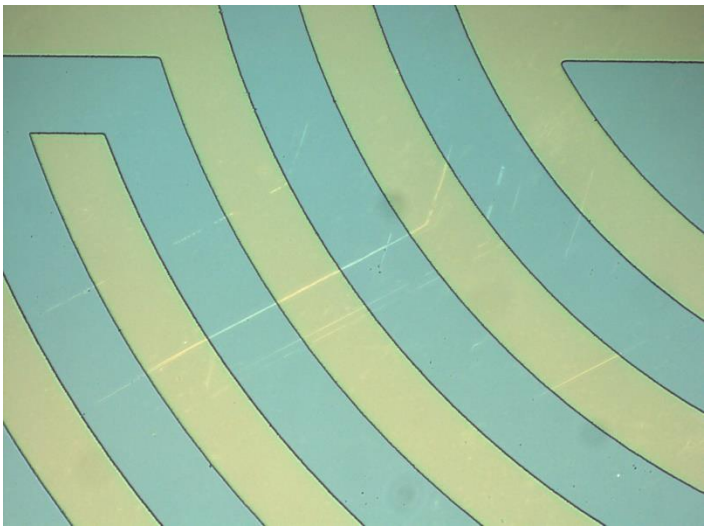

Figure 101 - reverse light image showing the same scratch does not break any connections

15.1.7 Sample 7

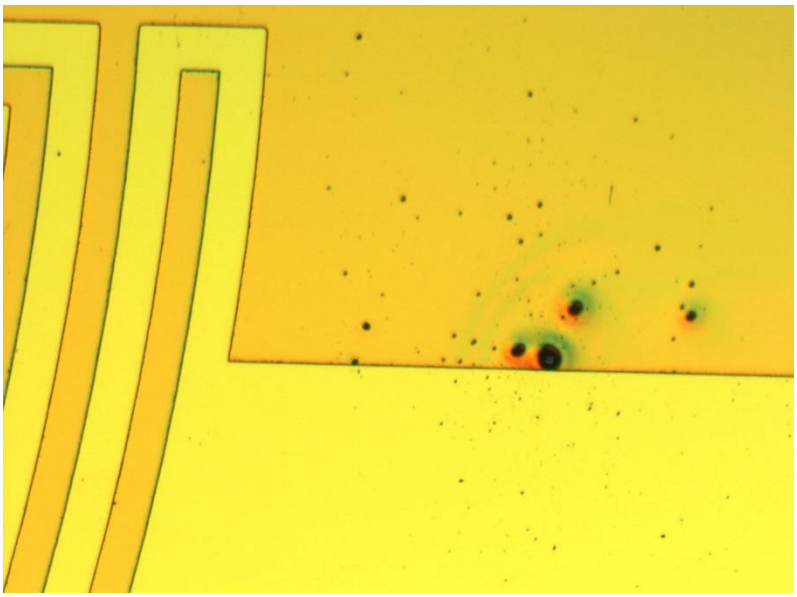

Figure 102 - image showing some dirt on sample 7

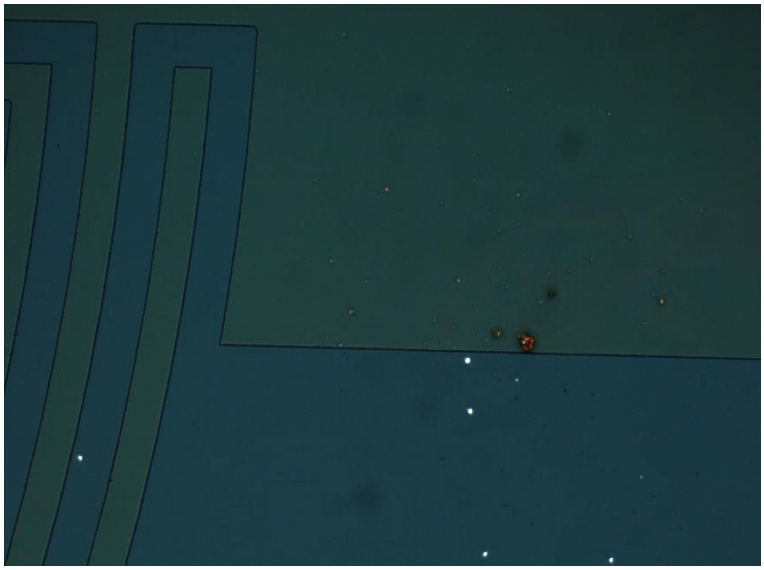

Figure 103 - image shows the same section under reverse light with some light thorough damage on the gold

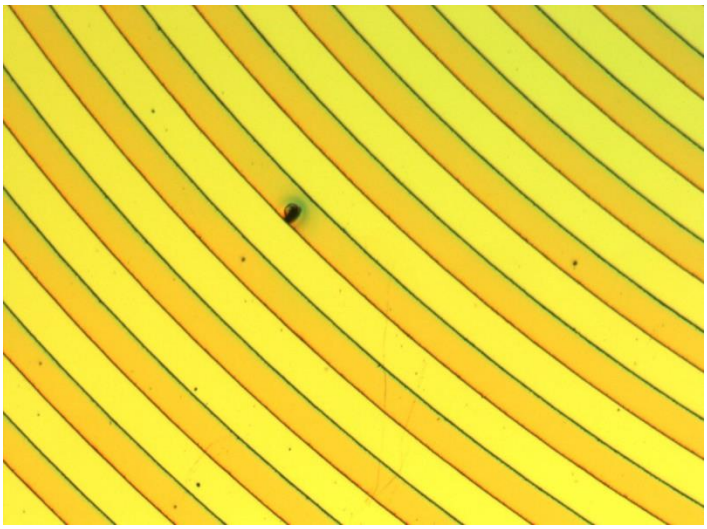

Figure 104 - image showing some dirt on a loop

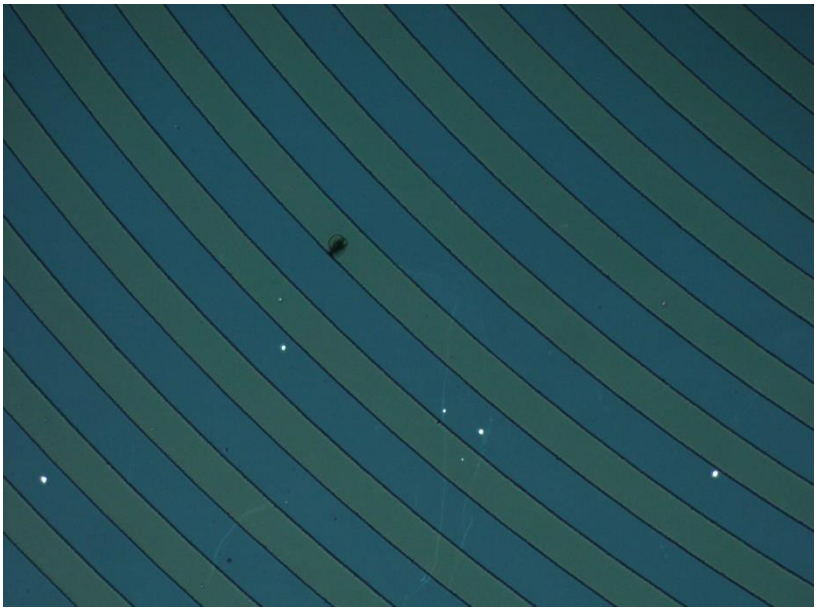

Figure 105 - image shows the reverse light on the same section, with some light thorough damage

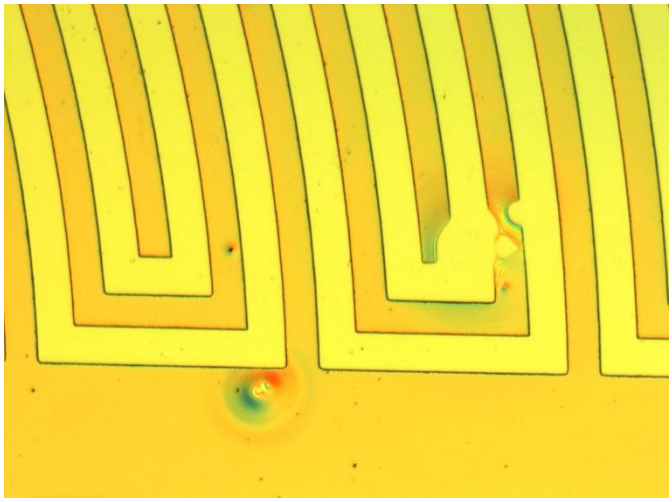

Figure 106 - image showing damage on the loop

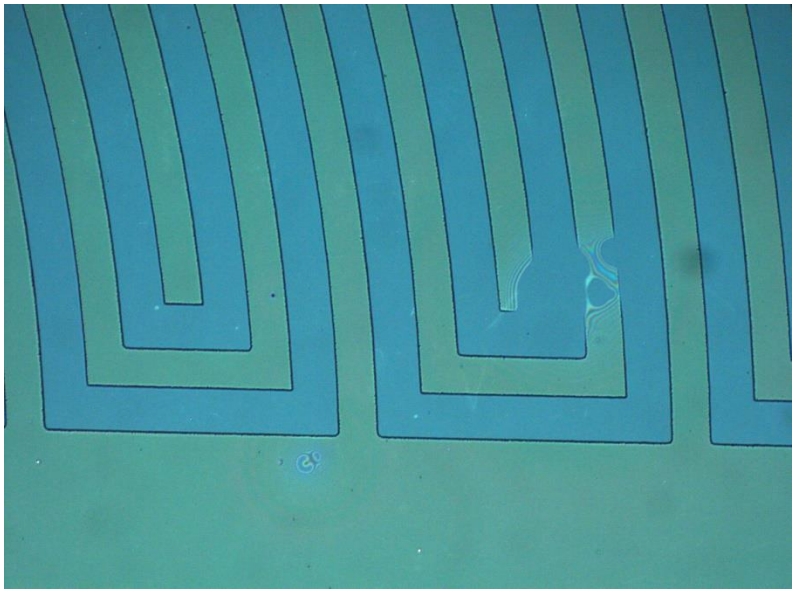

Figure 107 - image showing the reverse light for the same damage on the loop

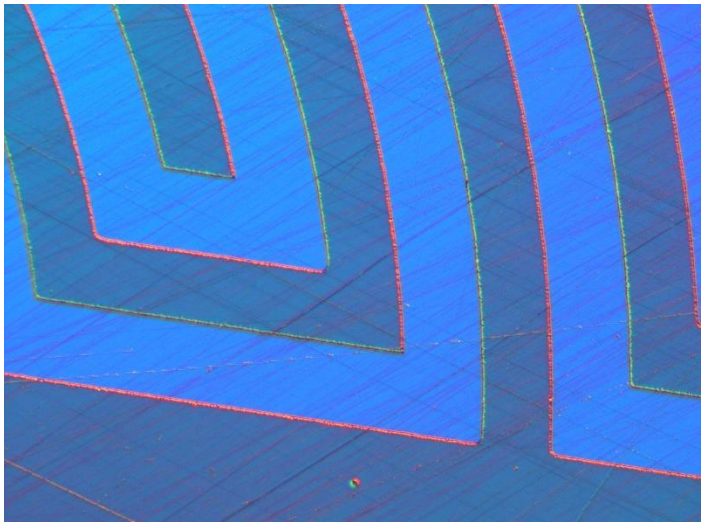

Figure 108 - image showing some scratches on sample 7

15.1.8 Sample 8

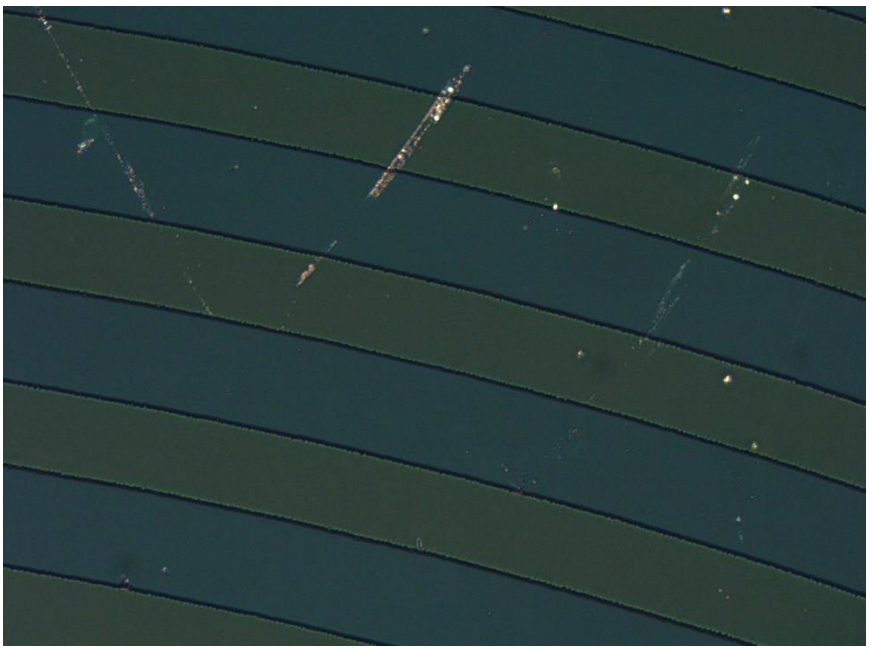

Figure 109 - image showing some scratches on sample 8

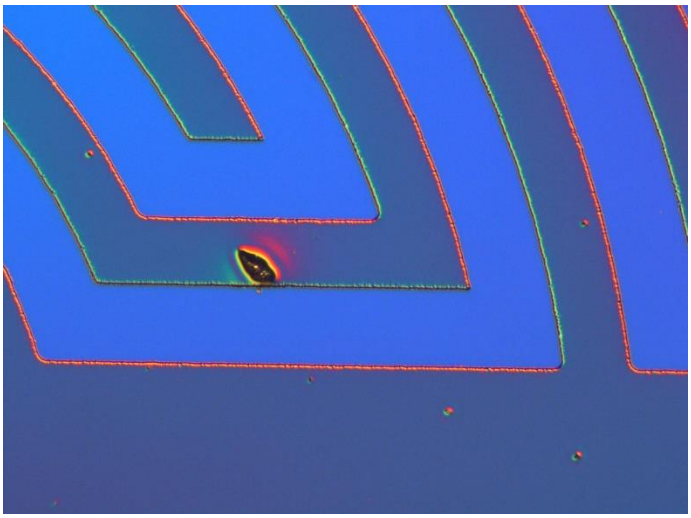

Figure 110 - image showing some dirt on sample 8

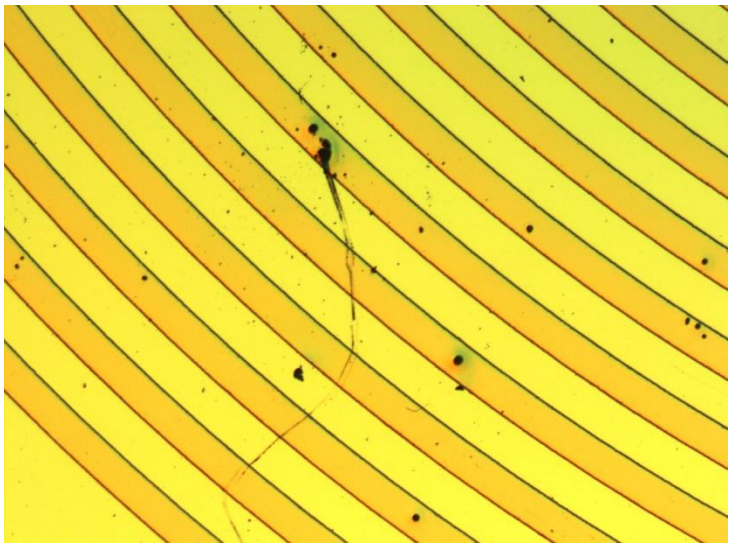

Figure 111 - image showing more dirt on sample 8

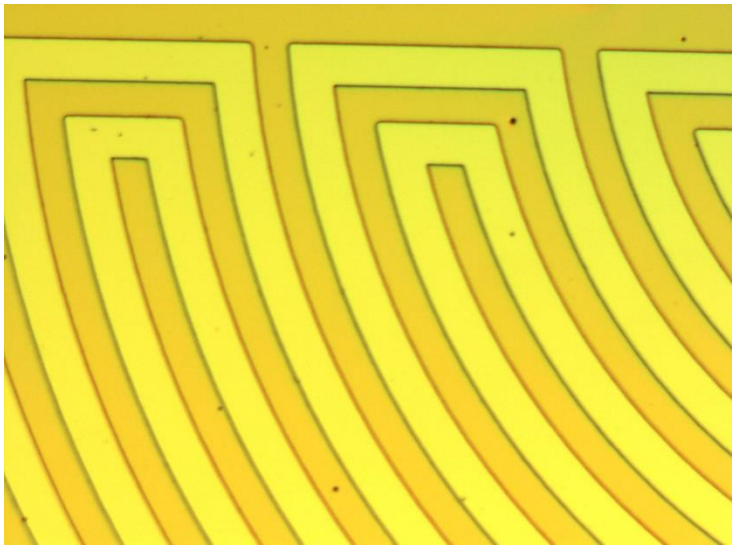

Figure 112 - image showing some light dirt on sample 8

15.2 Post-etch images

These images were taken after chemical etching and photoresist removal.

15.2.1 Sample 1

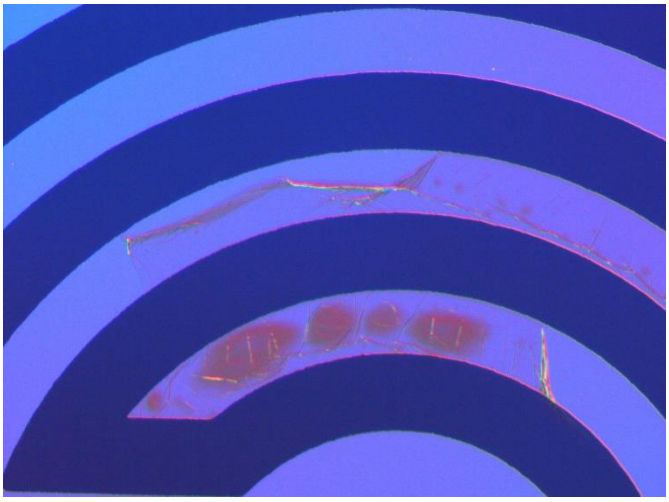

Figure 113 - image showing remaining photoresist on sample 1

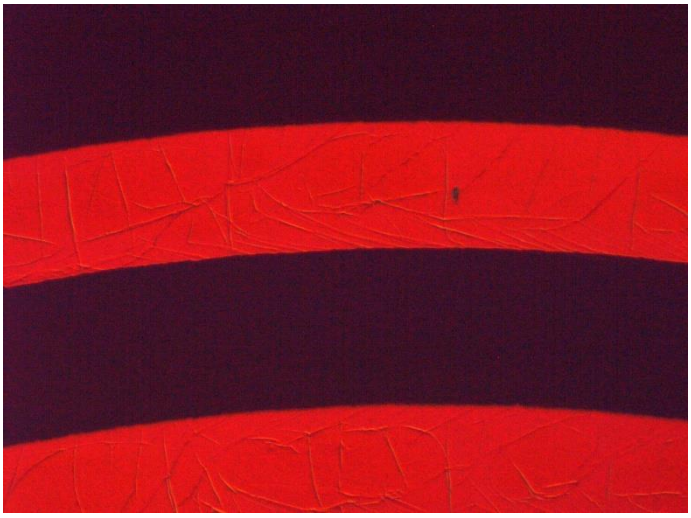

Figure 114 - image showing some cracking of hardened photoresist on sample 1

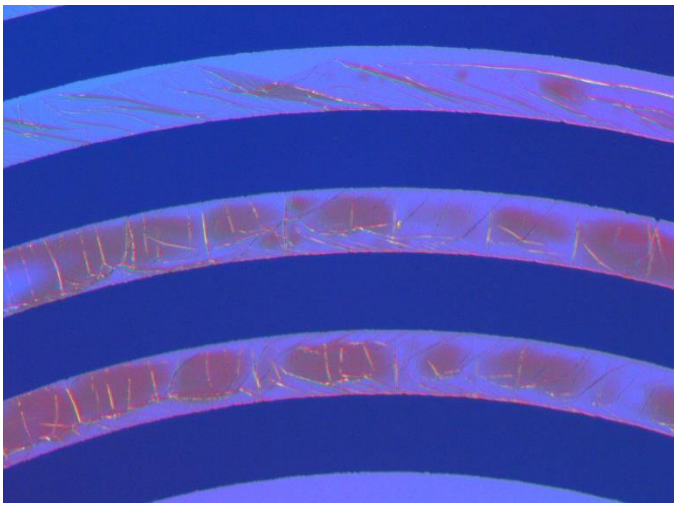

Figure 115 - image showing excess photoresist on sample 1

15.2.2 Sample 2

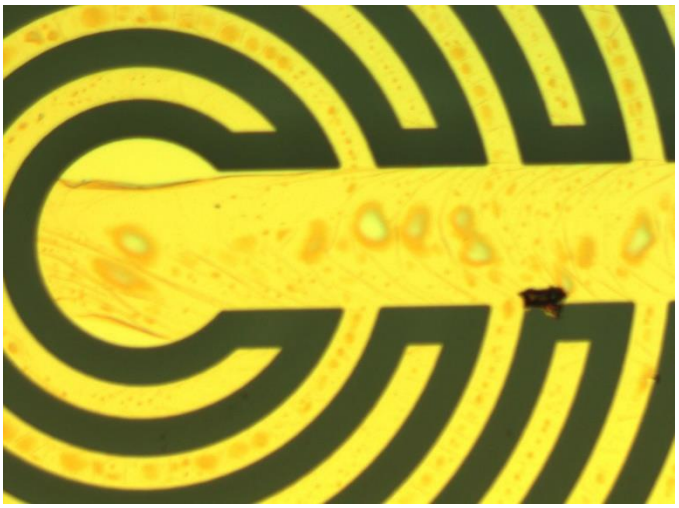

Figure 116 - image showing excess photoresist on sample 2

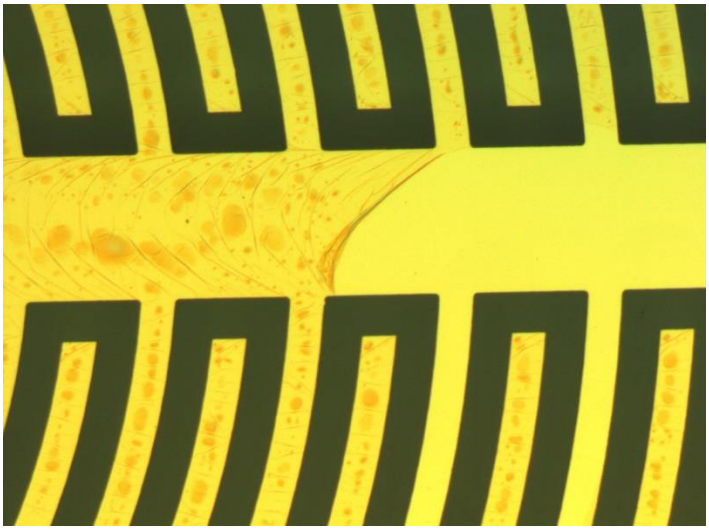

Figure 117 - image showing the pealing effect of excess photoresist on sample 2

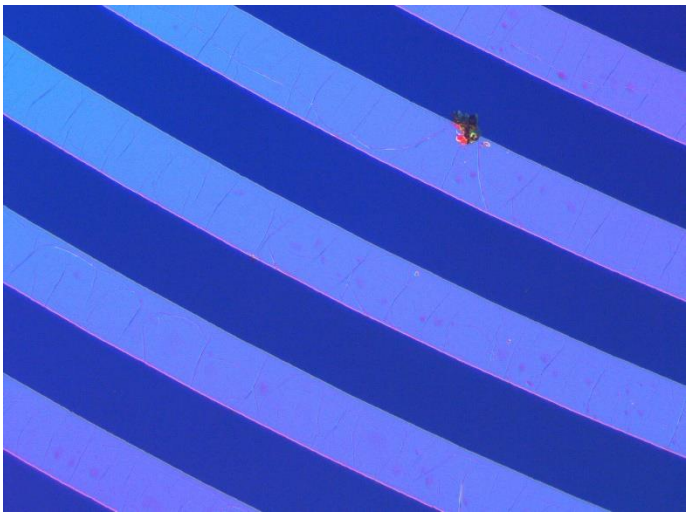

Figure 118 - image showing excess dirt on sample 2

15.2.3 Sample 3

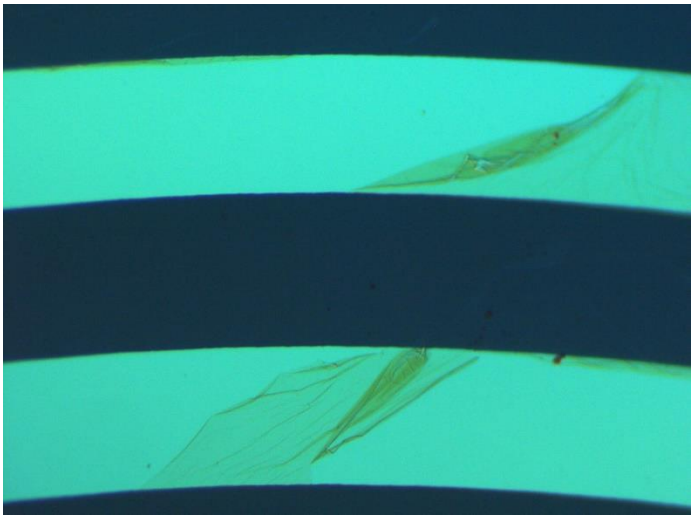

Figure 119 - image showing some excess photoresist and pealing on sample 3

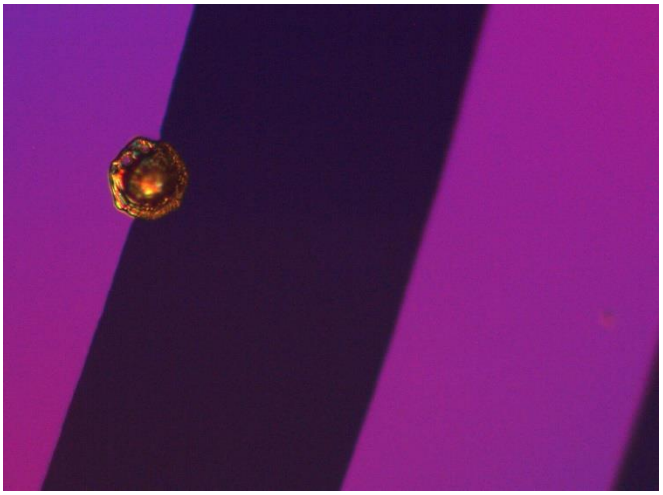

Figure 120 - image showing some dirt on sample 3

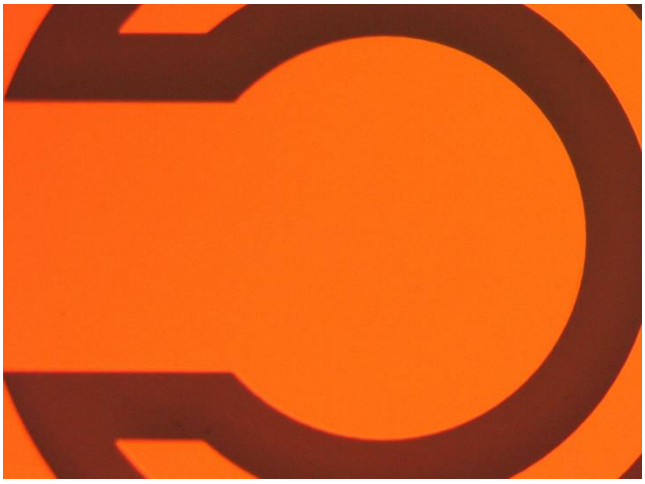

Figure 121 - image showing the central capacitive area on sample 3

15.2.4 Sample 4

Figure 122 - image showing sample 4, the darker blue areas represent the gap between the gold

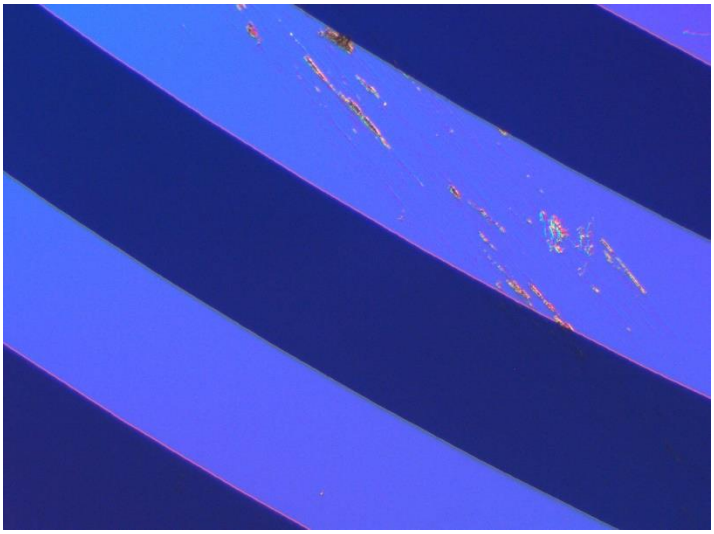

Figure 123 - image shows the some scratching on sample 4

Figure 124 - image showing the central capacitive area of sample 4

15.2.5 Sample 5

Figure 125 - image showing the central loop with some photoresist pealing on sample 5

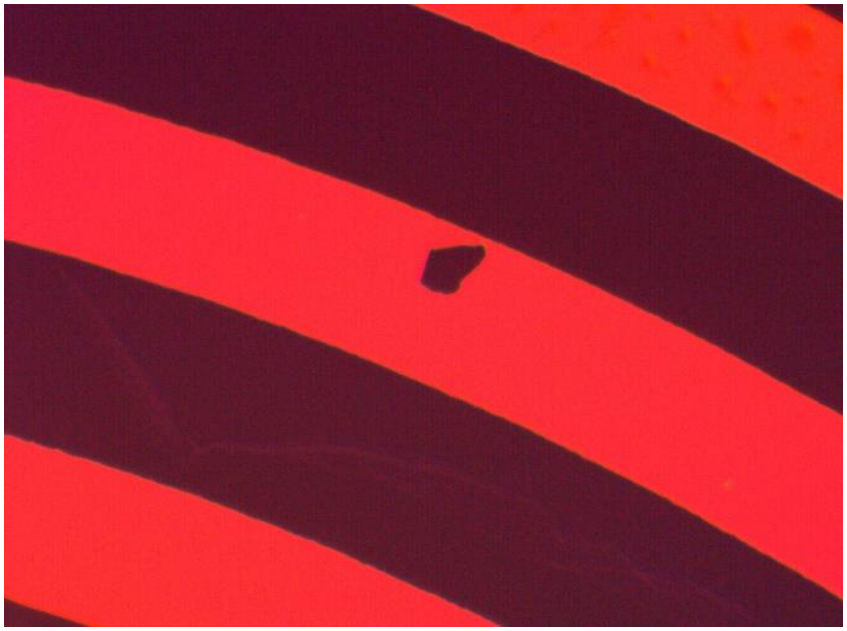

Figure 126 - image showing some breakage on the gold on sample 5

Figure 127 - image showing some dirt on sample 5

15.2.6 Sample 6

Figure 128 - image showing some light scratches and excess photoresist on sample 6

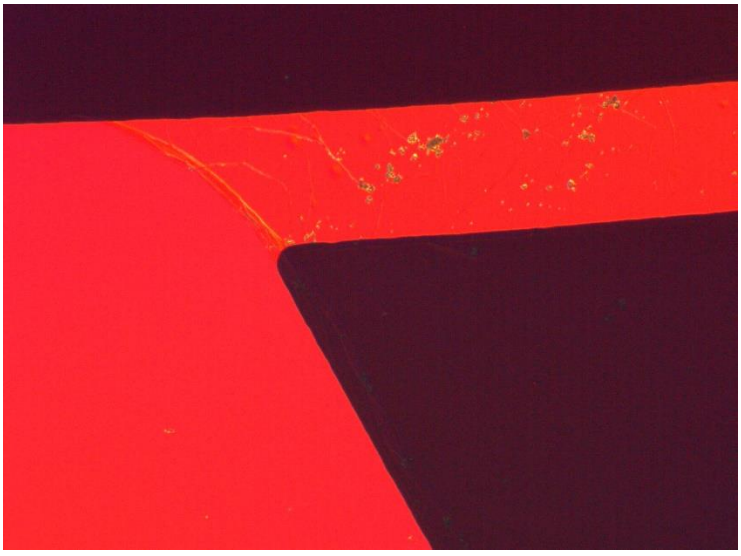

Figure 129 - image showing excess photoresist on sample 6

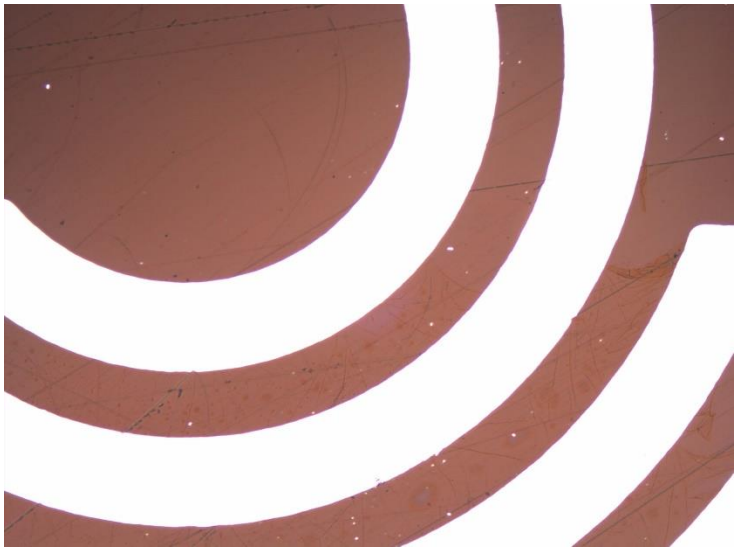

Figure 130 - image showing some light thorough damage on sample 6

15.2.7 Sample 7

Figure 131 - image showing excess photoresist on sample 7

Figure 132 - image showing excess photoresist on sample 7

15.2.8 Sample 8

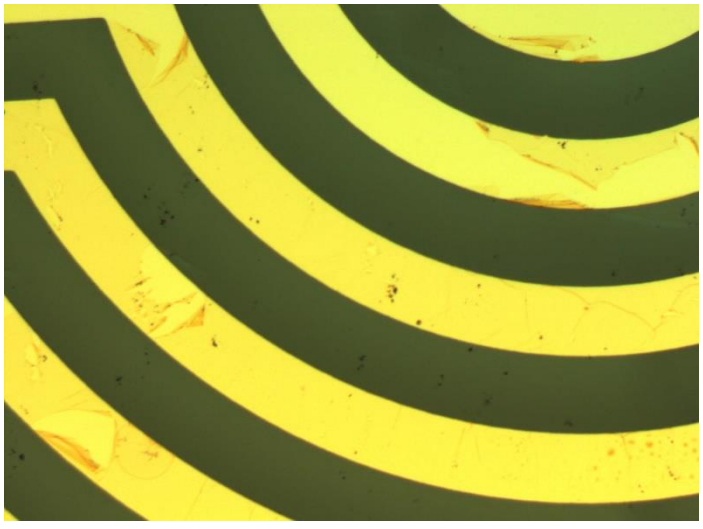

Figure 133 - image showing excess photoresist on sample 8

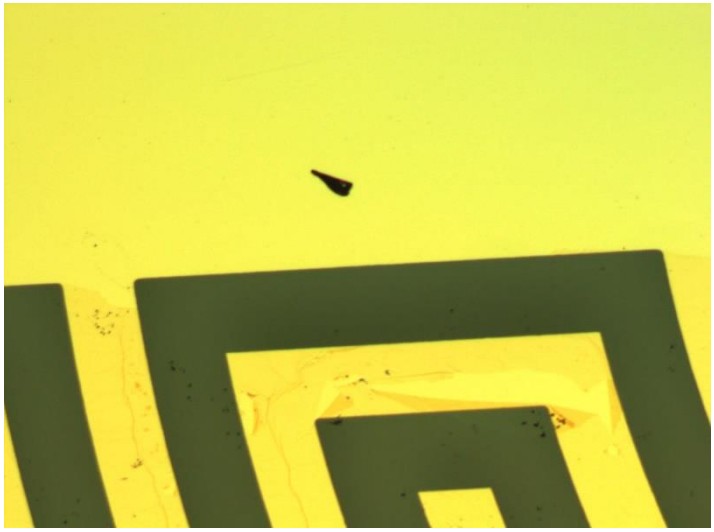

Figure 134 - image showing excess photoresist and some dirt on sample 8

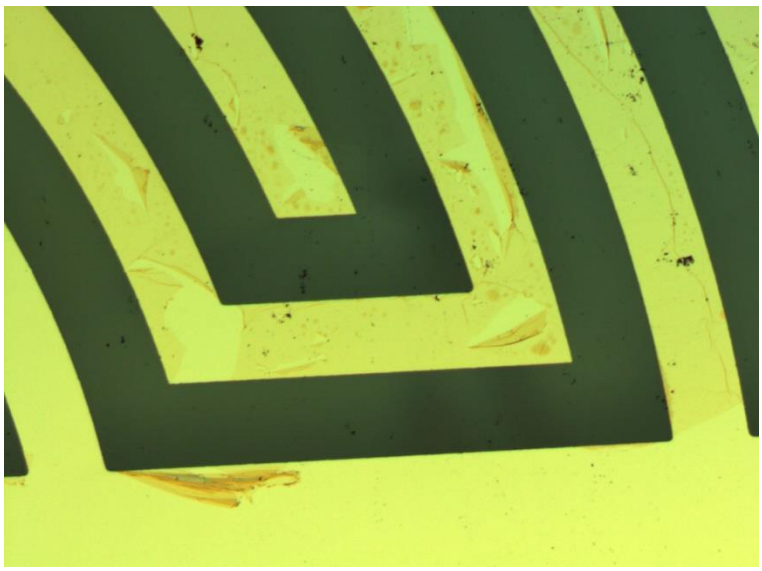

Figure 135 - image showing excess photoresist some of which are pealing

15.3 Experimental tables

15.3.1 Nanofabricated Electrode Experiments

Table 7 - Table of 96 volt plate voltage readings

time (minutes)	voltage (volts)	difference (milivolts)	total change (milivolts)
0	2.02	0	0
10	1.6	420	420
20	1.27	330	750
30	1.08	190	940
40	0.99	90	1030
50	0.94	50	1080
60	0.89	50	1130

Table 8 - Table showing 84 voltage voltage readings

time (minutes)	voltage (volts)	difference (milivolts)	Total change (milivolts)
0	2.12	0	0
10	2.09	30	30
20	1.88	210	240
30	1.61	270	510
40	1.41	200	710
50	1.26	150	860
60	1.17	90	950

Table 9- Table showing 76 volt plate voltage readings

time (minutes)	voltage (volts)	difference (milivolts)	total change (milivolts)
0	2.08	0	0
10	2.01	70	70
20	1.66	350	420
30	1.38	280	700
40	1.24	140	840
50	1.12	120	960
60	1.06	60	1020

Table 10 - table showing 64volt plate voltage readings

time (minutes)	voltage (volts)	difference (milivolts)	total change (milivolts)
0	2.08	0	0
10	2.01	70	70
22	1.61	400	470
30	1.45	160	630
40	1.29	160	790
50	1.2	90	880
60	1.14	60	940

Table 11 - table showing 58 volt plate voltage readings

time (minutes)	voltage (volts)	difference (milivolts)	total change (milivolts)

0	2.09	0	0
10	2.07	20	20
20	1.75	320	340
30	1.38	370	710
40	1.2	180	890
50	1.12	80	970
60	1.04	80	1050

Table 12 - table showing voltage differences for each plate in millivolts

time (minutes)	96V	84V	76V	67V	58V
0	0	0	0	0	0
10	420	30	70	70	20
20	330	210	350	#N/A	320
22	#N/A	#N/A	#N/A	400	#N/A
30	190	270	280	160	370
40	90	200	140	160	180
50	50	150	120	90	80
60	50	90	60	60	80

Table 13 - table showing total voltage changes for each plate in millivolts

time (minutes)	96V	84V	76V	67V	58V
0	0	0	0	0	0
10	420	30	70	70	20
20	750	240	420	#N/A	340
22	#N/A	#N/A	#N/A	470	#N/A
30	940	510	700	630	710
40	1030	710	840	790	890
50	1080	860	960	880	970
60	1130	950	1020	940	1050

15.3.2 Ionic transfer experiment

Table 14 - table showing voltage change over time for ionic transfer experiment

time	voltage input	voltage output
0	1	1.96
10	1	1.88
15	1	1.68
20	1	1.16
25	1	0.48
30	1	0.12
35	1	0.05
40	1	0.044

15.3.3 Double Mesh Experiments

These tables represent input voltage ranges, output voltage ranges, averages of the inputs and output voltage values and the gains for each of the double mesh experiments. Time is represented in minutes while input and output voltages are represented in millivolts.

15.3.3.1 The effect of Electrostatic field on Salt Solution

Table 15 - table showing input, output and gain voltage readings for plateless 5% salt solution

time	input 1	input 2	output1	output2	averageinput	averageoutput	gain/loss
0	992	1000	54	56	996	55	0.055221
5	992	1000	54	56	996	55	0.055221
10	992	1000	54	56	996	55	0.055221
15	992	1000	54	56	996	55	0.055221
20	992	1000	54	56	996	55	0.055221
25	992	1000	54	56	996	55	0.055221
30	992	1000	54	56	996	55	0.055221
35	992	1000	56	58	996	57	0.057229
40	992	1000	56	60	996	58	0.058233
45	984	992	62	60	988	61	0.061741
50	984	992	66	68	988	67	0.067814
55	976	984	70	72	980	71	0.072449
60	976	984	80	82	980	81	0.082653
65	976	984	88	90	980	89	0.090816
70	968	976	98	100	972	99	0.101852
75	968	976	106	108	972	107	0.110082
80	960	968	118	120	964	119	0.123444
85	960	968	130	132	964	131	0.135892

90	952	960	140	142	956	141	0.14749
95	944	952	150	152	948	151	0.159283
100	944	952	160	162	948	161	0.169831
105	936	944	172	174	940	173	0.184043
110	928	936	180	182	932	181	0.194206
115	920	928	182	184	924	183	0.198052
120	912	920	200	202	916	201	0.219432

Table 16 - table showing input, output and gain voltage readings for plateless 10% salt solution

time	input 1	input 2	output1	output2	averageinput	averageoutput	gain/loss
0	992	1000	50	52	996	51	0.051205
5	992	1000	50	52	996	51	0.051205
10	992	1000	50	52	996	51	0.051205
15	992	1000	50	52	996	51	0.051205
20	992	1000	50	52	996	51	0.051205
25	992	1000	50	52	996	51	0.051205
30	992	1000	50	52	996	51	0.051205
35	992	1000	52	54	996	53	0.053213
40	992	1000	56	58	996	57	0.057229
45	984	992	60	62	988	61	0.061741
50	984	992	66	68	988	67	0.067814
55	976	984	74	76	980	75	0.076531
60	976	984	84	86	980	85	0.086735
65	976	984	96	98	980	97	0.09898
70	968	976	110	112	972	111	0.114198
75	960	968	124	126	964	125	0.129668
80	952	960	138	140	956	139	0.145397
85	944	952	154	156	948	155	0.163502
90	936	944	170	172	940	171	0.181915
95	928	936	186	188	932	187	0.200644
100	912	920	200	202	916	201	0.219432
105	912	920	216	218	916	217	0.2369
110	912	920	230	232	916	231	0.252183
115	896	904	244	246	900	245	0.272222
120	896	904	256	258	900	257	0.285556

Table 17 - table showing input, output and gain voltage readings for plateless 15% salt solution

time	input 1	input 2	output1	output2	averageinput	averageoutput	gain/loss
0	992	1000	50	52	996	51	0.051205
10	992	1000	50	52	996	51	0.051205
15	992	1000	50	52	996	51	0.051205

20	992	1000	50	52	996	51	0.051205
25	992	1000	50	52	996	51	0.051205
30	992	1000	50	54	996	52	0.052209
35	992	1000	56	58	996	57	0.057229
40	984	992	60	62	988	61	0.061741
45	976	984	68	72	980	70	0.071429
50	976	984	80	82	980	81	0.082653
55	968	976	94	96	972	95	0.097737
62	960	968	120	122	964	121	0.125519
65	960	968	132	134	964	133	0.137967
70	944	952	152	154	948	153	0.161392
75	928	936	174	176	932	175	0.187768
80	920	928	196	198	924	197	0.213203
85	912	920	218	220	916	219	0.239083
90	896	904	238	240	900	239	0.265556
95	896	904	256	258	900	257	0.285556
100	880	888	272	274	884	273	0.308824
105	872	880	288	290	876	289	0.329909
110	864	872	302	304	868	303	0.349078
115	864	872	316	318	868	317	0.365207
120	848	856	328	330	852	329	0.38615

Table 18 - table showing input, output and gain voltage readings for plateless 20% salt solution

time	input1	input2	output1	output2	averageinput	averageoutput	gain/loss
0	992	1000	48	50	996	49	0.049196787
5	992	1000	48	50	996	49	0.049196787
10	992	1000	50	52	996	51	0.051204819
15	992	1000	50	52	996	51	0.051204819
20	992	1000	50	52	996	51	0.051204819
25	992	1000	50	52	996	51	0.051204819
30	992	1000	54	56	996	55	0.055220884
35	984	992	60	62	988	61	0.061740891
40	976	984	72	74	980	73	0.074489796
45	976	984	88	90	980	89	0.090816327
50	968	976	110	112	972	111	0.114197531
55	960	968	140	142	964	141	0.14626556
60	936	944	172	174	940	173	0.184042553
65	920	928	204	206	924	205	0.221861472
70	904	912	240	242	908	241	0.265418502
75	888	896	272	274	892	273	0.306053812

80	880	888	300	302	884	301	0.340497738
85	864	872	328	330	868	329	0.379032258
90	848	856	352	354	852	353	0.414319249
95	832	848	372	374	840	373	0.444047619
100	816	824	390	396	820	393	0.479268293
105	816	824	412	416	820	414	0.504878049
110	808	816	424	428	812	426	0.524630542
115	800	808	440	444	804	442	0.549751244
120	800	808	448	452	804	450	0.559701493

Table 19 - table showing input, output and gain voltage readings for plateless 25% salt solution

time	input1	input2	output1	output2	averageinput	averageoutput	gain/loss
0	992	1000	50	52	996	51	0.051204819
5	992	1000	50	52	996	51	0.051204819
10	992	1000	50	52	996	51	0.051204819
15	992	1000	50	52	996	51	0.051204819
20	992	1000	50	52	996	51	0.051204819
25	992	1000	50	52	996	51	0.051204819
30	-	-	-	-	-	-	-
35	984	992	62	64	988	63	0.063765182
40	976	984	76	78	980	77	0.078571429
45	-	-	-	-	-	-	-
50	960	968	116	118	964	117	0.121369295
55	944	952	148	150	948	149	0.157172996
60	928	936	180	182	932	181	0.194206009
65	912	920	218	220	916	219	0.239082969
70	888	912	248	250	900	249	0.276666667
75	880	888	280	282	884	281	0.317873303
80	872	880	308	310	876	309	0.352739726
85	848	856	332	334	852	333	0.39084507
90	840	848	354	356	844	355	0.420616114
95	832	840	374	376	836	375	0.448564593
100	816	824	394	400	820	397	0.484146341
105	808	816	412	416	812	414	0.509852217
110	800	808	424	428	804	426	0.529850746
115	800	800	436	440	800	438	0.5475
120	800	800	448	452	800	450	0.5625

Table 20 - table showing input, output and gain voltage readings for 200v plate field strength at 5% salt solution

time	input1	input2	output1	output2	averageinput	averageoutput	gain/loss

0	992	1000	50	52	996	51	0.051205
5	992	1000	50	52	996	51	0.051205
10	992	1000	50	52	996	51	0.051205
15	992	1000	50	52	996	51	0.051205
20	992	1000	50	52	996	51	0.051205
25	992	1000	50	52	996	51	0.051205
30	992	1000	50	52	996	51	0.051205
35	992	1000	54	56	996	55	0.055221
40	992	1000	56	58	996	57	0.057229
45	992	1000	60	62	996	61	0.061245
50	984	992	66	68	988	67	0.067814
55	976	984	74	76	980	75	0.076531
60	976	984	82	84	980	83	0.084694
65	968	976	90	92	972	91	0.093621
70	968	976	102	104	972	103	0.105967
75	960	968	116	118	964	117	0.121369
80	952	960	128	130	956	129	0.134937
85	952	960	142	144	956	143	0.149582
90	944	952	156	158	948	157	0.165612
95	936	944	170	172	940	171	0.181915
100	928	936	184	186	932	185	0.198498
105	920	928	198	200	924	199	0.215368
110	912	920	212	214	916	213	0.232533
115	912	920	224	226	916	225	0.245633
120	904	912	236	238	908	237	0.261013

Table 21- table showing input, output and gain voltage readings for 200v plate field strength at 10% salt solution

time	input 1	input 2	output1	output2	averageinput	averageoutput	gain/loss
0	992	1000	58	60	996	59	0.059236948
5	992	1000	58	60	996	59	0.059236948
10	992	1000	58	60	996	59	0.059236948
15	992	1000	58	60	996	59	0.059236948
20	992	1000	58	62	996	60	0.060240964
25	992	1000	58	62	996	60	0.060240964
30	992	1000	60	62	996	61	0.06124498
35	992	1000	64	66	996	65	0.065261044
40	984	992	68	70	988	69	0.069838057
45	976	984	78	80	980	79	0.080612245
50	976	984	88	90	980	89	0.090816327

55	968	976	102	104	972	103	0.105967078
60	960	968	116	118	964	117	0.121369295
65	952	960	134	136	956	135	0.141213389
70	944	952	154	156	948	155	0.16350211
75	936	944	172	174	940	173	0.184042553
80	928	936	188	192	932	190	0.203862661
85	912	920	206	210	916	208	0.227074236
90	912	920	226	228	916	227	0.247816594
95	896	904	242	246	900	244	0.271111111
100	896	904	256	260	900	258	0.286666667
105	880	896	274	276	888	275	0.309684685
110	880	888	288	290	884	289	0.326923077
115	872	880	300	302	876	301	0.343607306
120	864	872	312	314	868	313	0.360599078

Table 22 - table showing input, output and gain voltage readings for 200v plate field strength at 15% salt solution

200v, 15% salt solution							
time	input 1	input 2	output1	output2	averageinput	averageoutput	gain/loss
0	992	1000	52	56	996	54	0.054217
5	992	1000	52	56	996	54	0.054217
10	992	1000	52	56	996	54	0.054217
15	992	1000	52	56	996	54	0.054217
20	992	1000	52	56	996	54	0.054217
25	992	1000	52	56	996	54	0.054217
30	992	1000	56	58	996	57	0.057229
35	984	992	60	64	988	62	0.062753
40	984	992	66	68	988	67	0.067814
45	976	984	76	78	980	77	0.078571
50	976	984	90	92	980	91	0.092857
55	968	976	108	110	972	109	0.11214
60	960	968	126	128	964	127	0.131743
65	944	952	146	148	948	147	0.155063
70	936	944	168	170	940	169	0.179787
75	928	936	190	192	932	191	0.204936
80	912	920	210	212	916	211	0.230349
85	904	912	230	232	908	231	0.254405
90	896	904	250	252	900	251	0.278889
95	880	888	268	270	884	269	0.304299
100	880	888	286	288	884	287	0.324661
105	864	872	300	302	868	301	0.346774

110	856	864	314	316	860	315	0.366279
115	856	864	326	328	860	327	0.380233
120	848	856	336	340	852	338	0.396714

Table 23 - table showing input, output and gain voltage readings for 200v plate field strength at 20% solution

time	input1	input2	output1	output2	averageinput	averageoutput	gain/loss
0	992	1000	54	56	996	55	0.055220884
5	992	1000	54	56	996	55	0.055220884
10	992	1000	54	56	996	55	0.055220884
15	992	1000	54	56	996	55	0.055220884
20	992	1000	54	56	996	55	0.055220884
25	992	1000	54	56	996	55	0.055220884
30	992	1000	54	56	996	55	0.055220884
35	984	992	62	64	988	63	0.063765182
40	984	992	68	70	988	69	0.069838057
45	976	984	78	80	980	79	0.080612245
50	968	976	88	90	972	89	0.091563786
55	968	976	104	106	972	105	0.108024691
60	960	968	120	122	964	121	0.125518672
65	952	960	138	140	956	139	0.14539749
70	944	952	160	162	948	161	0.169831224
75	928	936	180	182	932	181	0.194206009
80	920	928	198	200	924	199	0.215367965
85	912	920	218	220	916	219	0.239082969
90	904	912	236	238	908	237	0.261013216
95	896	904	252	254	900	253	0.281111111
100	888	896	268	270	892	269	0.301569507
105	880	888	282	284	884	283	0.320135747
110	872	880	294	296	876	295	0.336757991
115	864	880	306	308	872	307	0.35206422
120	864	872	316	318	868	317	0.365207373

Table 24 - table showing input, output and gain voltage readings for 200v plate field strength at 25% salt solution

time	input1	input2	output1	output2	averageinput	averageoutput	gain/loss
0	992	1000	56	60	996	58	0.058232932
5	992	1000	56	60	996	58	0.058232932
10	992	1000	56	60	996	58	0.058232932
15	992	1000	56	60	996	58	0.058232932
20	992	1000	56	60	996	58	0.058232932
25	984	992	58	60	988	59	0.059716599

30	984	992	62	64	988	63	0.063765182
35	976	984	68	74	980	71	0.07244898
40	976	984	84	86	980	85	0.086734694
45	968	976	104	106	972	105	0.108024691
50	960	968	128	130	964	129	0.133817427
55	944	952	158	160	948	159	0.167721519
60	920	928	192	194	924	193	0.208874459
65	912	920	224	226	916	225	0.245633188
70	888	896	256	258	892	257	0.288116592
75	872	880	286	288	876	287	0.327625571
80	864	872	312	314	868	313	0.360599078
85	-	-	-	-	-	-	-
90	840	848	358	360	844	359	0.42535545
95	824	840	378	380	832	379	0.455528846
100	816	824	394	400	820	397	0.484146341
105	808	816	412	416	812	414	0.509852217
110	800	808	424	428	804	426	0.529850746
115	800	808	436	440	804	438	0.544776119
120	800	800	452	456	800	454	0.5675

16 Bibliography

University of Cambridge; “DoITPoMS - TLP Library Dielectric materials - Variation of the dielectric constant in alternating fields", Doitpoms.ac.uk. [Online]. Available: https://www.doitpoms.ac.uk/tlplib/dielectrics/variation.php.

MSI Sensing; "Broadband Dielectrics", Msi-sensing.com. 2015 [Online]. Available: http://www.msi-sensing.com/broadband_dielectrics.htm.

D.R.Caprette; "Introduction to SDS-PAGE", Ruf.rice.edu. 18-Nov-2012 [Online]. Available: http://www.ruf.rice.edu/~bioslabs/studies/sds-page/gellab2.html.

"Basics of EIS: Electrochemical Research-Impedance", Gamry.com. [Online]. Available: https://www.gamry.com/application-notes/EIS/basics-of-electrochemical-impedance-spectroscopy/.

"HyperPhysics", Hyperphysics.phy-astr.gsu.edu. [Online]. Available: http://hyperphysics.phy-astr.gsu.edu/hbase/hframe.html.

17 References

[1]“ Accelerating Intelligence.,” KurzweilAI A wearable graphene based biomedical device to monitor and treat diabetes. 22-March-2016 [Online]. Available: http://www.kurzweilai.net/a-wearable-graphene-based-biomedical-device-to-monitor-and-treat-diabetes.

[2] Center for Responsible Nanotechnology “Medical Nanotechnology: Benefits of Molecular Manufacturing.” [Online]. May-12-2003 Available: http://www.crnano.org/medical.htm.

[3] G. Glass, “Pharmaceutical patent challenges — time for reassessment?,” Nature News, 01-Dec-2004. Nature Reviews Drug Discovery volume 3, pages 1057–1062 (2004) doi:10.1038/nrd1581 [Online]. Available: https://www.nature.com/articles/nrd1581.

[4] I. Patringenaru “Nanoparticles Disguised as Red Blood Cells Will Deliver Cancer-Fighting Drugs,” UC San Diego Jacobs School of Engineering. [Online].June-20-2011. Available: http://jacobsschool.ucsd.edu/news/news_releases/release.sfe?id=1086.

[5] B. Kisliuk, “Tiny capsule effectively kills cancer cells,” UCLA Newsroom, 06-Feb-2013. [Online]. Available: http://newsroom.ucla.edu/releases/tiny-capsule-effectively-treats-243192.

[6] NHS Choices. [Online]. Available: https://www.nhs.uk/conditions/coronary-heart-disease/.

[7] M. Karimi, H. Zare, A. B. Nik, N. Yazdani, M. Hamrang, E. Mohamed, P. S. Zangabad, S. M. M. Basri, L. Bakhtiari, and M. R. Hamblin, “Nanotechnology in diagnosis and treatment of coronary artery disease,” Nanomedicine, Mar-2016. Nanomedicine (Lond). 2016 Mar; 11(5): 513–530. Published online 2016 Feb 23; doi : 10.2217/nnm.16.3 [Online]. Available: https://www.ncbi.nlm.nih.gov/pmc/articles/PMC4794112/.

[8] J.P Cobb, R.S. Hotchkiss, I.E. Karl and T.G Buchman, “Mechanisms of Cell Injury During Death”, British Journal of Anaesthesia 1996; 77: page 3-10

[9] M.Peran, M.A. Garcia, E. Lopez-Ruiz, G. Jimenez, J.A Marchal, “How Can Nanotechnology Help to Repair the Body? Advances in Cardiac, Skin, Bone, Cartilage and Nerve Tissue Regeneration” Materials 2013, 6, 1333-1359; doi:10.3390/ma6041333 [Online]. Available: https://www.ncbi.nlm.nih.gov/pmc/articles/PMC5452318/pdf/materials-06-01333.pdf

[10] "Nanotechnology May Be Used to Regenerate Tissues, Organs: Northwestern University News", Northwestern.edu. [Online]. Available: http://www.northwestern.edu/newscenter/stories/2007/05/stupp.html.

[11] M.Mitra “Medical Nanobot for Cell and Tissue Repair”, Journal of Analytical and Pharmaceutical Research, Volume 2 issue 6 – 2017

[12] S. Kumar, J. Xuan, M. Lee, H. Tolley, A. Hawkins and A. Woolley, "Thin-film microfabricated nanofluidic arrays for size-selective protein fractionation". Lab Chip. 2013

Dec 7; 13(23): 4591–4598. doi: 10.1039/c3lc50869b
[Online]. Available: https://www.ncbi.nlm.nih.gov/pmc/articles/PMC3864585/
[13]P. Floriano, N. Christodoulides, C. Miller, J. Ebersole, J. Spertus, B. Rose, D. Kinane, M. Novak, S. Steinhubl, S. Acosta, S. Mohanty, P. Dharshan, C. Yeh, S. Redding, W. Furmaga and J. McDevitt, "Use of Saliva-Based Nano-Biochip Tests for Acute Myocardial Infarction at the Point of Care: A Feasibility Study", Clinical Chemistry, vol. 55, no. 8, pp. 1530-1538, 2009.
[14] P. Malik, V. Katyal, V. Malik, A. Asatkar, G. Inwati and T. Mukherjee, "Nanobiosensors: Concepts and Variations", ISRN Nanomaterials, vol. 2013, pp. 1-9, 2013.
[15] Azimzadeh, Mostafa & Rahaie, Mahdi & Nasirizadeh, Navid & Daneshpour, Maryam & Naderi-Manesh, Hossein. (2017). Electrochemical miRNA Biosensors: The Benefits of Nanotechnology. Nanomedicine Research Journal (NMRJ). 1. 158-171. 10.7508/nmrj.2017.03.005.
[16]"1.1. What Is a Biosensor?", Gatewaycoalition.org. [Online]. Available: http://www.gatewaycoalition.org/files/hidden/sensr/ch1/1_1f.htm.
[17] M. Chaplin, "What are biosensors?", Www1.lsbu.ac.uk, 2004. [Online]. Available: http://www1.lsbu.ac.uk/water/enztech/biosensors.html.
[18] L. Zheng, J. Wei, X. Lv, Y. Bi, P. Wu, Z. Zhang, P. Wang, R. Liu, J. Jiang, H. Cong, J. Liang, W. Chen, H. Cao, W. Liu, G. Gao, Y. Du, X. Jiang and X. Li, "Detection and differentiation of influenza viruses with glycan-functionalized gold nanoparticles", Biosensors and Bioelectronics, vol. 91, pp. 46-52, 2017.
[19] S. Fahmy, "UGA researchers use gold nanoparticles to diagnose flu in minutes - UGA Today", UGA Today, 2011. [Online]. Available: https://news.uga.edu/uga-researchers-use-gold-nanoparticles-to-diagnose-flu-in-minutes/.
[20] "Quantum Dots", Sigma-Aldrich. [Online]. Available: https://www.sigmaaldrich.com/technical-documents/articles/materials-science/nanomaterials/quantum-dots.html.
[21] "Immunolabeling | Thermo Fisher Scientific", Thermofisher.com. [Online]. Available: https://www.thermofisher.com/uk/en/home/life-science/cell-analysis/cell-analysis-learning-center/molecular-probes-school-of-fluorescence/imaging-basics/labeling-your-samples/immunolabeling.html.
[22] T. Zdobnova, S. Dorofeev, P. Tananaev, R. Vasiliev, T. Balandin, E. Edelweiss, O. Stremovskiy, I. Balalaeva, I. Turchin, E. Lebedenko, V. Zlomanov and S. Deyev, "Fluorescent immunolabeling of cancer cells by quantum dots and antibody scFv fragment", Journal of Biomedical Optics, vol. 14, no. 2, p. 021004, 2009.
[23] T. Chu, F. Shieh, L. Lavery, M. Levy, R. Richards-Kortum, B. Korgel and A. Ellington, "Labeling tumor cells with fluorescent nanocrystal–aptamer bioconjugates", Biosensors and Bioelectronics, vol. 21, no. 10, pp. 1859-1866, 2006.

[24] Z. Kaul, T. Yaguchi, S. Kaul, T. Hirano, R. Wadhwa and K. Taira, "Mortalin imaging in normal and cancer cells with quantum dot immuno-conjugates", Cell Research, vol. 13, no. 6, pp. 503-507, 2003.
[25] H. Wang, H. Wang, R. Liang and K. Ruan, "Detection of Tumor Marker CA125 in Ovarian Carcinoma Using Quantum Dots", Acta Biochimica et Biophysica Sinica, vol. 36, no. 10, pp. 681-686, 2004.
[26] H. Colton, J. Falls, H. Ni, P. Kwanyuen, D. Creech, E. McNeil, W. Casey, G. Hamilton and N. Cariello, "Visualization and Quantitation of Peroxisomes Using Fluorescent Nanocrystals: Treatment of Rats and Monkeys with Fibrates and Detection in the Liver", Toxicological Sciences, vol. 80, no. 1, pp. 183-192, 2004.
[27] Kahn E et al, "Analysis of CD36 expression on human monocytic cells and atherosclerotic tissue sections with quantum dots: investigation by flow cytometry and spe... - PubMed - NCBI", Ncbi.nlm.nih.gov, 2006. [Online]. Available: https://www.ncbi.nlm.nih.gov/pubmed/16566276.
[28] J. Bocsi, D. Lenz, A. Mittag, V. Varga, B. Molnar, Z. Tulassay, U. Sack and A. Tárnok, "Automated four-color analysis of leukocytes by scanning fluorescence microscopy using quantum dots", Cytometry Part A, vol. 69, no. 3, pp. 131-134, 2006.
[29] Y. Chu, D. Engebretson and J. Carey, "Bioconjugated Magnetic Nanoparticles for the Detection of Bacteria", Journal of Biomedical Nanotechnology, vol. 9, no. 12, pp. 1951-1961, 2013.
[30] H. Hathaway, K. Butler, N. Adolphi, D. Lovato, R. Belfon, D. Fegan, T. Monson, J. Trujillo, T. Tessier, H. Bryant, D. Huber, R. Larson and E. Flynn, "Detection of breast cancer cells using targeted magnetic nanoparticles and ultra-sensitive magnetic field sensors", Breast Cancer Research, vol. 13, no. 5, 2011.
[31]"Static Fields: 1. What are static electric and magnetic fields?", Greenfacts.org. [Online]. Available: https://www.greenfacts.org/en/static-fields/l-2/1-what-are-static-fields.htm.
[32]M. Rouse, "What is permittivity (electric permittivity)? - Definition from WhatIs.com", WhatIs.com, 2005. [Online]. Available: http://whatis.techtarget.com/definition/permittivity-electric-permittivity.
[33]Miami College of Arts and Sciences "Supplemental Materials", Physics.miami.edu. Phy 207, Section H, Spring 2005 [Online]. Available: http://www.physics.miami.edu/~zuo/class/fall_05/lecture%20supp.html.
[34]"Visualizing DNA After Agarose Gel Electrophoresis", Edvotek.com. [Online]. Available: http://www.edvotek.com/M36.
[35]"Britannica.com", Media1.britannica.com. [Online]. Available: https://media1.britannica.com/eb-media/07/130907-004-537354FB.jpg
[36]"wikimedia.org", Upload.wikimedia.org. [Online]. Available: https://upload.wikimedia.org/wikipedia/commons/thumb/6/6c/Dielectric_responses.svg/90

8px-Dielectric_responses.svg.png.
[37]S. Chan Lee, S. Some, S. Wook Kim, S. Jun Kim, J. Seo, J. Lee, T. Lee, J. Ahn, H. Choi and S. Chan Jun, "Efficient Direct Reduction of Graphene Oxide by Silicon Substrate", Scientific Reports, vol. 5, no. 1, 2015.
[38]L. Jeurgens, W. Sloof, F. Tichelaar, C. Borsboom and E. Mittemeijer, "Determination of thickness and composition of aluminium-oxide overlayers on aluminium substrates", Applied Surface Science, vol. 144-145, pp. 11-15, 1999.
[39]T. Nakasu, W. Sun, S. Yamashita, T. Aiba, K. Taguri, M. Kobayashi, T. Asahi and H. Togo, "MBE growth and characterization of ZnTe epilayers on m-plane sapphire substrates", physica status solidi (c), vol. 11, no. 7-8, pp. 1182-1185, 2014.
[40]G. Wang, M. Zhang, Y. Zhu, G. Ding, D. Jiang, Q. Guo, S. Liu, X. Xie, P. Chu, Z. Di and X. Wang, "Direct Growth of Graphene Film on Germanium Substrate", Scientific Reports, vol. 3, no. 1, 2013.
[41]D. Stirland and B. Straughan, "A review of etching and defect characterisation of gallium arsenide substrate material", Thin Solid Films, vol. 31, no. 1-2, pp. 139-170, 1976.
[42]M. Cameron, "Iodine: Inhalation Hazards, Detection and Protection", State of California Department of Justice, 2002. [Online]. Available: https://oag.ca.gov/sites/all/files/agweb/pdfs/cci/safety/iodine_hazards.pdf.